2004

The role of ribosomal protein L11 and the L11-binding rRNA in protein synthesis on the prokaryotic ribosome

William Sean Bowen
The University of Montana

NOTE TO USERS

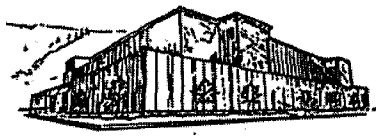

THE UNIVERSITY OF MONTANA

THE ROLE OF RIBOSOMAL PROTEIN L11 AND THE L11-BINDING rRNA IN PROTEIN SYNTHESIS ON THE PROKARYOTIC RIBOSOME

by

William Sean Bowen

B.A. University of Montana 1998

A dissertation submitted in partial fulfillment
of the requirements for the degree of
Doctor of Philosophy
Division of Biological Sciences
in The University of Montana
November 2004

Approved by:

Chairman

Graduate School Dean

11-8-04
Date

Bowen, William S., Ph.D., November 2004 **Biochemistry/Microbiology**

Chairman: J. Stephen Lodmell

The Role of Ribosomal Protein L11 and the L11-Binding rRNA in Protein Synthesis on the Prokaryotic Ribosome

The purpose of this study was to investigate the role of ribosomal protein L11 and the L11-binding rRNA in translation on the prokaryotic ribosome. The L11 and L11-binding rRNA forms a complex on the inter-subunit face of the large ribosomal subunit, and is part of a group of ribosomal protein and rRNA elements that are separated in the secondary structure of the large subunit, but that are all linked to the functions of soluble translation factors during their interactions with ribosomes. Together the elements are referred to as the GTPase-associated region (GAR) due to their link to factor-dependent hydrolysis of guanosine triphosphate on the ribosome. Here we used structural and functional biochemical studies to specifically characterize the proximity of the L11/L11-binding rRNA complex to other elements of the GAR, and to elucidate the role of L11 and the L11-binding rRNA in factor interactions during translation.

The evidence provided herein suggests that the L11/L11-binding rRNA complex is proximal to other important elements of the GAR in the tertiary structure of the large subunit, and both L11 and the L11-binding rRNA are involved in the function of elongation factor G (EF-G) on the ribosome. Translation factor EF-G participates in elongation of a nascent peptide on the ribosome by catalyzing the translocation of transfer RNA across the ribosome as they decode messenger RNA. L11-binding rRNA is found to be important for binding of elongation factor G (EF-G) on the ribosome, while L11 is linked to EF-G-dependent GTP hydrolysis and/or turnover of EF-G during its cyclical interaction with the ribosome. The C-terminal domain of L11 stabilizes the structure of the L11-binding rRNA to allow its interaction with EF-G, while presence of the N-terminal domain of L11 increases the efficiency of EF-G-dependent GTP hydrolysis and/or turnover of the factor in the process of protein synthesis.

Don't give up, don't ever give up!

ACKNOWLEDGMENTS

You cannot do it alone. As friends, colleagues, and family share in the tribulations along the way, they also share in the congratulations. I would like to thank my committee members for their wisdom, advice, and patience. Thanks to the members of the Hill and Lodmell labs. To Jean Marc Lanchy: You have taught me a lot about science, politics, and friendship. To Scott Hennelly: There is no way I get here without your help. From excellent technical advice, to honest friendship, to quick wit; you gave it all. To Marty Rice: Somehow, you got me through. I am a much better person for knowing you and I will never forget you. To my advisors, Steve Lodmell and Walt Hill: Walt, you are truly an inspiration in how you do science and in how you live life. Steve, I do not know how I can repay what you have done for me the last five years. I only hope I can make both of you proud to call me your student. To my family: It has been a long, hard journey, and I would not have had the courage to start without your confidence, guidance, and love. To my sister Jacqui: What do you think of your little brother now? Thank you for being my ally when I needed a sympathetic ear. Finally, to my long-suffering wife Jonelle: We did it baby! Now I believe we can do anything together. Thank you for never giving up and never losing faith. You have my unconditional love in return.

TABLE OF CONTENTS

LIST OF APPENDICES

Appendix

LIST OF FIGURES

LIST OF TABLES

Chapter 1
Introduction

The research described in this dissertation was designed to characterize the structure and function of an RNA domain of the prokaryotic ribosome known to interact with translation factors during protein biosynthesis. This domain consists of ribosomal protein L11 and the region of ribosomal RNA (rRNA) to which it binds (L11BR).

The first chapter introduces the concepts that are critical for understanding the function of the L11/L11BR on the prokaryotic ribosome. After describing the importance of the translation of proteins on ribosomes to living organisms, we outline the aspects of translation that are related to our study. Then we describe the soluble translation factors that assist in the function of the ribosome during translation, with particular attention on those factors that require the coupled hydrolysis of GTP. Next we describe the phylogenetically conserved role of rRNA in translation and the postulated translational functions of several important domains. Particular emphasis is placed on the role of those regions linked to interactions with translation factors and GTP hydrolysis, including the L11BR. We move on to explain the importance of L11 in the translation process and speculate on the mechanism of translation inhibition by thiostrepton, an antibiotic that binds in the L11/L11BR domain and disrupts translation factor interactions with the ribosome. After this, we provide a background on a variety of methods used to study ribosome structure and their importance for understanding the function of the

ribosome. This section includes background on the chemical modification and chemical nuclease probing techniques that were utilized in our study. Finally, the last section of the introduction includes an overview of the specific aims that guided our research and the hypotheses that were tested in the following chapters.

Chapter 2 details experiments that localized this domain with respect to other structural landmarks on the large subunit of prokaryotic ribosomes. We found that the L11BR is proximal in the tertiary structure of the ribosomal large subunit to another element of large subunit rRNA previously linked to translation factor interactions with the ribosome, a domain known as the sarcin/ricin stem-loop domain.

Our second section of research, detailed in the first part of Chapter 3, describes experiments designed to address the hypothesis that the structural flexibility of the L11BR is governed by the interaction of ribosomal protein L11 with the rRNA in this domain of the ribosome. We found that mutations of the eubacterium *Escherichia coli* that result in the absence of L11 from ribosomes significantly alter the structure of the L11BR. However, mutations that result in the loss of only the N-terminal domain of L11 do not alter L11BR structure significantly.

Finally, the last part of Chapter 3 and all of Chapter 4 address the hypothesis that mutations resulting in the loss of all or part of L11 on prokaryotic ribosomes have adverse effects on translation elongation factor functions on the ribosome. We found that the loss of L11 significantly reduced the interaction of elongation factor G (EF-G) with the ribosome and significantly decreased the rate of translation elongation. The loss of the N-terminal domain did not significantly affect the EF-G interactions with the ribosome, but it did reduce both the rate of translation elongation and the rate of EF-G-

dependent hydrolysis of guanosine triphosphate (GTP), a function of the factor that is coupled to its interaction with ribosomes and its role during protein synthesis. In Chapter 5 we summarize the results of our studies and analyze their importance in the context of ribosome function.

Gene Expression

One of the fundamental challenges all organisms face is to accurately and efficiently express the information encoded in their genetic material in such a way that vital cellular processes continue even in ever-changing environmental conditions. Without converting this information into a functional protein, organisms would be limited to the chemical and molecular potential of the deoxyribonucleic acid (DNA) itself to provide cellular functions. This would significantly reduce the structural and functional complexities possible for biological organisms. To overcome this limitation, evolution has provided organisms with an ingenious strategy for gene expression (Figure 1.1).

First, the carrier of genetic information, a linear molecular sequence of the DNA bases adenine, guanine, thymine, and cytosine (A,G,T,C) connected through a sugar-phosphate backbone, is transcribed into the linear molecular sequence of messenger ribonucleic acid (mRNA). mRNA is a faithful copy of the genetic information from DNA that differs from DNA by the substitution of uridine (U) for thymine in the coding sequence and by the addition of a hydroxyl group on the sugar ring (not shown). mRNA is a complementary copy of DNA in the sense that ribonucleoside monomers are incorporated into the copy strand based upon their potential for hydrogen bond base-pairing with the deoxyribonucleoside bases of the template DNA strand (C:G; U:A) (Figure 1.1). The transcription from DNA to mRNA allows the genetic information to be

amplified into several copies, to be transported to other regions of the cell, and to be disposed of when no longer useful. This strategy provides several points on the pathway to regulate gene expression and allows the DNA to remain protected from sources of mutation.

Finally, the linear molecular sequence of mRNA is used to direct assembly of a linear molecular sequence of amino acids. This process is termed translation. The sequence of amino acids in the translated protein directs the tertiary folding of the protein and determines the diversity of structures it can form and, therefore, the structural or catalytic roles it can fulfill in the cell. The resulting protein is the functional expression of the genetic information.

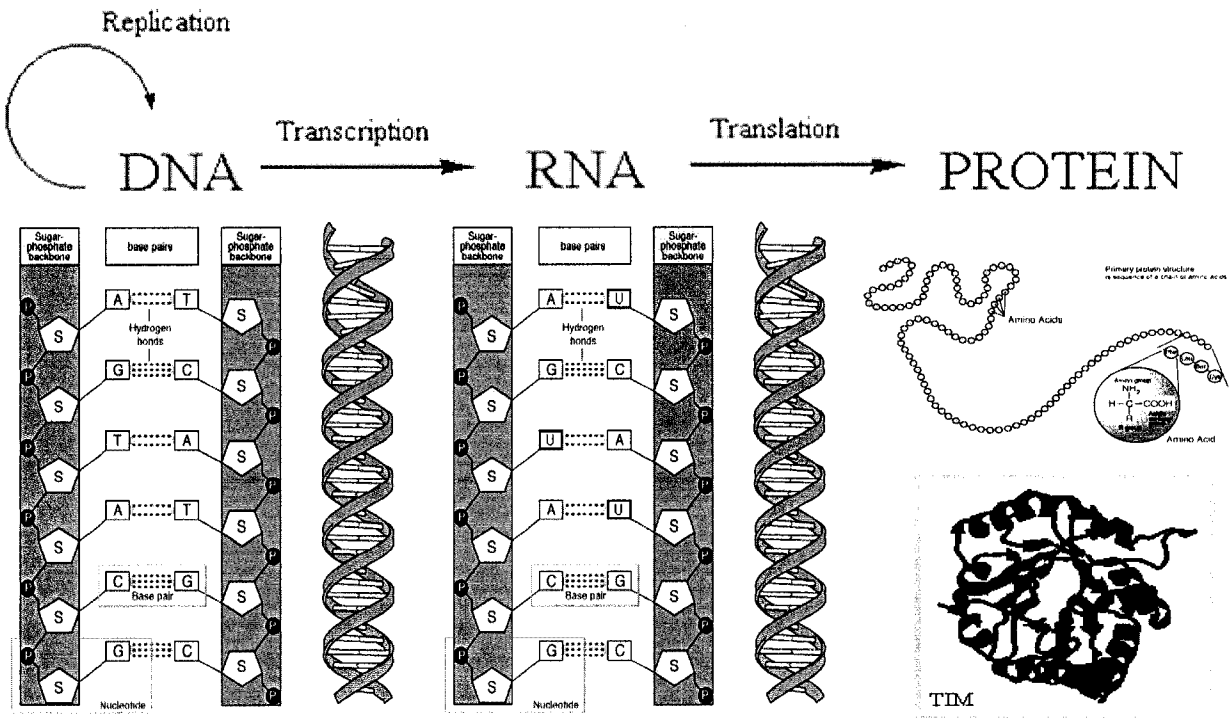

Figure 1.1. Transformation of Genetic Information from DNA Sequence into Functional Protein. The "central dogma" of molecular biology: DNA (left) is transcribed into messenger RNA (middle). Messenger RNA is then translated into the linear sequence of amino acids (above right) that folds into a functional protein (below right). DNA, RNA, and Protein structures were modified from figures by Darryl Leja at the National Human Genome Research Institute (NHGRI) (http://www.genome.gov/page.cfm). A, adenine; T, thymine; C, cytosine; G, guanosine; U, uridine.

The Ribosome and Translation

During transcription, mRNA is synthesized as a complementary copy of the DNA template sequence by the enzyme RNA polymerase. In the eubacterium, *Escherichia coli*, this enzyme complex, consisting of six polypeptide subunits, polymerizes nucleotide triphosphates into a polynucleotide copy of the DNA sequence. Once mRNA is synthesized, the mRNA sequence must be translated into the amino acid sequence of the desired protein. Translation takes place on a large, intracellular ribonucleoprotein particle called the ribosome. Ribosomes of similar size and structure fulfill this function in all cells of bacteria, plants, and animals.

Ribosomes are large complexes of ribosomal proteins and rRNA. In the eubacteria, these large macromolecular complexes have a sedimentation coefficient of 70S, a molecular weight of nearly 2.5 million daltons, and consist of two asymmetric subunits with sedimentation coefficients of 30S (small subunit) and 50S (large subunit) (Figure 1.2). The 50S subunit itself is made up of two molecules of ribosomal rRNA, with sedimentation coefficients of 23S and 5S and 34 ribosomal proteins. The 30S subunit contains one molecule of 16S rRNA and 21 ribosomal proteins. Transfer RNA (tRNA) serves as the adaptor molecule to link the information contained in the mRNA sequence to the incorporation of a specific amino acid in the growing polypeptide on the ribosome. Complementarity between the three base codon of the mRNA molecule with the anticodon of the tRNA molecule (Figure 1.2) assures proper incorporation of the specifically attached amino acid into the polypeptide.

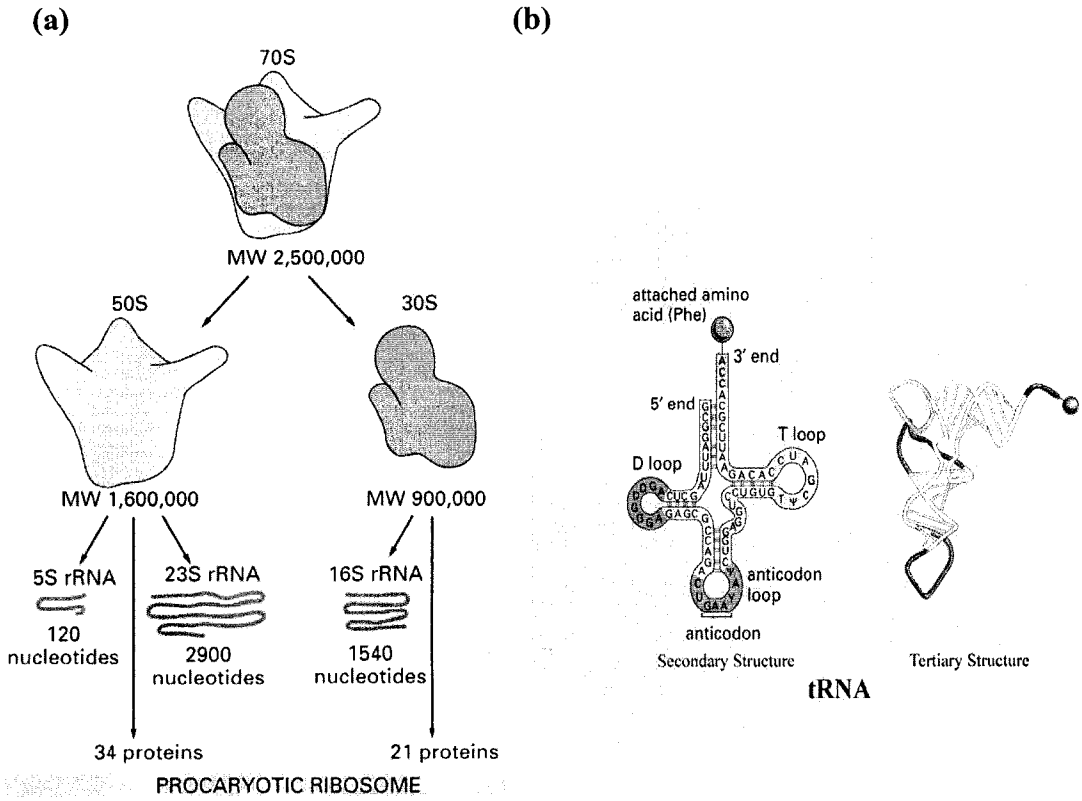

Figure 1.2: Ribosomes and tRNA. (a) Components of prokaryotic ribosome structure. (b) The structure of tRNA. Modified from Alberts *et al.*(2)

After the landmark discovery of the "little cellular granules," or ribosomes, by George Palade in 1955 (11), the race was on to uncover the molecular basis for translation, a race that continues today. About forty years of intensive study of ribosome structure and biochemistry has greatly elucidated the mechanisms by which organisms synthesize protein from genetic information. Although translation in eukaryotic cells has been found to be somewhat more complex and to require a larger number of cellular co-factors than in prokaryotic cells, researchers have found that the fundamental machinery and methods of the translation process are closely related in all domains of life. For

instance, for all organisms the process of translation is believed to take place in a series of three principal stages: initiation, elongation, and termination. For the purpose of this study we will focus on prokaryotic translation.

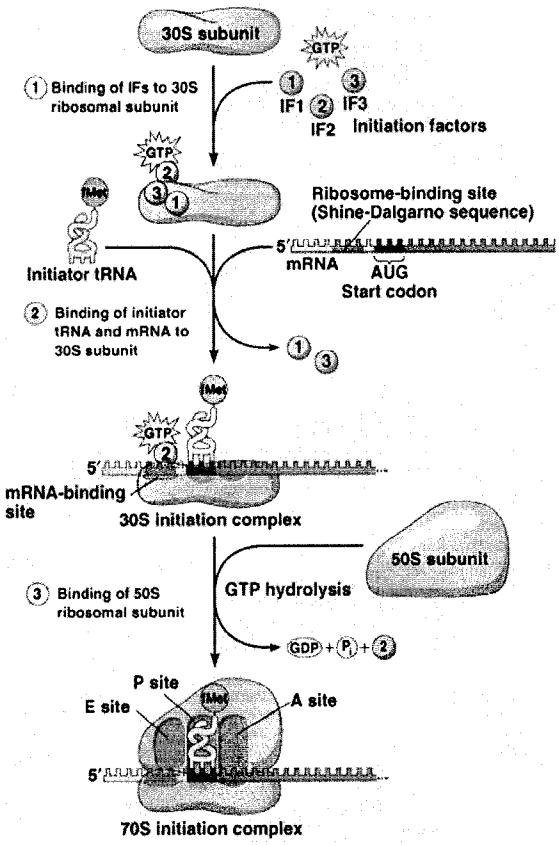

Figure 1.3: Initiation of Translation in Prokaryotes. The depiction shows formation of the 70S initiation complex from ribosomal subunits with the aid of initiation factors. Reproduced from Tortura *et al.* (1).

Translation Initiation

Translation initiation is a vital step in efficient protein synthesis. Selection of the appropriate start codon establishes the correct reading frame, ensuring accuracy of translation. In addition, the "bottleneck" at the initiation step (initation is the rate-limiting step of translation *in vivo*) makes it a prime locus for translation regulation strategies. Prokaryotic translation initiation follows the pathway outlined in Figure 1.3. First, if the ribosome is initiating after a previous round of translation, initiation factor 3 (IF3) associates with the 30S subunit and removes deacylated tRNA and mRNA (12). Next, a new mRNA binds to the 30S subunit, and an interaction between the mRNA Shine-Dalgarno sequence and the anti-Shine-Dalgarno sequence near the 3' end of 16S rRNA helps to place the mRNA start codon (AUG) in the 30S subunit peptidyl (P) site (13,14). Immediately, formyl-methionyl (fMet)-tRNA^{fMet} with a complementary anticodon sequence and in complex with IF2 and GTP binds to the 30S subunit, placing

the initiator tRNA in the P site. Comparatively little is known about the function of initiation factor 1 (IF1), but it seems to stimulate the binding and activity of IF2 and IF3 and helps ensure binding of the initiator tRNA-IF2-GTP complex in the P site before formation of the 70S initiation complex (15,16). Finally, the 50S subunit binds to the 30S initiation complex and induces the hydrolysis of GTP bound to IF2 that aids subunit association and allows the initiation factor to exit the ribosome (17).

Translation Elongation

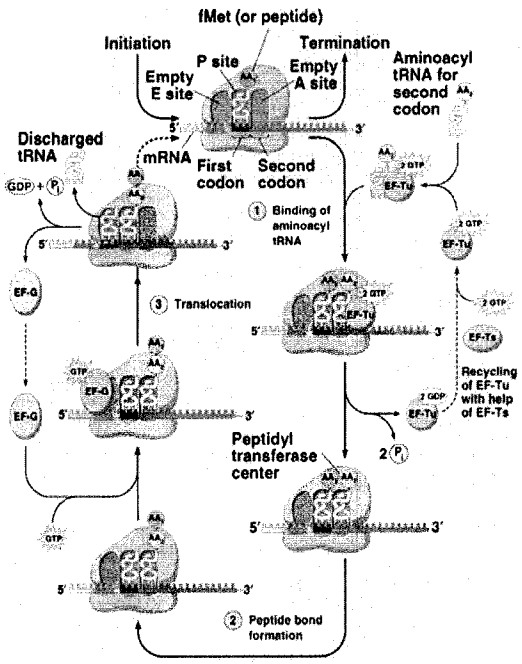

Figure 1.4. Translation Elongation Cycle in Prokaryotes. Depicted is the cycle that adds a single amino acid to the growing polypeptide attached to P site tRNA. Reproduced from Tortura *et al.* (1)

The elongation cycle of prokaryotic translation is shown in Figure 1.4. The process requires three distinct steps: binding of aminoacyl-tRNA, peptide bond formation, and translocation (18). In the first step of elongation, elongation factor Tu (EF-Tu), in a ternary complex with GTP and aminoacyl tRNA, protects the fragile amino acid-tRNA ester link against hydrolysis and delivers the appropriate tRNA to the aminoacyl (A) site of the ribosome in a reaction that is dependent upon the proper matching of the aminoacyl tRNA anticodon to mRNA codon in that site (19,20). Proper codon recognition leads to GTP hydrolysis and the exit of EF-Tu-GTP from the ribosome. In step 2, the aminoacyl end of the A site tRNA is accommodated in the ribosome peptidyl transferase center of the 50S subunit, where the growing peptide on the P site tRNA is

transferred to the amino-terminus of the amino acid attached to the 3' end of the A site tRNA. Recycling of EF-Tu to the ternary complex with GTP and tRNA requires the assistance of a third elongation factor, EF-Ts, that catalyzes removal of GDP bound to EF-Tu, allowing association of a fresh molecule of GTP and binding of a new aminoacyl-tRNA. Finally, in step 3, elongation factor G (EF-G), in complex with GTP, binds to the ribosome and catalyzes the displacement of A site peptidyl tRNA to the P site and P site deacylated tRNA to the exit (E) site where it dissociates. This reaction requires the hydrolysis of the EF-G-bound GTP and ends with the P site tRNA-bound peptide incremented by one amino acid and the A site open for the beginning of another cycle.

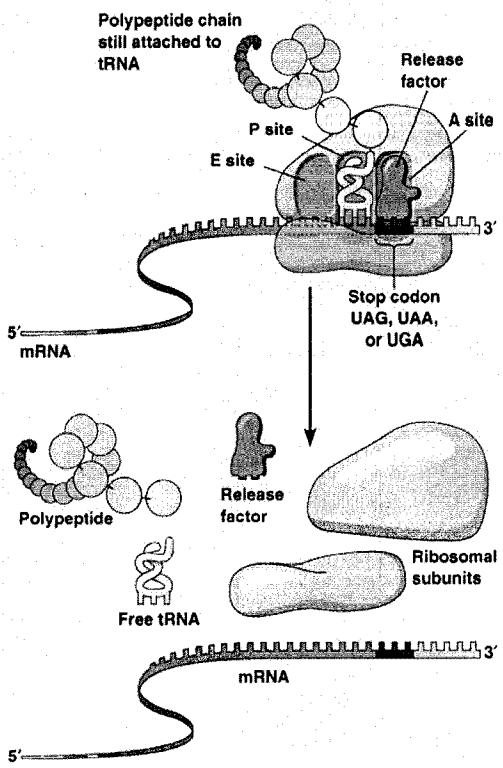

Figure 1.5. Termination of Translation in Prokaryotes. Release of the completed peptide from the ribosome and preparation for re-initiation. Reproduced from Tortura *et al.* (1)

Translation Termination

The last stage of translation, termination, occurs when the ribosome has reached the end of the mRNA and a stop codon resides in the A site on the ribosome. Stop codons include UAA, UAG, and UGA that normally do not specify incorporation of an amino acid as there is no tRNA with a matching anticodon for each (21,22). When the ribosome reaches a stop codon, appropriate release factor (RF) binds (RF1 for UAA and UAG; RF2 for UAA or UGA) binds in the A site of the ribosome and catalyzes hydrolysis of the peptide from

peptidyl tRNA in the P site (22-24). Upon hydrolysis of the peptide, RF3, in complex with GDP, binds to the ribosome. Exchange of bound GTP for GDP on the ribosome induces a structural change in RF3 that catalyzes removal of the bound release factor (not shown) (25). Finally, ribosome recycling factor (RRF), in conjuction with EF-G, induces dissociation of the terminated ribosome into subunits, preparing it for re-initiation (not shown) (26-28).

The amazing degree of conservation in the mechanism of translation and the function of many translation factors in all organisms underlies the central importance of template-driven protein synthesis to all life forms. In fact, of the three major cellular information processing systems; replication, transcription, and translation, translational components have the most universal distribution among Bacteria, Archaea, and Eukarya. Both rRNA and most ribosomal proteins share uncanny conservation in structure and function among the three domains, as well as the elongation factors, tRNAs, and aminoacyl-tRNA synthetases, the enzymes that catalyze attachment of amino acids to the 3' end of tRNAs for incorporation into proteins on the ribosome during translation (29,30).

Translation Factors

It is evident from the descriptions above that translation on prokaryotic ribosomes requires the assistance of many soluble cellular factors (Table 1.1). In fact, eukaryotic translation, especially translation initiation, requires many additional factors compared with translation initiation in prokaryotes. These differences mainly reflect the spatial uncoupling of transcription and translation (transcription in the nucleus and translation in

the cytoplasm) and the necessity for additional levels of temporal and spatial translational regulation in eukaryotes, and not fundamental differences in the translation mechanism. Most of the prokaryotic translation factors have a functional counterpart in eukaryotes (Table 1.1).

Table 1.1. Soluble Protein Factors in Prokaryotic and Eukarytic Translation*

Prokaryotic Factor	*Eukaryotic Factor*	*Function*
Initiation		
IF1		formation of initiation complex
IF2	eIF2	formation of initiation complex
IF3	eIF3,e1F4C	formation of initiation complex
	CBPI	mRNA cap binding
	eIF4A,eIF4B,eIF4F	scanning to start codon
	eIF5	dissociation of eIF2,eIF3,eIF4C
	eIF6	dissociation of large subunit after termination
Elongation		
EF-Tu	eEF1α	binding of aminoacyl tRNA to ribosomes
EF-Ts	eEF1ßγ	recycling of GTP on EF-Tu/EF1α
EF-G	eEF2	translocation of tRNA on the ribosome
Termination		
RF1	eRF1	hydrolysis of completed peptide from tRNA
RF2		hydrolysis of completed peptide from tRNA
RF3	eRF3	removal of release factors from terminated ribosome
RRF		disassembly of ribosome termination complex

*Factor information adapted from Mathews and van Holde (31).

The translation cartoons above outline the immense leaps that have been made in our understanding of the fundamental steps involved in protein synthesis on ribosomes in the last four decades. However, they suggest that the ribosome serves as a passive platform to guide the functions of the factors (tRNA, mRNA, initiation factors, elongation factors, and termination factors) in translation. More and more, ribosome researchers have begun to realize that components of the ribosome, both ribosomal proteins and rRNA, play essential parts in supporting and even catalyzing translation at the molecular level.

Translational GTPases

GTPase or G proteins constitute a highly conserved family of proteins that provide a wide range of important cellular functions in all domains of life. Judging from the conservation of the functional mechanism and core structures of GTPase proteins, it appears that they may have evolved from a primordial precursor ((32) cited in (33)), with an original function probably in translation (34). These ubiquitous proteins have been linked to functions in such diverse cellular processes as membrane signaling pathways (eukaryotes), cell division (all domains), membrane trafficking (eukaryotes), protein secretion (all domains), cell cycle control (all domains), stress response (prokaryotes) and of course, protein synthesis on the ribosome (all domains) (for a recent review see (35)). They belong to a superfamily of cellular NTPases that contain the most common protein fold, and that comprise greater than 10% of the gene products in most cellular organisms (36). Some of the most conserved of the translation factors are the translational GTPases. In prokaryotes they include IF2, EF-G, EF-Tu, and RF3.

What distinguishes GTPase proteins from other cellular proteins is the canonical mechanism governing their function. As suggested by their name, GTPase proteins bind and hydrolyze GTP to regulate cellular functions. These proteins share a conserved GTP-binding or G domain structure. (Figure 1.6) (35). The basic structure of the G domain consists of a mixed six-stranded ß-sheet with five α-helices surrounding. The flexible P-loop of the G domain binds the α- and ß-phosphates of the guanine nucleotide, while residues from the switch I and switch II regions of the domain coordinate the γ-phosphate in position for hydrolysis (34). Local conformational changes in the switch I and switch II regions are magnified and relayed to other domains in the protein to modulate the activity of the protein or its affinity for downstream effectors.

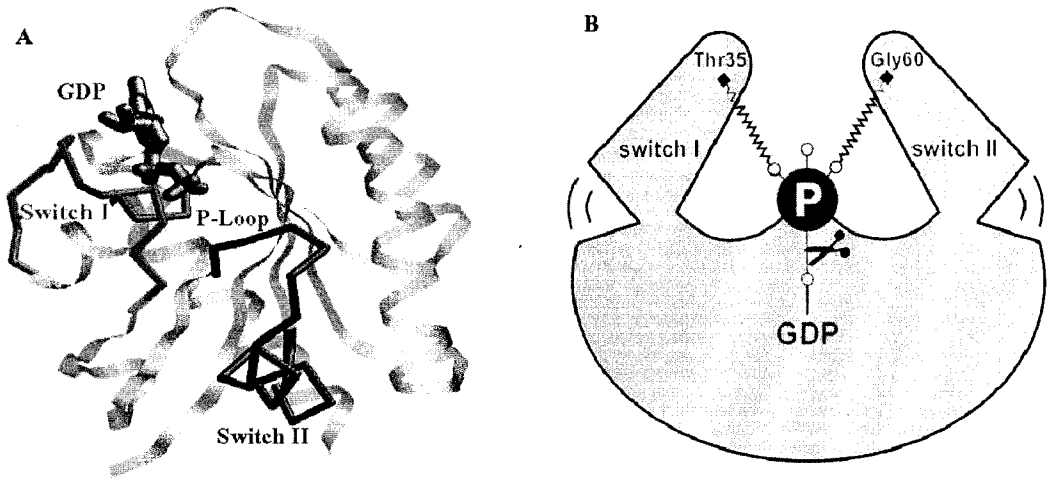

Figure 1.6. G Domain Structure and Diagram. (A) Structure of minimal G domain structure (Ras p21) (7), showing P-loop (red), switch I (dark green), and switch II (cyan). (B) Diagram of GTP "switch" mechanism. Hydrolysis of the γ-phosphate (scissors) allows local conformational change of the coordinating switch I and switch II regions upon phosphate release. Adapted from Vetter and Wittinghofer (10).

Most GTPase proteins have very low rates of intrinsic GTPase activity and require accessory factors, termed GTPase activating proteins (GAPs), for efficient on/off switching (37,38). For many, the mechanism of GTPase activation involves the GAP protein donating residues to the GTPase active site to stabilize the transition state in hydrolysis. Two such examples are the small GTPase proteins Ras and Rho that function in signaling and cell cycle control in eukaryotic cells. For these proteins, GTPase activation requires their respective GAP proteins to donate an arginine residue, termed an "arginine finger," in *trans* to the active site of the GTPase proteins to stabilize a catalytic glutamine residue and to neutralize developing charges in the transition state (39). Still other GTPase proteins, including the G_α subunit of heterotrimeric G proteins involved in signal transduction in eukaryotic cells, do not require insertion of a catalytic arginine, but contain an intrinsic arginine that is stabilized in a catalytically active position by an interaction with regulators of G protein signaling (RGSs). Therefore, the switch from GTP-bound "on" state to GDP-bound "off" state of these G proteins is accelerated by association with the cognate target or downstream effector RGS in a conformation that favors hydrolysis of the bound GTP (40,41).

To switch back to the GTP-bound "on" conformation and finish the GTPase cyle, G proteins must interact with a guanine nucleotide exchange factor (GEF) to dissociate bound GDP and allow GTP binding, or, they must have a significantly higher intrinsic affinity for binding GTP than GDP. The Ras family are examples of GTPases with specific GEFs to facilitate release of tightly bound GDP and replacement with GTP. SOS, CDC25, and Vav proteins are three such protein factors that stabilize the nucleotide-free or intermediate form of Ras proteins to favor exchange (42). For the G_α

subunit of heterotrimeric G proteins, interaction of the ßγ-subunits of the heterotrimer with the G_α subunit at the cell membrane stabilizes binding of GDP and locks the heterotrimer in an inactive state. In this case, extracellular stimulation of a receptor associated with the heterotrimer leads to a conformational change in the heterotrimer that destabilizes the bound GDP and allows exchange for a molecule of GTP (41). Therefore the stimulated receptor serves as an exchange factor.

Several of the translational GTPases differ significantly in the mechanisms for guanine nucleotide exchange. EF-Ts serves as an exchange factor for EF-Tu by binding to the EF-Tu-GDP complex and forcing a conformational change in the G domain that displaces a magnesium ion (43). This bound magnesium ion normally stabilizes GDP in the G domain (44), and its disruption allows GDP to dissociate and to be replaced by GTP to complete the GTPase cycle. EF-Tu with bound GTP assumes a structure that favors binding of aminoacyl-tRNA and formation of the translation competent, EF-Tu:aminoacyl-tRNA:GTP complex (45,46). IF2, EF-G, and RF3 on the other hand, have comparable affinities for GTP and GDP (47-49), allowing unaided reloading of GTP after GTP hydrolysis. This possibly provides a mechanism for sensing the energy state of the cell, with high levels of GTP in the cell leading to maximal cycling of these translation factors.

The translational GTPases share the common structural core and significant sequence homology with both the small GTPase proteins of the Ras superfamily and G_α subunit GTPases (50). For translational GTPases, the GAP or activation effector is the ribosome itself (51-55). Decades of intense research, however, have not revealed an element on ribosomes that is solely responsible for activating any of the translational

GTPases and, therefore, the mechanism by which the ribosome stimulates GTPase activity remains unknown. Researchers have found that the GAP elements probably reside on the large subunit ((56-58), for reviews see (59-61)). In fact, at least four structural features of the 50S subunit have been implicated in GTPase activation: a protein stalk consisting of two dimers of the 12 kDa protein L7/L12 (62-66) (L12 differs from L7 only by having an N-terminal acetylation), ribosomal protein L10 (57,67-69), ribosomal protein L11 (69-71), the L11-binding region of 23S rRNA (70-76), and the sarcin/ricin loop of 23S rRNA (70,72,76-80), so called as it is the target site of the translation inactivation activity of the ribotoxins sarcin and ricin (81).

Researchers have so far been unable to locate a specific catalytic arginine residue on a ribosomal protein that might induce GTPase activation of the translational GTPases. Instead, the mechanism for GTPase activation by the ribosome probably more closely resembles that of the G_α subunits of heterotrimeric G proteins, with elements of the ribosome serving as the RGSs to stabilize the catalytically active state of the G domain. The intrinsic arginine residues of EF-G and EF-Tu that are in homologous positions to those in the active site of G_α subunits are not required for GTPase activity (82,83). Interestingly, a residue 11 angstroms from the bound nucleotide in EF-G of *E. coli.*, arginine-29, was found to be essential for GTPase activity for the factor. A direct role for this residue in catalysis, however, would require an extensive conformational change in the G domain, and a homologous residue is not found in EF-Tu (61). Likewise, no residue that fulfills a role analogous to the intrinsic catalytic arginine of G_α subunits has been found for IF2, and little is known about GTPase activation for this factor (84,85). Still less is known about the GTPase activity of RF3 during translation (47).

As translation is one of the most fundamental cellular processes for all living organisms, it is not surprising that the establishment of the translational GTPases pre-dates the divergence of the bacteria, eukarya, and archaea lineages, and that they were probably the first to develop from a likely universal common ancestor of GTPase proteins (33). EF-Tu, EF-G, IF2, and RF3 all have functional equivalents in eukarya and archaea (see Table 1.1 for eukaryotic equivalents). Therefore, mechanisms for GTPase activation among other GTPase families (Ras and Rho and G_α subunits) probably evolved from or diverged from the original model of translational GTPases.

The Ribosome is a Ribozyme (More or Less)

A clue to the mechanisms of translation may come from the concept of an RNA-centric world pre-dating and serving as an evolutionary intermediate to the DNA-centric world of life forms today. This concept was first put forth by Crick in 1968 upon considering the function of ribosomes in protein synthesis (86), and gained significant support from the discovery of catalytic RNAs or ribozymes in the 1980s (86,87). In the RNA world, RNAs serve as both genetic material and biological catalysts (for reviews and discussion of the RNA world concept see (88-90). Proponents of this model postulate the existence of an early proto-ribosome made up completely of RNA. The active sites of modern ribosomes, those involved in catalysis of peptidyl transferase, in decoding the interaction of the mRNA codon and tRNA anticodon, and in translocation, coordinating the movements of mRNA and tRNA across the ribosome, may have evolved as separate ribozymes with functions outside of translation.

For instance, Poole *et al.* postulate evolution of a proto-ribosome from an early RNA replicase (Figure 1.7) (9). In this model, a proto-16S rRNA decodes the tRNA anticodon and template RNA codon and catalyzes the cleavage and ligation of three ribonucleotides to add to the growing nascent RNA copy strand. Later in evolution, the cleavage and ligation functions would have been lost and decoding of the tRNA and mRNA interaction would remain the function of 16S rRNA.

The interactions and orientation of the aminoacylated tRNA ends and cleavage of the amino acid after ribonucleotide incorporation may have been the purview of a proto-23S rRNA (Figure 1.7). In this case, selection and orientation of the aminoacylated ends of tRNA, amino acid cleavage, and release of deacylated tRNA would have evolved into the peptidyl transferase, tRNA selection, and translocation functions of the large subunit

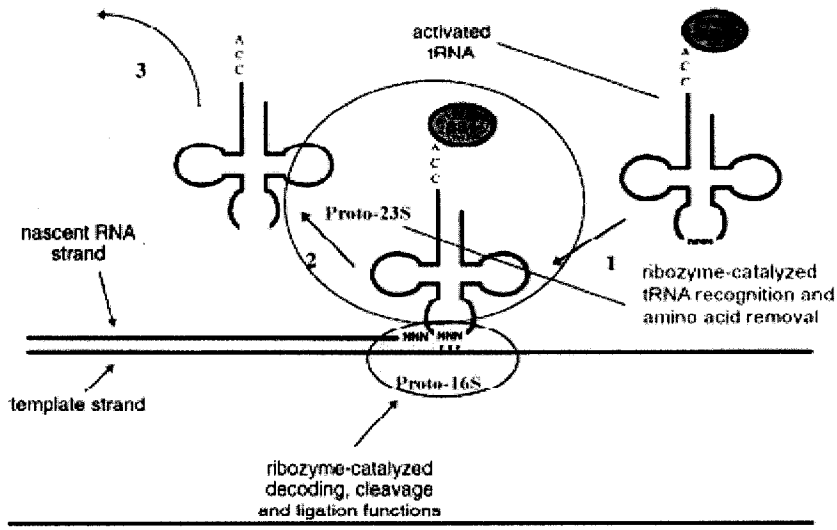

Figure 1.7. RNA Replicase, a Possible Precursor to an RNA Proto-Ribosome. (1) An early tRNA analog, activated by attachment of an amino acid, serves as a carrier for three ribonucleotides in the anticodon position. The attached amino acid provides a tag for the proto-23S rRNA to recognize and orient the tRNA. (2) The proto-16S rRNA decodes matching of the tRNA "anticodon" to the template "codon," and cleavage and ligation adds the ribonucleotides to the growing RNA copy in a manner similar to today's splicing mechanisms. (3) The proto-23S rRNA cleaves the amino acid and the used tRNA is released. Figure adapted from Poole *et al.* (9).

rRNAs seen today. Each of these functional RNAs could have been joined by recombination once replication fidelity could reliably reproduce an entire 23 S rRNA-like molecule.

Of course, the selective pressure to retain the protein synthesis activities of a proto-ribosome would have been the evolutionary advantage of synthesized protein in support of fundamental metabolic processes. At first, simple peptides could have served a supportive role, stabilizing the conformation and increasing the catalytic efficiency of RNA during replication. The first of these catalytic ribonucleoprotein (RNP) enzymes would have been a more efficient and accurate proto-ribosome. This would create a positive feedback mechanism for the production of increasingly functional peptides.

Later, as the synthesized peptides grew in size and complexity, their inherent supremacy for biochemical catalysis would have led to subjugation and possible replacement of the role of catalytic RNAs in cellular functions by protein enzymes (for an in-depth discussion of this progession from an RNA world see (9)).

Given this scenario, and the pre-eminence of protein catalysis in cells today, we might predict that the ribosome would evolve to become a platform of catalytic ribosomal proteins. Protein catalysts have faster turnover and reaction times than ribozymes, and the diversity of the chemical groups on amino acid side chains allows for a wider variety of reaction mechanisms. However, two fundamental characteristics of translation may have prevented complete replacement of catalytic RNAs by proteins in the process (91).

First, protein synthesis is a central process to many metabolic functions in cellular organisms, making it difficult to replace the original components. Second, the improvement on the rates of reactions afforded by protein catalysts is ultimately limited by the rate of diffusion of the substrates, and Graham's Law of Diffusion requires that the diffusion rate is inversely proportional to the square root of the molecular weight of the substrate. Therefore, the rates of the fundamental reactions in translation would be limited by the diffusion rate of the relatively large tRNA and mRNA molecules, reducing the potential rate advantage of protein catalysis.

If translation evolved from an RNA proto-ribosome, therefore, we would predict that the domains of rRNA involved in central functions would be the most conserved features of modern ribosomes. Consistently the most conserved features of rRNAs we recognize today are also those regions that have been linked to functions that are fundamental to translation. These domains were primarily linked to the three basic functions of translation; decoding, peptidyl transferase, and translocation. Below, we briefly review the important functions of these conserved centers, focusing on prokaryotic ribosomes. Little is known about the function of 5S rRNA and, therefore, we will not review this enigmatic molecule here.

16S rRNA

Decoding on the ribosome ensures the accurate selection of an incoming aminoacyl-tRNA into the ribosomal A site by measuring correct Watson-Crick base-pairing between the mRNA codon and tRNA anticodon. To do this, the ribosome recognizes the structural geometry of the Watson-Crick base-pair (92-95). Although some diversity is allowed in the third or "wobble" base-pair (96), this mechanism ensures that only a

correct codon-anticodon base-pair is accepted. The region of the 30S subunit associated with A site tRNA interactions and decoding is referred to as the decoding center (97). The decoding center consists of two short phylogenetically conserved sequences of rRNA at the 3' end of 16S rRNA (Figure 7) around nucleotides 1400-1500

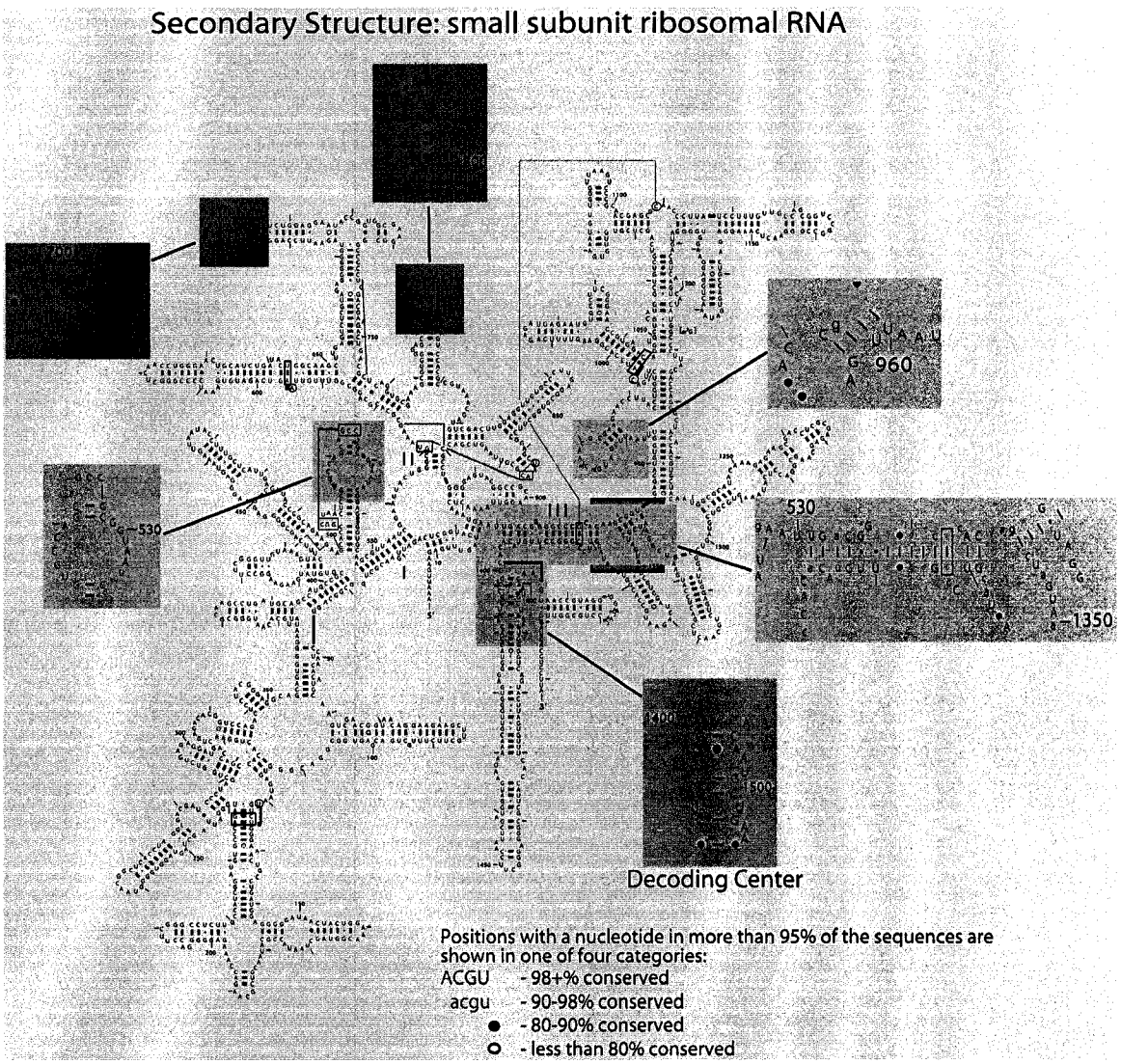

Figure 1.8. Phylogenetic Conservation of 16S rRNA. 16S rRNA regions involved in the decoding function of the ribosome are highlighted in green (the 530 stem-loop and the decoding center). Regions involved in tRNA binding in the P and E sites are highlighted in orange and blue respectively. The highlighted regions are enlarged to show the phylogenetically conserved nucleotides (from analysis of 5591 sequences of Bacteria, Archaea, and Eukarya small subunit rRNA). Structure and analysis from Cannone *et al.* (6).

(Figure 1.8; green box) (97), although at least one nucleotide near a stem-loop including the conserved nucleotide G530 (*E. coli* numbering for rRNA nucleotides will be used throughout this study), has also been implicated (Figure 1.8; green box) (93). Interactions between conserved nucleotides and the codon-anticodon base-pair in the decoding center specifically enhance the stability of tRNA binding and favor selection of cognate over non-cognate or near-cognate base-pairs (92,93). rRNA seems to be the primary component of the decoding site (98), although recent studies have indicated that the "tails" of a few ribosomal proteins may stabilize the binding site (99). Similarly, conserved nucleotides in 16S are involved in the binding of P site and Exit (E) site tRNA as the tRNA traverse the 30S subunit (Figure 1.8; orange and blue boxes respectively), with somewhat more contribution from ribosomal proteins (99,100).

23S rRNA

As with 16S rRNA, 23S rRNA has several phylogenetically conserved regions that have been linked to fundamental functions in translation. Figure 1.9 illustrates the nucleotide conservation among large subunit rRNAs from Bacteria, Archaea, and Eukarya, superimposed upon the 23S rRNA secondary structure of *Escherichia coli*. The phylogenetically conserved regions are highlighted and discussed below.

Peptidyl Transferase

Munro first attributed peptidyl transferase activity to the large subunit of *Escherichia coli* ribosomes in 1967 (101). Although early investigators attempted to find a single catalytic large ribosomal subunit protein, they could only establish that peptidyl transferase activity persists in a complex of 23S rRNA with strictly limited set of ribosomal proteins (reviewed in (102)), resists vigorous procedures employed to remove

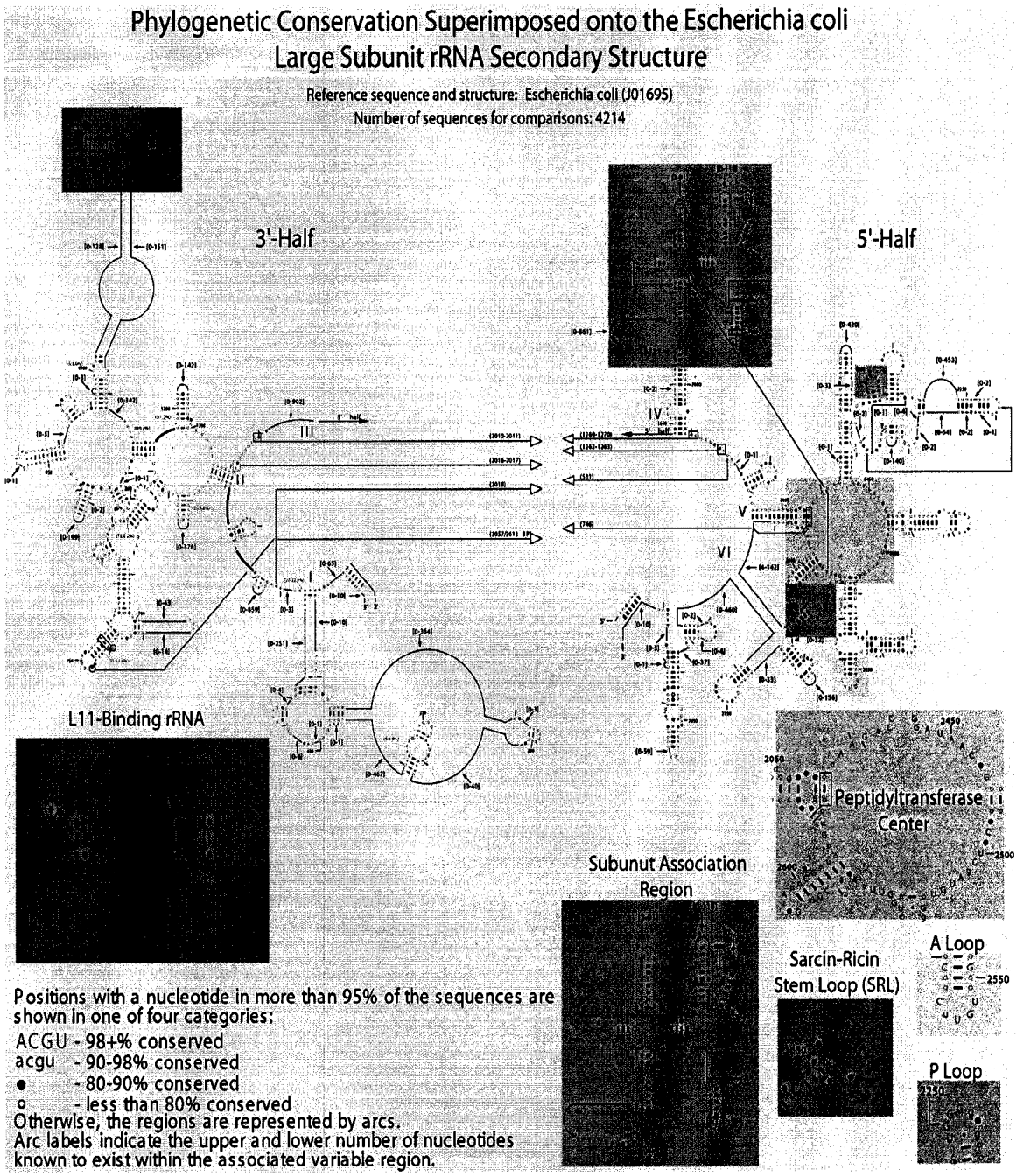

Figure 1.9. Phylogenetic Conservation of 23S rRNA. The figure shows the conservation of nucleotides at equivalent positions in the 3'- and 5'-halves of 23S rRNA for Bacteria (23S), Eukarya (28S + 5.8S), and Archaea (23S) (total of 4214 sequences) superimposed upon the secondary structure of *Escherichia coli* 23S rRNA (figure and phylogenetic comparison adapted from Cannone *et al.* (6)). The most conserved features are highlighted and enlarged in insets for clarity. Dark pink, L11-binding rRNA involved in ribosomal protein L11 binding and factor interactions; dark yellow, subunit association region; light pink, P loop involved in tRNA interactions in the P site; light yellow, A loop involved in tRNA interactions in the A site; light green, sarcin/ricin stem loop (SRL) involved in factor interactions; light blue, the peptidyl transferase region involved in peptide transfer from P to A site tRNA during elongation; orange, site of interactions with E site tRNA.

all proteins from large subunit rRNA (103), and does not reside with any combination of RNA-free ribosomal proteins (cited in (102)). Meanwhile, biochemical evidence mounted implicating rRNA in the reaction. Several groups provided evidence for specific cross-linking between derivatived aminoacyl moieties attached to the 3' (acceptor) end of tRNA and 23S rRNA when the tRNA was bound to the A or P sites of ribosomes (104-107). Later, chemical modification protection experiments also revealed 23S rRNA as part of the tRNA ribosomal binding sites (108). Finally, the binding sites and resistance mutations for antibiotics that affect peptidyl transferase and/or tRNA binding on the large subunit map virtually exclusively to 23S rRNA residues (for reviews see (109-112)). The experiments described above consistently linked nucleotides in domain V of 23S rRNA (Figure 1.9) to peptidyl transferase and interactions with A and P site tRNA. One element of this domain, termed the peptidyl transferase center (Figure 1.9; light blue square) includes a large central loop that contains most rRNA nucleotides associated with peptide transfer catalysis and resistance mutations to inhibitors of peptidyl transferase (113). Adjacent to the peptidyl transferase center are the A and P loops (Figure 1.9; light yellow and rose squares respectively), two 23S rRNA elements linked to interactions of the 3'-aminoacylated and 3'-peptidyl ends of tRNA in the A and P sites respectively ((108,114-118) and for review see (100)).

Subunit Interface

Another conserved feature of the 23S rRNA, a region encompassing domain IV (Figure 1.9; dark yellow box) also forms part of the interaction sites for tRNA on the 50S subunit (115). This region maps to the large and small subunit interface (99,119,120) and its has been suggested that it may either help maintain the accuracy of tRNA selection or

be involved in translocation of tRNAs by serving as a communication pathway between the decoding center of 16S rRNA and the peptidyl transferase center (99,119).

Sarcin/Ricin Stem-Loop

The sarcin/ricin stem-loop (SRL) is one of the most conserved sequences of rRNA on ribosomes from all domains of life (Figure 1.9; dark green box), and gets its name from being the site of activity of two ribotoxins, α-sarcin and ricin. α-Sarcin is a cytotoxic protein secreted by filamentous fungus that hydrolyzes the phosphodiester bond on the 3' side of G4325 (the equivalent is G2662 on *Escherichia coli* 23S rRNA) in the 28S rRNA of eukaryotic ribosomes (81), inhibiting protein synthesis on eukaryotic prokaryotic ribosomes (121). Although the affected rRNA sequence is nearly universally conserved between 23S rRNA of Bacteria and Archaea, and 28S rRNA of Eukarya, cleavage of 23S rRNA in bacterial ribosomes requires concentrations of α-sarcin an order of magnitude higher, and inhibition of protein synthesis is significantly reduced (81). Ricin and related cytotoxins from plants inactivate eukaryotic ribosomes by hydrolyzing the *N*-glycosidic bond of A4324 (the equivalent position is A2661 on *Escherichia coli* 23S rRNA), resulting in depurination of the residue on rRNA (122). These toxins are inactive against bacterial ribosomes, but hydrolyze the equivalent residue in 23S rRNA stripped of ribosomal proteins (123). Also from the ricin group are the Shiga toxins from bacteria with similar activities (124).

Both α-sarcin and ricin-related ribotoxins inhibit peptide chain elongation on affected ribosomes, and studies of their activities have shed light onto the function of the SRL in translation. For instance, the activity of both ribotoxins inhibits EF-1α (the eukaryotic equivalent of EF-Tu in bacteria)-dependent binding of aminoacyl-tRNA to

elongating ribosomes (125,126), and the activity of both inhibits ribosomal binding of EF-2 (EF-G in bacteria) (126,127). Furthermore, binding of elongation factors of both eukaryotes and prokaryotes has been localized to the SRL (72,128,129). In addition, mutational studies have identified specific nucleotides in the SRL associated with factor interactions (78,79,130-132) and led to the suggestion that the SRL may undergo a functionally-important conformational change during translation (133,134).

L11-Binding rRNA

The L11BR is not only the site of ribosomal protein L11 binding, but also has been linked to interactions with both elongation factor complexes (71,72,76,80,135); the tRNA:GTP:EF-Tu (EF-1α in eukaryotes) complex that brings aminoacyl-tRNA to the empty A site, and the GTP:EF-G (EF-2 in eukaryotes) complex that catalyzes translocation of the P site, deacylated and A site peptidyl (after peptidyl transferase) tRNA's to the E site and P site, respectively, during elongation.

The L11BR shows high phylogenetic conservation (Figure 1.9; dark rose box) and folds into a distinctive tertiary structure (Figure 10) that brings the two distal stem-loops within the domain into close proximity (8,136). Structural studies on a fragment of the L11BR indicated that this tertiary structure is formed by conserved interactions of bases between the stem-loops (for example the base triples; G1056:U1082:A1086, C1100:G1091:G1071, and G1099:C1092:C1072) (136-139), and that the structure is stabilized by the binding of L11 (136,140). Foot-printing L11 on the L11BR detected binding of the protein only in the minor groove of the stem-loop that includes nucleotide A1067 (Figure 1.10) (141), however, and the protein does not appear to contact the

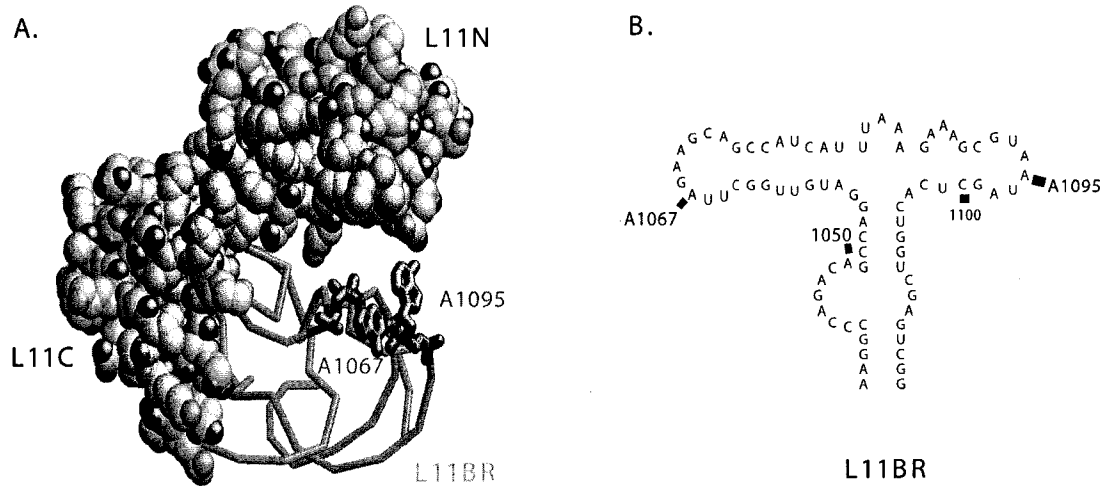

Figure 1.10. Tertiary and Secondary Structure of the L11-Binding rRNA. (A) Tertiary structure of the a fragment of L11 bound to the L11-binding rRNA (8). (B) Secondary structure of the L11-binding rRNA (6). L11N, N-terminal domain of L11; L11C, C-terminal domain of L11; L11BR, L11-binding rRNA.

nucleotides involved in the conserved interactions (8,136). Interestingly, binding of the antibiotic thiostrepton to the L11BR stabilizes the same structure of the rRNA (137,139,142), although it does not bind to a site overlapping that of L11 (142,143). These studies led to the hypothesis that this inherently unstable rRNA structure may cycle between distinct conformations during translation, and that binding of thiostrepton may "trap" the rRNA in a particular conformation, preventing a functionally important transition (137,138). In fact, studies of the ribosome interactions and activity of the antibiotic thiostepton were the first to implicate the L11BR of rRNA in translation functions.

Ribosomal Protein L11

Suggestions of the importance of the rRNA to such conserved activities of the ribosome as decoding, peptidyl transferase, and translocation begs the question, "What is the function of the ribosomal proteins?" Perhaps the proteins serve as somewhat inert molecular scaffolding that holds the rRNA in the appropriate position and orientation for catalytic activity. Perhaps the proteins serve to fine-tune the central functions of translation that developed on a proto-ribosome. In fact, structural evidence from recent x-ray crystallographic and cryo-electron microscopic studies of prokarytotic ribosomes and ribosomal ligands, as well as volumes of historical biochemical evidence, suggest ribosomal proteins have a direct role in many important ribosomal activities. Documented functions include forming part of the exit site for deacylated tRNA binding just before it is ejected from the ribosome (144), gating the exit tunnel where the growing peptide leaves the large subunit (145), helping to check the accuracy of tRNA selection during decoding (146,147), and determining the position, timing, and affinity of translation factor interactions with the ribosome (61,71,148,149).

Ribosomal protein L11 is another example of a protein that plays a significant role in ribosome functions. Past studies on L11-deficient ribosomes implicated the protein in binding of EF-G on the ribosome (150,151) and EF-G-coupled GTPase activation (69). Cross-linking and biochemical studies linked L11 to RF-1-mediated translation termination (152-154) and guanosine pentaphosphate (pppGpp) synthesis by the stringent factor, RelA, during the stringent response to amino acid starvation in bacteria (155-157). L11 has two domains (158) (Figure 10), a C-terminal domain (approximately 75 amino acids) that mediates binding to the L11BR (136,142), and an N-

terminal domain (approximately 65 amino acids) that associates only loosely with rRNA (8,136). The C-terminal domain not only anchors L11 on the ribosome, but also stabilizes the tertiary structure of the L11BR (140,159). Alternatively, the N-terminal domain mediates interactions with stringent factor (157) and RF-1 (152-154).

Little is known of the molecular mechanisms involved in L11 mediation of factor interactions and coupled GTPase activation. L11 may affect factor interactions and GTPase indirectly by stabilizing the proper conformation of the L11BR, or directly by forming part of a GTPase activation domain on the ribosome. A cryo-electron microscopy study recently suggested that the N-terminal domain of L11 may be flexible, reversibly dissociating from the L11BR to interact with the GDP:EF-G complex in a translation step following coupled GTP hydrolysis (71).

Thiostrepton

Thiostrepton is a multicyclic thiopeptide antibiotic produced by *Streptomyces sp.* that binds to ribosomes with high affinity and disrupts translation. Although thiostrepton is known to affect reactions during the elongation steps of translation, the molecular basis for its inhibition is uncertain. Previous studies have reported that thiostrepton inhibits IF2-dependent P site binding of fMet-tRNA^{fMet}, EF-Tu-dependent A site binding of aminoacyl-tRNA, and EF-G-dependent translocation on the ribosome (160-164). However, conflicting studies have shown that the ribosome-dependent GTPase activities of the three factors are alternatively inhibited (164-166), unaffected (60,167), or even stimulated (166,168) by the presence of the antibiotic. These results can be reconciled if the presence of thiostrepton induces changes on the ribosome that inhibit productive ribosome binding for some factors prior to GTPase activation and that prevent an

important post-GTPase function on the ribosome for others (for a discussion see (166,168,169)).

Studies of the binding of thiostrepton and L11 to the L11BR have suggested several possibilities for the role of this domain in translation and the inhibition by thiostrepton. Weisblum and Demohn first recognized 50S subunits as the site of action of thiostrepton translation inhibition (170), and it was later discovered that L11 was necessary for thiostrepton binding to ribosomes and absent in resistant mutants (171,172). Evidence for the involvement of rRNA in binding thiostrepton came from studies of the resistance mechanisms of *Streptomyces sp.* In each case, resistance was conferred by the action of an RNA-pentose methylase that methylates one residue (A1067 in *Escherichia coli*) in the L11BR, rendering ribosomes refractory to thiostrepton binding (173,174). In addition, mutation of A1067 or equivalent to G, C, or U severely reduced the efficacy of antibiotic inhibition (175).

Thiostrepton binds to a complex of 23S rRNA and L11 with high affinity. However, binding to 23S rRNA alone is orders of magnitude lower (175,176), suggesting the necessity of both ribosomal components for binding. Foot-printing of thiostrepton on 23S rRNA by chemical probing (143) and structural studies on a complex of the L11BR fragment and L11 (8,136,137,139,142) suggested that thiostrepton probably binds in a cleft formed between the the rRNA and the N-terminal domain of the protein, and that the tertiary structure of the L11BR is inherently unstable. Based on these results, the authors postulated that thiostrepton binding to ribosomes inhibits translation elongation either by steric hindrance of elongation factor binding or by preventing a conformational change in

the L11BR/L11 complex that is necessary for steps in elongation (discussed in (137) and (8)). This intriguing possibility is investigated in the research presented in this study.

Structural Studies on Prokaryotic Ribosomes

X-Ray Crystallography

Thus far, a thorough understanding of the mechanisms of ribosome function at the molecular level has not yet been attained, and researchers are employing a battery of techniques to improve our understanding of ribosome structure at greater resolution. For instance, remarkable advances have been made in the last two decades in the analysis of ribosomes using biophysical techniques such as x-ray crystallography and cryo-electron microscopy. The relatively large size of the ribosome macromolecular complex (~2.5 MDa), previously an impediment to x-ray crystallographic techniques, is increasingly being overcome by new methods of crystal generation, by the availability of high energy x-ray sources (synchrotron radiation), and by improvements in the collection and analysis of x-ray diffraction data to resolve structures (177). As a result, relatively high resolution structures of the entire 70S ribosome from the thermophilic bacterium, *Thermus thermophilus* (99,178), of the 50S subunits from the archaea, *Haloarcula marismortui* (179) and the mesophilic bacterium *Deinococcus radiodurans* (180), and of the 30S subunits from *Thermus thermophilus* (144,181) have recently become available that greatly increase our understanding of protein synthesis at the molecular level.

Cryo-Electron Microscopy

Ribosome researchers have also used cryo-electon microscopic techniques successfully for structural analysis of functional ribosome complexes, albeit at lower resolutions than for x-ray crystallography. Cryo-electron microscopy allows the study of

ribosomes in conditions that are more physiological than those in x-ray crystals, and the ribosome complexes can more easily be "frozen" in functional states while associated with mRNA, tRNA, and translation factors, allowing the dissection of "snapshots" in the stages of translation. Improved methods for freezing particles and of computational techniques for single-particle reconstruction from multiple electron diffraction images have recently led to the possibility of imaging of particles at unprecedented resolutions (182). By analyzing low resolution (10-20 Å) cryo-electron images of functional ribosome complexes in relation to higher resolution x-ray crystallographic structures from related organisms, investigators have been able to accurately identify the positions on ribosome reconstructions of rRNA, ribosomal proteins, and factors interacting with ribosomes in functional complexes.

Cross-linking

Biochemical approaches to ribosome structure analysis have also provided valuable insight into ribosome function. One method widely used to identify the positions of ribosome components and interacting factors is to chemically cross-link those features that are proximal in tertiary structures. Cross-linking is commonly induced by treatment of ribosomes with ultra-violet radiation, by treatment of ribosomes with chemical cross-linking reagents, or by introduction of tethered cross-linking reagents at specific positions on rRNA, ribosomal proteins, or ribosome ligands. For instance, chemical cross-linking of ribosome constituents has enabled researchers to evaluate the proximity and dynamics of rRNA domains and of rRNA and ribosomal protein in the ribosome (for a review see (183)). Cross-linking ribosome ligands in functional ribosome complexes has identified ribosomal components interacting with mRNA (184-

190), tRNA (191-196), and translation factors (24,197-202). In addition, DNA oligonucleotides, complementary to stretches of rRNA and derivatized with photolabile cross-linking agents, have been hybridized to ribosomes and were used to identify ribosomal proteins and regions of rRNA proximal to the hybridized probe (203-207).

Cross-linking studies have the advantage of directly identifying regions of proximity between ribosomal components or between the ribosome and interacting factors, as the cross-linked molecules must lie within the range of the reactive group. However, the low efficiency of cross-linking often requires the use of relatively high levels of interacting ligands to increase the level of occupancy, making the technique susceptible to the detection of artifacts due to occupancy of non-specific sites.

Chemical and Enzymatic Probing

Structural probing using chemical and enzymatic reagents has also been useful for structural studies on ribosomes. Enzymatic nucleases such as RNase T1, U2, and RNase V1 have different specificities for hydrolysis of RNA structures (see (208,209) for reviews of RNases and methods) and, therefore, they have been used extensively to probe both the secondary structure of rRNA and to identify rRNA domains protected from their activity by interactions with ribosomal proteins (210-213), translation factors, and tRNAs.

The use of chemical modification reagents, including dimethyl sulfate (DMS), 1-cyclohexyl-3-(2-morpholinoethyl)-carbodiimide-*p*-toluene sulfate (CMCT), 2-keto-3-ethoxybutyraldehyde (kethoxal), and diethylpyrocarbonate (DEPC), that modify specific positions on the nitrogenous bases of nucleic acids, to probe RNA structure and interactions with proteins was pioneered by Peattie (214,215) and has been used to study

ribosome structure extensively by both Garrett and Noller. The principle is simple. Changes in the position or extent of chemical modification of the RNA bases under different probing conditions or in the presence of potential ligands represents a change in the structure of the RNA or "protection" of the RNA base by interaction with a ligand. These methods have been used in the past to identify rRNA regions protected by the binding of ribosomal proteins (137,212,213,216-219) and to "foot-print" the protection of rRNA by tRNA (108,115-117,220-222), mRNA (223), and translation factors (72,224-228) on ribosomes. RNase and chemical modification methods are limited, however by the availability and reactivity of RNA or specific bases in the native structure of the RNA, and changes in reactivity due to direct interactions or to indirect changes in rRNA conformation cannot be easily distinguished.

Chemical Nucleases

Alternatively, the category of nucleic acid probes known as chemical nucleases, that includes such commonly used metal coordinating complexes as ethylene-diaminetetraacetic acid (EDTA):Fe^{2+}, metalloporphyrins, and 1,10-ortho-phenanthroline:Cu^{2+}, cause lesions in the nucleic acid backbone by oxidative attack on the ribose or deoxyribose primarily, or, less frequently, on the nitrogenous base. Strand scission from oxidative attack makes the lesion more readily detectable than chemical modification, and is not limited to specific nucleobases positions. However, the principle for probing RNA structure and interactions is the same as for chemical modification techniques.

Diffusible hydroxyl radicals, generated from the oxidation of EDTA-chelated Fe^{2+} in the presence of hydrogen peroxide (modified Fenton reaction), cleave the nucleic acid

backbone by abstracting a hydrogen atom from the ribose or deoxyribose C_4' carbon primarily, leading to rearrangement, elimination, and scission (see Appendix B for background on metal complex cleavage) ((229) and references therein). The radicals produced induce cleavage of double or single stranded cleavage without preference for the base at each position. However, cleavage is attenuated when the backbone is shielded by contact with other macromolecules or by the tertiary structure of the nucleic acid.

EDTA:Fe^{2+} probing has previously been used with great success in by Noller *et al.* to elucidate structural and mechanistic features of the ribosome. Tethered cleavage from ribosomal proteins, tRNA, and translation factors localized their interactions to regions of rRNA in the 70S ribosome (see (100,230) for reviews). To identify proximal regions of rRNA, Noller and co-workers tethered EDTA:Fe^{2+} directly to an interruption in the rRNA backbone (231). These studies illustrate the power of chemical nucleases for elucidating rRNA structure.

Experimental Stategy

The aim of the first part of this study was to identify elements of rRNA in the large subunit of the prokaryotic ribosome that are proximal to the sarcin/ricin stem-loop (SRL). As discussed above, both the L11BR and SRL domains have previously been linked to binding and GTPase activity of elongation factors on the ribosome. In fact these two components, along with a pentameric complex including ribosomal protein L10 and two dimers of proteins L7 and L12 (L10.$(L7/L12)_2$) that forms a protein stalk on the 50S subunit (232,233), are referred to as the GTPase-associated region (GAR) due to their involvement in factor interactions and GTPase activation (8). Some circumstantial evidence also linked the SRL directly with the L11BR. For instance, the initial binding

of thiostrepton to ribosomes prevents the rRNA hydrolytic activity at the SRL (234), and the activity of α-sarcin and ricin at the SRL cause structural changes at the L11BR (235). Therefore, we postulated that the two regions, distal in the secondary structure of 23S rRNA (Figure 8), may be proximal in the tertiary structure of the 50S subunit. Alternatively, the two regions might be distal in the tertiary structure and affect translation by interacting with distinct domains of the translation factors. To test our prediction, and to characterize the rRNA environment surrounding the GAR, we designed a system to localize a chemical probe to a specific position within the functional domain. The results of our probing studies suggested that the SRL and L11BR are indeed proximal on the 50S subunit of prokaryotes and also revealed several additional elements of rRNA proximal to the SRL. These results preceded the publication of high resolution x-ray crystal structures of the large subunit (179,180) that confirmed the proximity of the same elements.

The location of the chemical cleavage in the L11BR, proximal to the known binding site of the antibiotic thiostrepton, prompted us to ask if binding of the antibiotic might change our cleavage results. Our studies revealed that rRNA cleavage in the L11BR from the SRL-bound oligonucleotide were severely attenuated in in the presence of thiostrepton. As the cleavages were not localized to the thiostrepton binding cleft, they could not be explained as direct steric protection from the bound antibiotic.

Building on the results of our probing studies, we next sought to further elucidate the potential conformational change identified in the L11BR. The aim in the second part of this study (Chapter 3) was to identify the structural changes in the L11BR associated with thiostrepton binding. As discussed above, thiostrepton is believed to bind in a cleft

between the L11BR and L11. Therefore, we hypothesized that antibiotic binding might "trap" a conformation of the rRNA within the L11BR that would explains its effects on translation. Alternatively, the effects of thiostrepton binding might be localized to the binding site, directly preventing the association of translation factors, or antibiotic binding might induce a conformational change in ribosomal protein L11 that protects the affected region of L11BR from oligonucleotide-directed cleavage from the SRL.

As ribosomal protein L11 also binds in the L11BR and is known to regulate its structure, we also sought to characterize the structural changes in the L11BR that accompany mutations in L11. We chose to probe the L11BR structure on ribosomes that were isolated from a strain of *Escherichia coli* that had the chromosomal gene for L11 knocked out. To further elucidate the role of L11 we also probed, with or without thiostrepton present, isolated ribosomes from the L11 knockout strain with the C-terminal domain of L11 or the entire protein (as a control) supplied by expression from an inducible plasmid *in vivo*. Binding of the C-terminal domain of L11 is thought to stabilize the structure of the L11BR, but the function of the N-terminal domain of the protein is largely unknown. Therefore, we hypothesized that the absence of the entire protein would cause a dramatic destabilization of the rRNA in the L11BR, while the absence of only the N-terminal domain would have less significant effects. Alternatively, the structure of the L11BR might be stabilized by surrounding elements of the ribosome, and binding of L11 in this domain might position the protein for a functional role in translation.

From these studies, we found that thiostrepton binding induces structural changes in the L11BR outside of the antibiotic binding site, suggesting that the antibiotic indeed

induces a distinct structure of the L11BR. In addition, the results indicated that the structure of the L11-binding rRNA becomes fully conformationally flexible when ribosomes lack the entire L11 protein, but not when ribosomes lack only the N-terminal domain. The effects of the absence of the N-terminal domain of L11 were localized to only a few residues on the surface of the L11BR, suggesting that this domain is only loosely associated with the rRNA.

Our use of the L11-mutant ribosomes for structural studies presented the opportunity to help understand the function of this phylogenetically conserved ribosomal protein during translation. Our aim was to decipher the particular effects of the L11 mutations on translation functions. A review of past research allowed us to formulate several hypotheses to explore with functional studies. Based on the inhibitory effect of the absence of the equivalent ribosomal protein (BM11) in thiostrepton-resistant mutants of *Bacillus megaterium*, we postulated that ribosomes from *Escherichia coli* mutants lacking L11 would be severely inhibited in *in vitro* translation relative to wild type ribosomes. Similarly, we expected that mutant ribosomes with only the C-terminal domain of L11 would suffer significant decreases in translation efficiency. Therefore, simultaneous to our structure probing, we performed *in vitro* translation tests. We found that *in vitro* translation on mutant ribosomes lacking L11 was severely inhibited, while only moderate inhibition was noted for ribosomes lacking the N-terminal domain of the protein. N-terminal domain mutants of L11 were specifically inhibited in the function of EF-G during the elongation phase of translation, while mutants lacking the entire protein were inhibited in both the functions of EF-G and EF-Tu during this phase. These results led us to compare the binding of translation factors to L11-mutant ribosomes and to

compare the efficiency of the hydrolysis of GTP by EF-G on mutant and wild type ribosomes. The results of these studies provided evidence that suggests that the entire L11 protein and, therefore, the structure of the L11BR is necessary for the functions and interactions of the elongation factors with the ribosome. In addition, the absence of the N-terminal domain of L11 inhibits the GTPase activity of the EF-G associated with ribosome interactions.

CHAPTER 2

Proximity of Elements of the GTPase-Associated Region on the Large Subunit of Prokaryotic Ribosomes

Introduction

The sarcin/ricin stem-loop (SRL), around nucleotides 2647-2674 (*E. coli* numbering), is involved in interactions with the elongation factors EF-G and EF-Tu during translation on the ribosome (72). The nuclease activity of the ribotoxin α-sarcin and the N-glycosidic activity of the ribotoxin ricin in the terminal loop of the SRL prevent association of these factors with the ribosome and inhibit factor-dependent steps in translation (236). Together with ribosomal proteins L7/12, L10, L11, and the L11-binding region of 23S rRNA, the SRL forms the factor binding and GTPase-associated region (GAR) on the 50S subunit of prokaryotic ribosomes. Because each of these components is involved in factor binding and/or GTPase activation, we hypothesized that they form a functional unit with elements that are close in the tertiary structure of the ribosome. To test this hypothesis, we utilized a chemical nuclease, the 1-10-orthophenanthroline:Cu^{2+} complex, which was chemically tethered to a DNA oligonucleotide probe with base complementarity to the SRL. After hybridizing the probe to the SRL, we induced chemical cleavage of surrounding rRNA to identify those regions that were within the reach of the tethered nuclease.

As the L11-binding rRNA region (L11BR) has also been implicated in factor interactions on the ribosome, we hypothesized that this region would be proximal to the SRL in the tertiary structure of the large subunit. Alternatively, these regions may be distal in the tertiary structure of the ribosome and affect factor interactions with distinct domains of the elongation factors. Upon scanning the length of the 23S rRNA for chemical cleavage from the hybridized probe we indeed found evidence for cleavage of

the L11BR. In addition, we identified two elements, the 2530 stem-loop and the 2750 stem-loop regions, that were proximal to the SRL. Interestingly, when we added thiostrepton, an antibiotic known to bind in the L11BR, we found that the chemical cleavage induced from the SRL was attenuated, suggesting that binding of this antibiotic may induce a significant conformational change in the region. Our results brought new insight to the structure of the factor binding region of the ribosome and suggested an inherent flexibility of the rRNA in this region.

Phenanthroline:Cu Mediated Cleavage of Nucleic Acids

The nucleotytic activity of the redox-active phenathroline:Cu^{2+} (OP:Cu) coordination complex against DNA was first discovered in 1979 (237). Since that time, similar nucleolytic activity of a significant number of synthetic coordination complexes, such as the ethylenediaminetetraacetic acid (EDTA):Fe^{2+} complex and the porphyrin:Ni^{2+} complex have been described (for a review of chemical nucleases see (238)). Cleavage of the DNA or RNA by the OP:Cu complex occurs if the copper component is present in the complex as an highly oxidized species (229). This is accomplished in a series of steps.

First, Cu^{2+} in the complex is reduced to Cu^{+} by the addition of a reducing agent to the solution (commonly mercaptopropionic (MPA) or ascorbic acid are used). Next, association of the phenathroline moiety with the nucleic acid localizes the complex to the target DNA or RNA, preventing unproductive quenching of the reactive species by buffer components and placing the Cu species in correct position and orientation to induce scission of the nucleic acid. Association of the complex with nucleic acids can occur in two ways. For double stranded DNA, a reduced *bis* phenanthroline-copper complex

$((OP)_2Cu^+)$, with two molecules of phenanthroline coordinating one copper ion (Figure 2.1) docks in a non-intercalative manner into the minor groove of the B-form DNA helix. For RNA, the minor groove of the A form helix in single or double stranded RNA is too shallow for docking of phenanthroline and, therefore, the phenanthroline-copper complex is believed to intercalate between nucleobases in a single-stranded region that is strained

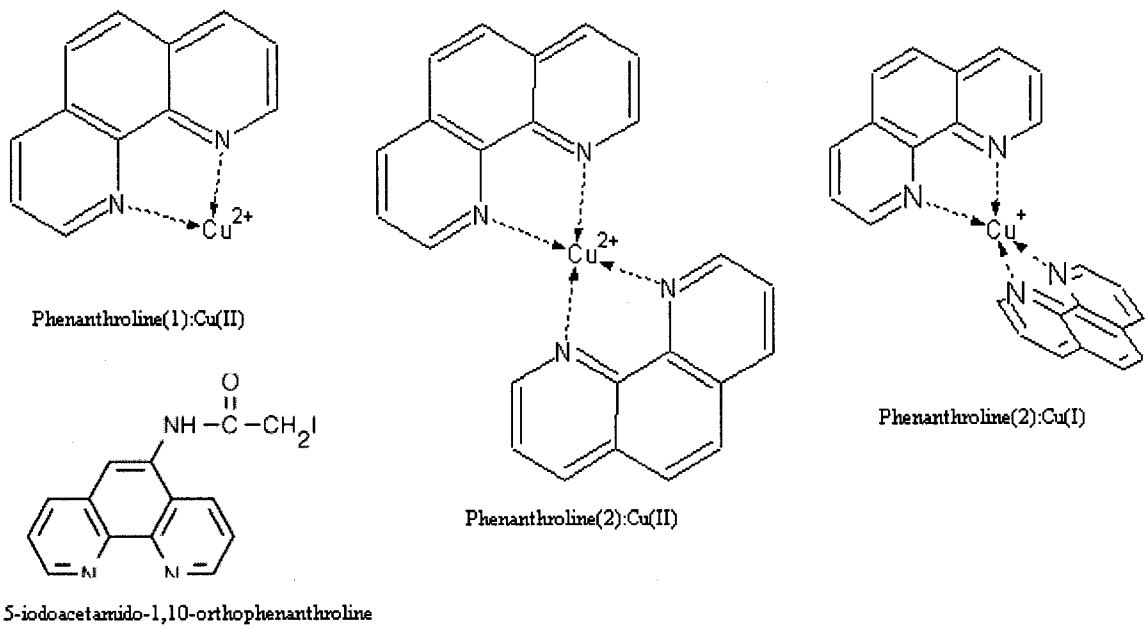

Figure 2.1. Structure of Phenanthroline and Complexes with Copper. The illustrations show the three different coordination complexes of phenanthroline and copper as well as the molecule (5-iodoacetamido-1,10-orthophenanthroline) used to tether phenanthroline to biomolecules. The phenathroline(2):Cu(II) complex shows a square-planar coordination while the phenanthroline(2):Cu(I) complex shows a tetrahedral coordination configuration.

or bulged enough to accommodate it (239,240). In the last stage of OP:Cu-mediated cleavage of nucleic acids, hydrogen peroxide, either produced endogenously from the reduction of Cu^{2+}, or added exogenously during the reaction, oxidizes the Cu^+ component to a highly reactive copper-oxo species such as $[CuO]^+$, $[CuOH]^{2+}$, or CuO_2H (229). It is

this species that abstracts a hydrogen atom from the ribose (primarily C_1' hydrogen) or deoxyribose (primarily C_2' hydrogen) in the minor groove. Figure 2.2 shows the postulated mechanism for cleavage of RNA by phenanthroline:Cu^{2+}. Abstraction of the hydrogen atom generates a ribose-centered radical that is then oxidized by the bound cupric complex to form a carbocation, followed by rearrangement and elimination to produce the free base, 5-methylenefuranone, and free 5'- and 3'-phosphate termini.

When phenanthroline is tethered to a biomolecule for probing as in the present study, it is generally utilized as the mono complex, with one phenanthroline molecule tethered to the biomolecule and coordinating a copper ion (Figure 2.1). This form has been found to be the most efficient for cleavage of RNA, possibly due to the preference

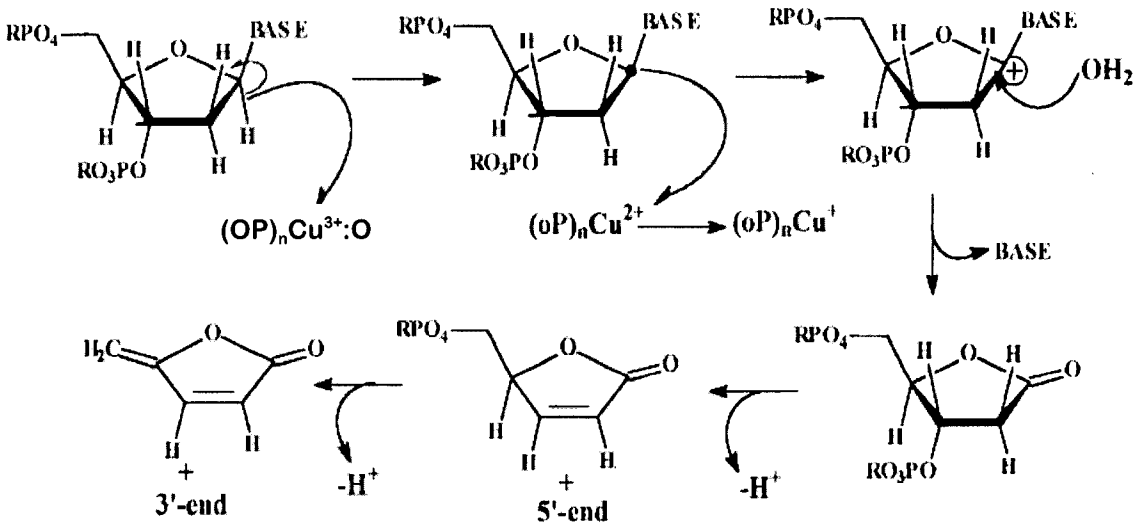

Figure 2.2. Mechanism of Cleavage of RNA by Phenathroline:Copper ($(OP)_n$) (3). The proposed reaction products are the free base, the cyclic lactone (5-methylenefuranone), and the 5'- and 3'- phosphate termini.

for intercalative binding rather than for association with the minor groove of DNA (240,241).

Complementary DNA Probe-Directed Phenanthroline:Cu Cleavage of 23S rRNA

Phenanthroline:Cu cleavage has become an important tool for elucidating the translation machinery at the molecular level. The free phenanthroline:Cu^{2+} complex has previously been used in structural studies of both tRNA and rRNA. Hermann and Heumann used the *bis* complex, consisting of two 1,10-*o*-phenanthroline molecules coordinating a single copper ion, to obtain structure and distance information between nucleotides in folded tRNA-Phe (242). In the Hill lab,tethered phenanthroline has previously been used as a tool for identifying the interactions of important factors with the ribosome. For instance, mRNA and tRNA were synthesized with a single 4-thiouracil at specific positions to serve as sites to attach 5-iodoacetamido-1,10-phenanthroline (5IOP) and probe the proximity of rRNA when the derivatized factors were bound (243-245). In more recent studies, Muth and colleagues used free and tethered phenanthroline:Cu cleavage for structural studies of the ribosome (3,240,246,247). Free phenanthroline:Cu cleavage was used to elucidate the structure of a functionally important rRNA pseudoknot on the large subunit of ribosomes (240), and phenanthroline:Cu tethered to DNA oligonucleotides complementary to rRNA was utilized to both to probe conformational changes that occur in a transition between inactive and active ribosomes (3), and to identify rRNA domains proximal to DNA oligonucleotides with tethered phenanthroline:Cu^{2+} when they were hybridized to specific positions on the ribosome (246).

In this section of our study, we outline experiments that were carried out to elucidate the position of the sarcin/ricin stem-loop (SRL) in relation to other domains of rRNA on the large subunit of the prokaryotic ribosome. To do this, we localized a tethered chemical nuclease to the SRL by hybridizing a complementary, derivatized oligonucleotide to the domain. Using this approach, we were able to identify three distinct rRNA elements in close proximity to the SRL in the tertiary structure of the large subunit. In addition, we discovered a conformational change that occurs in one of these domains, the ribosomal protein L11-binding domain, that undergoes a conformational change in response to binding of the antibiotic, thiostrepton, at a proximal position. In this way, the chemical nuclease, phenanthroline:Cu^{2+}, proved to be a valuable tool for uncovering both the static and dynamic characteristics of the ribosome.

Results

Design of Complementary DNA Probes

DNA oligonucleotide probes were designed to localize the reactive phenanthroline:Cu^{2+} group at or near the tip of the sarcin-ricin stem loop (SRL). The probe that provided the best binding results for 50S subunits (Figure 2.4) was a probe with complementarity to 23S rRNA residues A2654-G2664 and was designated the Sarcin2654 probe. A mismatch probe the same length as the Sarcin2654 probe was also designed with an unrelated sequence to use as a control during reactions (Table 2.1). The Sarcin2654 and mismatch probes were checked for complementarity to any stretch in all of the rest of 23S rRNA, in all of 16S rRNA, and in 5S rRNA sequences. Each oligonucleotide contained no more than five residues in a straight stretch complementary to another region of rRNA and no more than 6 total residues in complementary positions to rRNA outside of the SRL.

Table 2.1. DNA Oligonucleotides for Sarcin/Ricin Domain Probing	
Probe/rRNA Sequence	**Designation**
5'-HO- C C T C T C G T A C T - P(S)-3' 3'-(2664)- G G A G A G C A U G A- (2654)-5'	Sarcin2654
5'-HO- C C T C T C G T A C T - P-3' 3'-(2664)- G G A G A G C A U G A- (2654)-5'	Sarcin2654-phosphate
5'-HO- G C T G T T G T G A T - P(S)-3'	Sarcin2654-mismatch

P = phosphate group (PO_3) ; **P(S)** = phophorothioate group (PO_2S) ; **HO** = 5'-hydroxyl group; **C** = cytidine; **T** = thymidine; **U** = uridine; **G** = guanosine; **A** = adenosine. Numbers in paranthesis are the 23S rRNA residue numbers (*E. coli* numbering).

Synthesis and Purification of Probes

DNA oligonucleotide probes were prepared as described in the experimental section on an Applied Biosystems, Incorporated (ABI) DNA synthesizer using standard automated phosphoramidite synthesis methods (248) for incorporation of nucleosides. 3' -phosphates were incorporated by starting synthesis with a phosphate column. Where appropriate, a reagent was used to convert the 3'- phosphite intermediate group to a phorphorothioate (PO_2S) during synthesis (see MATERIALS AND METHODS section for details). In addition to the complementary oligonucleotide, an oligonucleotide with 3'- phosphates only (Sarcin2654-phosphate) and the same sequence as the probe, and an oligonucleotide with an unrelated sequence (Sarcin2654-mismatch), but synthesized in the same manner (mismatch control) were synthesized for use as controls.

Reaction of Phenanthroline with DNA Oligonucleotides

To attach phenanthroline to DNA oligonucleotides, we utilized the reaction first reported by Helene (249). Here, the thiophosphate sulfer anion nucleophile on the oligonucleotide displaces iodine from the α-haloamide group of 5-iodoacetamido-1,10-phenanthroline (5IOP) (Figure 2.1).

Attachment of the phenanthroline moiety to the phosphorothioate oligonucleotides was accomplished under conditions optimal for solubility of the hydrophobic phenanthroline and hydrophilic oligonucleotide reactants (1:1, DMSO:water). Efficiency of the phenanthroline attachment was checked through the use of affinity polyacrylamide gel electrophoresis (PAGE) with the addition of [(N-acryloylamino) phenyl]mercuric chloride (APM) before polymerization (5). This allowed covalent immobilization of the

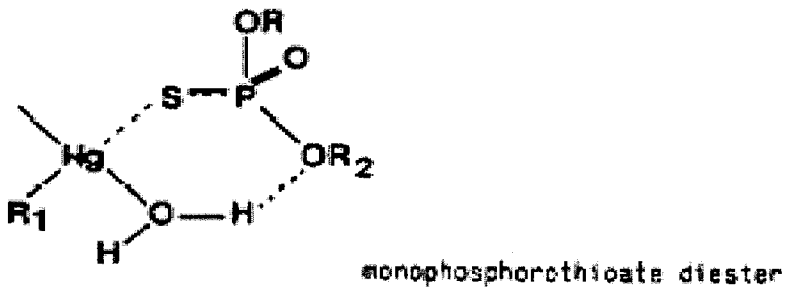

Figure 2.3. Coordination of a Phosphorothioate by Immobolized Mercury. $\mathbf{R_1}$ represents the gel matrix. **R** or $\mathbf{R_2}$ represent the oligonucleotidenucleotide. Adapted from Igloi (5).

mercury derivative in the PAGE gel for interaction with phosphorothioate oligonucleotides via a square planar coordination complex during electrophoresis (Figure

2.3). As derivatized phosphorothioates or oligonucleotides with terminal phosphates are not coordinated by the mercury derivative, comparison of the retardation of phenanthroline-derivatived and non-derivatized oligonucleotides on APM gels allowed us to estimate the efficiency of attachment of the phenantholine moiety to oligonucleotides. Figure 2.4 shows an APM gel run with a time titration for the phenanthroline-derivatization of the Sarcin2654 oligonucleotide. The reaction was essentially complete at the earliest time point (30 minutes) after the addition of 5IOP to the phosphorothioate oligonucleotide. Electrophoresis of underivatized oligonucleotide (lane 1) is retarded while electrophoresis of the derivatized oligonucleotide (lanes 2-4) and the the Sarcin2654-phosphate probe (lane 5) is not. The addition of the phenanthroline group to

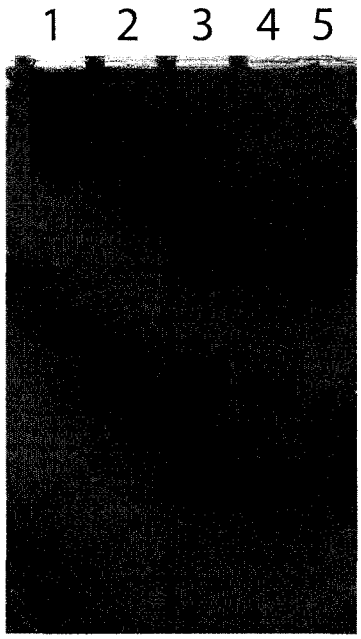

Figure 2.4. Analysis of Derivatized Oligonucleotides. The figure shows an [(N-acryloylamino) phenyl]mercuric chloride-12% polyacrylamide gel (APM-PAGE) with a time titration for the reaction of 5-iodoacetamido-1,10-orthophenanthroline (5IOP) with the 3'-phosphorothioate Sarcin2654 DNA oligonucleotide. (1) 3'-phosphorothioate probe without added 5IOP; (2) 30 minute reaction of 5IOP with phosphorothioate probe; (3) 1 hour reaction of 5IOP with phosphorothioate probe; (4) 2 hour reaction of 5IOP with phosphorothioate probe; (5) 3'-phosphate probe.

the Sarcin2654 oligonucleotide is detectable as a difference in the electrophoretic mobility of the derivatized oligonucleotide and the Sarcin2654-phosphate probe. An additional product, barely detectable to the naked eye and larger than the primary product, appeared after the reaction for each sample. Based on the persistence of this contaminating band and the need to remove unreacted 5IOP from reaction mixtures, we utilized HPLC of the reaction products to isolate derivatized oligonucleotides. The indicated peaks were collected, were dried down, and were resuspended in buffered solution for use in probing experiments. From UV spectroscopy of the isolated products, we determined that about 65-85% of the phenanthroline-derivatized product was collected after the reaction and purification procedures (data not shown).

Binding of Derivatized Oligonucleotides to 50S subunits

The next step in probing with the phenanthroline-derivatized probes was to determine the binding of the oligonucleotides to their target sequence on the large subunit of the ribosome. To do this, we used nitrocellulose filter binding assays with radiolabeled oligonucleotides. Derivatized oligonucleotides were 5'-radiolabeled using polynucleotide kinase exchange (see experimental methods for specifics). The radiolabeled oligonucleotides were purified and annealed to 50S subunits and the percent binding was determined based upon retention of radioactivity on nitrocellulose filters. Figure 2.5 shows the results of nitrocellulose filter binding assay with increasing amounts of radiolabeled Sarcin2654 probe added to 50S subunits and a second, competition assay, that includes binding of a constant amount of radiolabeled Sarcin2654 probe (10 uM—10:1 probe:subunit ratio) incubated with an increasing amount of unlabeled

A

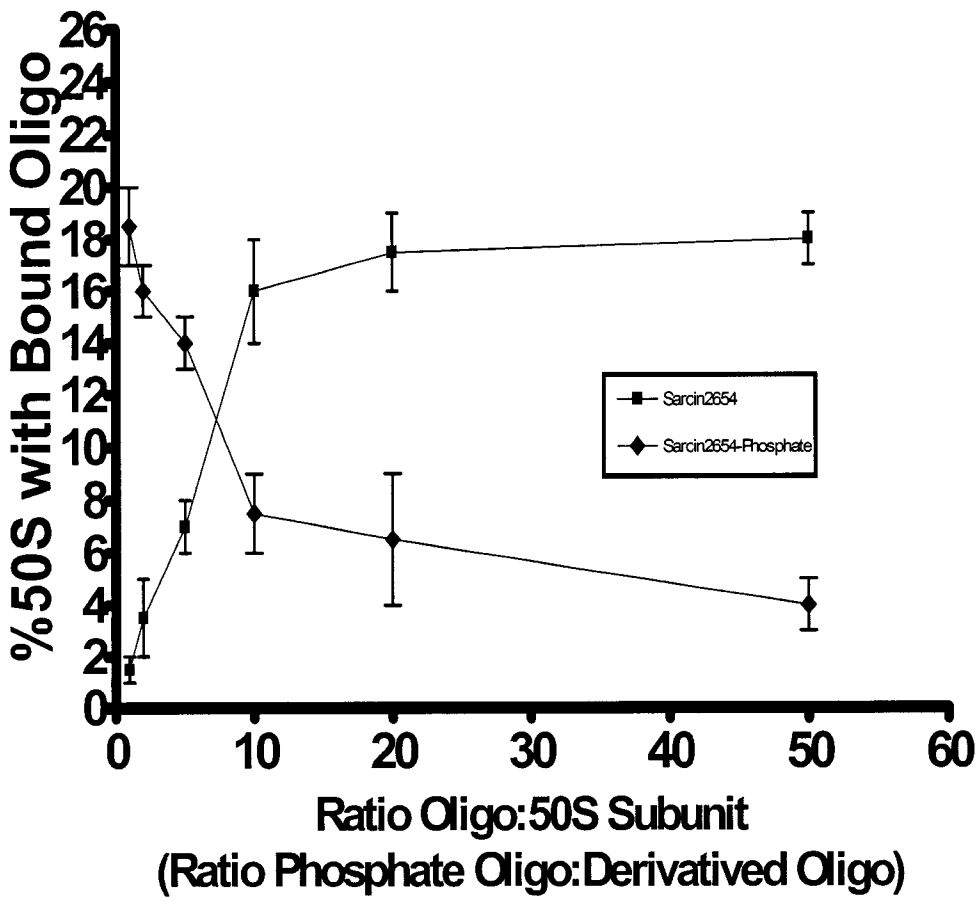

Figure 2.5. Binding of SRL-Directed Oligonucleotides to 50S Subunits. 50S subunits (0.5 μM) were incubated with increasing amounts of SRL-direct, radiolabeled probes, were filtered through nitrocellulose filters, and % binding was determined from scintillation counting of dried filters. For the competition assay, 50S subunits (0.5 μM) were incubated with radiolabeled Sarcin2654 (10 μM) and increasing amounts of unlabeled Sarcin2654-phosphate probe.

Sarcin2654-phosphate probe. The specificity of the binding was determined by two methods. First, we added increasing amounts of unlabeled, non- derivatized probe (Sarcin2654-phosphate) to reactions and determined the effect on binding. Second, we utilized the enzyme RNaseH to determine the localization of probe binding.

The percentage of 50S subunits with bound oligonucleotide saturated at levels around 18% for the Sarcin2654 probe. These results are consistent with those of Muralikrishna *et al.* (204), that showed ~20% binding of a slightly longer probe directed to the same region of the large subunit. The reason that targeted oligos do not reach a level approaching 100% binding, even at ratios of probe:subunit as high as 50:1 (a level where non-specific binding to related sequences becomes favorable), is not well understood, but is documented for oligonucleotide probing of both subunits (204,205,250,251). When the 50S subunits were combined with purified 30S subunits and were tested for activity in binding Phe-tRNA^{Phe} in the P site, they were found to be greater than 40% active (data not shown), suggesting that the population of subunits does not consist of a majority of inactive particles. Also, when rRNA is extracted from the 50S subunits, it can be resolved into 2 distinct bands, identified as 5S and 23S rRNA, by PAGE gel analysis (data not shown), indicating that the rRNA is not significantly degraded during isolation of the subunits. It is possible that the character of the subunits themselves prevents efficient binding. The compact structure of the rRNA and protein in the subunits and the negative phosphate backbone charge of the oligonucleotide may make the approach of macromolecules the size of DNA oligonucleotides less favorable. Although studies at higher temperatures, under different ionic conditions, and with longer incubation times have been done (251,252), they still did not reach levels approaching 100%.

Probe-Directed Phenanthroline-Cu^{2+} Cleavage of rRNA in the Sarcin/Ricin Domain

In order to explore the rRNA environment around the SRL, we hybridized the phenanthroline-derivatived Sarcin2654 probe in the presence of Cu^{2+} and reducing

reagent (MPA). The tethered phenanthroline:Cu^{2+} complex could then intercalate into surrounding rRNA structures and induce strand cleavage detectable by primer extension analysis (Figure 2.6). The results for the sarcin/ricin domain region indicated that increasing amounts of derivatized probe induce cleavage around positions A2654 and G2655 near the 3'-end of the hybridized probe and around positions A2749-A2753 in the

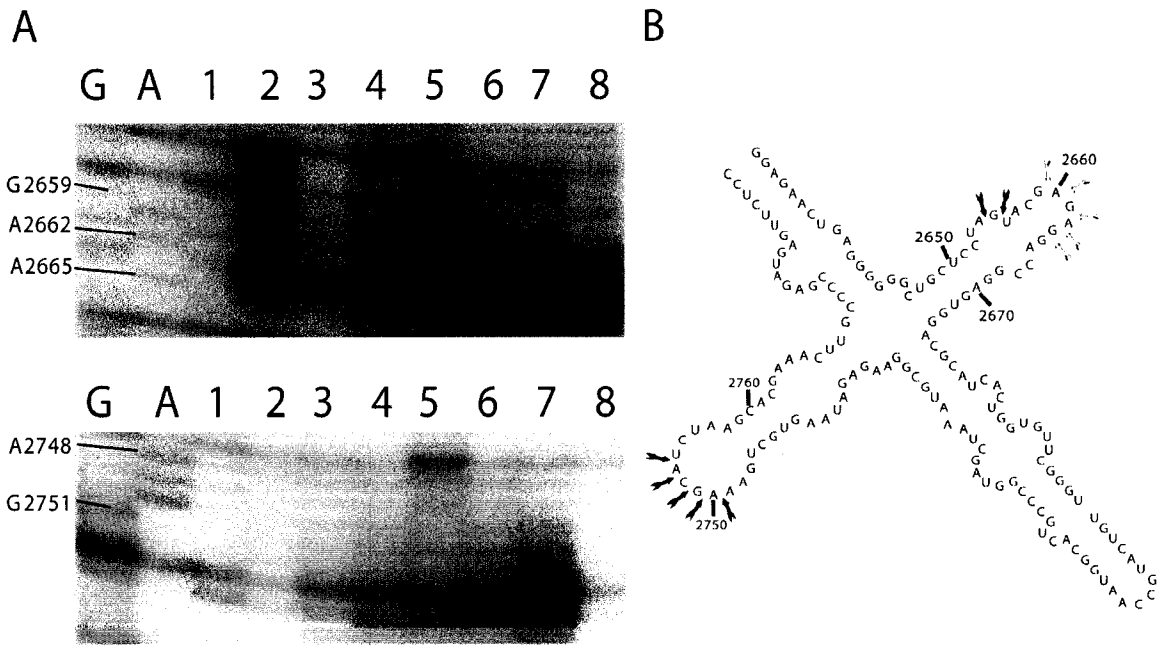

Figure 2.6(A). Sarcin2654 Probe-Directed Cleavage of rRNA in the Sarcin/Ricin Domain. Cleavage of rRNA was induced from phenanthroline:Cu^{2+} conjugated to the 3'-end of the DNA probe hybridized to 50S subunits (0.5 μM). (G), G sequencing lane; (A), A sequencing lane; (1), 50S control without conjugated probe; (2), extracted rRNA cleavage induced by conjugated probe (10 μM); (2), 50S subunits (0.5 μM) rRNA cleavage induced in the presence of the Sarcin2654-mismatch conjugated probe (20 μM); (3), 50S subunits (0.5 μM) rRNA cleavage induced in the presence of conjugated Sarcin2654 probe (0.5 μM); (4), 50S subunits (0.5 μM) rRNA cleavage induced in the presenceof conjugated Sarcin2654 probe (2.5 μM); (5), 50S subunits (0.5 μM) rRNA cleavage induced in the presence of conjugated Sarcin2654 probe (5 μM); (6) 50S subunits (0.5 μM) rRNA cleavage induced in the presence of conjugated Sarcin2654 probe (10 μM); (7), 50S subunits (0.5 μM) rRNA cleavage induced in the presence of conjugated Sarcin2654 probe (20 μM); (8) RNase H cleavage of 50S subunits (0.5 μM) in the presence of conjugated Sarcin2654 probe (10 μM). Specifics for the probing conditions are described in **Material and Methods. (B). Conjugated probe-induced cleavages of 50S subunit rRNA.** Positions of induced cleavages are indicated on the secondary structure representation of the sarcin/ricin domain of 23S rRNA. Black arrows represent probe-nduced cleavages; yellow arrows represent RNase H-induced cleavages in the presence of probe.

2750 stem-loop region (Figure 2.6; lanes 4-7). However, when a similar amount of derivatized Sarcin2654-mismatch probe was incubated with the derivatized probe, no cleavage of rRNA in this domain was detected (lane 3). When hybridized to rRNA from 50S subunits with the ribosomal proteins previously extracted (lane 2), the probe induces a similar but more robust pattern of cleavage around the SRL. However, no cleavage of the extracted rRNA was induced by the derivatized probe in the region of the 2750 stem-loop (lane 2). This result indicates that the rRNA may adopt a different tertiary structure in the absence of ribosomal proteins that prevents the hybridized probe-conjugated phenanthroline:Cu^{2+} from interacting with the 2750 stem-loop.

Finally, as a second control for probe binding, we localized RNase H cleavage of 50S subunits in the presence of derivatized probe RNase H cleavage. RNase H is a bacterial endoribonuclease that specifically hydrolyzes the phosphodiester bonds of RNA that is hybridized to DNA. Therefore, we expected cleavage of rRNA at the location of DNA probe hydridization to 50S subunits. Figure 2.6 also shows the results for RNase H cleavage on 50S subunits incubated with derivatized Sarcin2654 probe. RNase H-induced cleavage occurs at residues G2659-G2653 (Figure 2.6A, lane 8; Figure 2.5B). As indicated in an earlier study of the activity of this enzyme (253), cleavage occurs primarily at the 3'-end of the RNA segment complementary to the DNA probe. In contrast to suggestions from that study, cleavage of the hybrid structures occurs efficiently within a hairpin structure of the rRNA around positions G2659-G2664 (Figure 2.6B). This difference may be attributable to the effects on the stability of the stem-loop of the combination of the terminal GNRA tetraloop (2659-2662) and the internal loop (U2653-G2655:C2667-C2668) (Figure 2-5c) that form part of the structure, and the

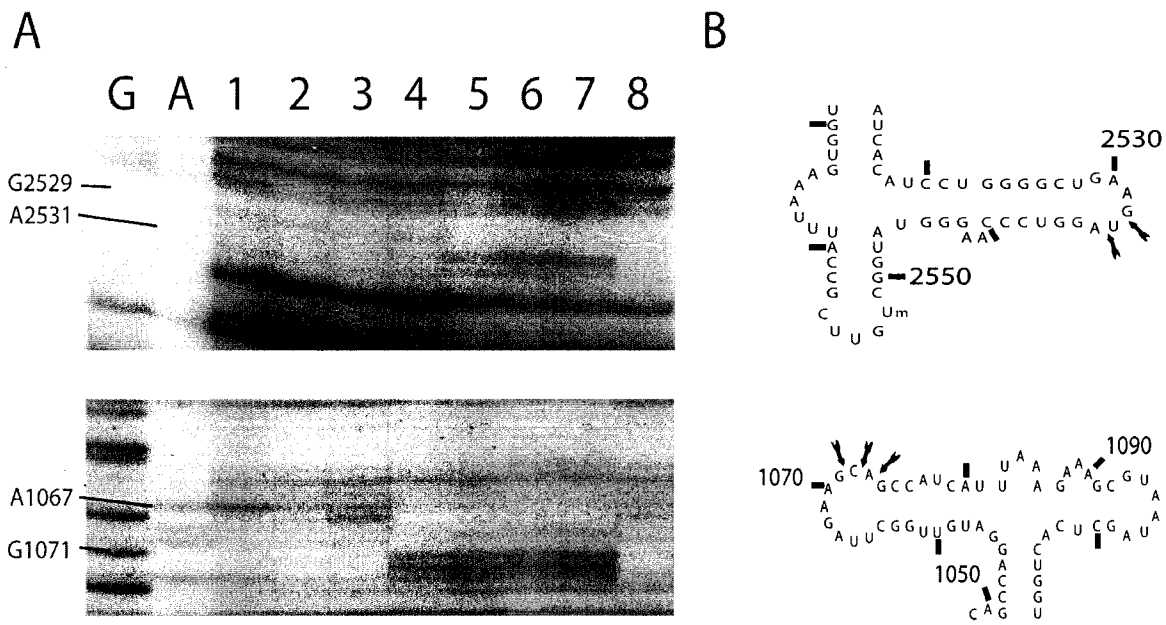

Figure 2.7(A). Sarcin2654 Probe-Directed Cleavage of rRNA Outside the Sarcin/Ricin Domain. Cleavage of rRNA was induced from phenanthroline:Cu^{2+} conjugated to the 3'-end of the DNA probe hybridized to 70S ribosomes (0.5 μM). (G), G sequencing lane; (A), A sequencing lane; (1), 70S control without conjugated probe; (2), extracted rRNA cleavage induced by conjugated probe (10 μM); (2), 70S ribosome (0.5 μM) rRNA cleavage induced in the presence of the Sarcin2654-mismatch conjugated probe (20 μM); (3), 70S ribosome (0.5 μM) rRNA cleavage induced in the presence of conjugated Sarcin2654 probe (0.5 μM); (4), 70S ribosome (0.5 μM) rRNA cleavage induced in the presenceof conjugated Sarcin2654 probe (2.5 μM); (5), 70S ribosome (0.5 μM) rRNA cleavage induced in the presence of conjugated Sarcin2654 probe (5 μM); (6) 70S ribosome (0.5 μM) rRNA cleavage induced in the presence of conjugated Sarcin2654 probe (10 μM); (7), 70S ribosome (0.5 μM) rRNA cleavage induced in the presence of conjugated Sarcin2654 probe (20 μM); (8) RNase H cleavage of 70S ribosome (0.5 μM) in the presence of conjugated Sarcin2654 probe (10 μM). Specifics for the probing conditions are described in **Material and Methods. (B). Derivatized probe-induced cleavages of 70S ribosome rRNA.** Positions of induced cleavages are indicated on the secondary structure representation of the 2530 stem-loop domain and the L11-binding domain of 23S rRNA. Black arrows represent the positions of probe-induced cleavages.

results are consistent with the susceptibility of this domain to melting of the stem as noted by Meyer *et al.* (250). As indicated by our results, this instability must make this structure amenable to hybridization with the derivatized probe.

Probe-Directed Cleavage of rRNA in Regions Outside the Sarcin/Ricin Domain

To ascertain what regions of rRNA might be proximal to the SRL, we performed reverse transcriptase primer extension analysis of rRNA extracted from 50S subunits that were probed with the derivatized Sarcin2654 probe. Upon "walking" the entire 23S rRNA with extension primers, we discovered two regions outside of the SRL domain where cleavage of rRNA was reproducibly induced by the presence of the derivatized probes. Cleavage was induced at rRNA residues in the 2550 stem-loop in domain V of 23S rRNA and in the L11-binding region of rRNA (~1050-1105) in domain II of 23S rRNA. Figure 2.7 shows results for derivatized-probe directed cleavage of these two regions. Cleavage of the 2530 stem-loop from the Sarcin 2654 probe is localized to U2533-A2534 in the terminal loop (Figure 2.6B). Cleavage in the loop region is consistent with the necessity of the phenanthroline:Cu^{2+} complex to bookmark in single-stranded and "strained" regions of RNA to induce cleavage (240,254).

Cleavage of the L11-binding region from the hybridized Sarcin2654 probe is localized to G1071-G1074. These residues are localized on one face of the tertiary structure of the L11-binding domain (Figure 2.7), at the junction where the two stem-loops (that containing A1067 in the loop and that containing A1095 in the loop) fold together. These cleavages also occur in a loop region with a structure that "presents" the susceptible residues for association with the phenanthroline:Cu^{2+} complex.

Protection of L11-Binding rRNA Cleavage by Thiostrepton

Based upon the cleavage we observed from the SRL to the L11-binding region and the previous results relating modifications in the SRL and changes in the structure of the L11-binding region, we then asked if the binding of thiostrepton in the L11-binding

region might change our probing results for that region. To ascertain the effects of thiostrepton on cleavage, we added the antibiotic to 50S subunits and probed them with the derivatized SRL probe. The results (Figure 2.8) indicated that the presence of the antibiotic protects the region of 23S rRNA around nucleotide G1071 from cleavage directed by the SRL-bound probe.

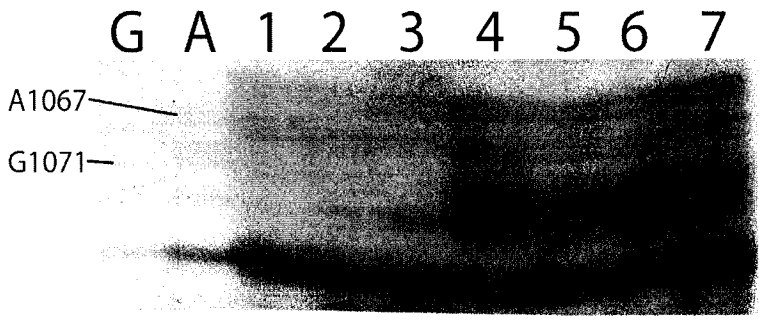

Figure 2.8 Thiostrepton Protection of Cleavage in the L11-Binding Region. Cleavage of rRNA was induced from phenanthroline:Cu^{2+} conjugated to the 3'-end of the DNA probe hybridized to 50S subunits (0.5 μM). (G), G sequencing lane; (A), A sequencing lane; (1), 70S control without conjugated probe; (2), 50S subunits incubated with un-derivatized Sarcin2654 probe and otherwise treated as in experimental lanes; (3), 50S subunits incubated with 10 μM Thiostrepton and underivatized Sarcin2654 probe and otherwise treated as in experimental lanes; (4), 50S subunits probed with the derivatized Sarcin2654 probe (conditions as in Figures 2.5 and 2.6 above); (5), 50S subunits incubated with 10 μM thiostrepton before probing with the derivatized Sarcin2654 probe; (6) 50S subunits probed with the derivatized Sarcin2654 probe as above; (7), 50S subunits probed by first hybridizing derivatized probe, then incubating with 10 μM thiostrepton, then inducing cleavage (adding MPA).

Discussion

Proximity of rRNA Residues to the Sarcin/Ricin Domain

The results of our directed probing studies allow us to define regions of the rRNA that are proximal in the tertiary structure of the large subunit of 70S ribosomes. From these results, we found that at least three regions of 23S rRNA that are distal from the

SRL in the secondary structure of the large subunit are proximal when the 23S rRNA folds into the tertiary structure of the ribosome. From knowledge of the length of the phenanthroline:Cu^{2+} complex and its tether to the hybridized probe, we can estimate the distance between the hybridized probes and these regions to be between 15 and 20 angstroms (Å).

Agreement of Probing Data with the Published Crystal Structures of Large Subunits

Near the conclusion of our probing studies, several high-resolution crystal structures of large ribosomal subunits were published that allowed us to judge the reliability of the directed probing for estimating the proximity of elements on the ribosome. Although the emergence of the crystal structures precluded publication of our data, the published structures confirmed that our probing studies accurately predicted the proximity of the rRNA elements. Figure 2.9 shows a model of the 50S subunit from *Deinococcus radiodurans* (180) with SRL identified along with the elements of rRNA identified in our study.

Some interesting points emerge from our data as well. First, the paucity of cleavage induced to each region when the derivatized probe is hybridized to 23S rRNA with the ribosomal proteins extracted suggests that the rRNA adopts a structure in this state that is distinct from the intact subunit. This change could be due to melting of the structure of the rRNA in the absence of ribosomal proteins. Stabilization of tertiary rRNA structure by ribosomal proteins has been previously documented in biophysical studies of rRNA with proteins extracted (255,256).

The crystal structure of the large subunit from *Haloarcula marismortui* was recently determined to 2.4 Å resolution. Analysis of this structure revealed that the

regions of the 23S rRNA, including the SRL and L11-binding domain, that are believed to interact with translation factors interact with a higher than average concentration of ribosomal proteins (257). The ribosomal proteins interacting in these regions include L6, L14, and L3 that interact with the SRL domain and L11 and the pentameric stalk complex ($L10(L7/L12)_2$ that interact with the L11-binding domain. These extensive interactions also suggest a strong dependence of the rRNA structure on interactions with ribosomal proteins.

Cleavage from the bound probe to the 2530 loop of 23S rRNA can be rationalized by the proximity of the SRL and this stem-loop in the crystal structures of 50S subunits. If we estimate the distance in the crystal structures between the backbone of 23S rRNA residue A2654, the residue that would be adjacent to the derivatized 5'-end of the bound oligonucleotide in a presumed rRNA:DNA double helix, and the backbone of the rRNA cleaved in the 2530 loop, we find that the it falls within the 15-20 Å threshold (approximately 18 Å) for the "reach" of the bound phenanthroline:Cu^{2+}. However, when we estimate the distance between the backbone at A2654 and the residues in the 2750 loop and the L11-binding rRNA that are cleaved, we find that the values are greater than twice the distance we would expect for efficient cleavage (~48 Å and ~50 Å respectively). These discrepancies suggest one of the following scenarios. First, formation of the helix between the DNA oligonucleotide probe and the SRL rRNA can be expected to change the structure and/or orientation of the SRL domain relative to the rest of the subunit, potentially placing the bound end of the probe in closer proximity to these

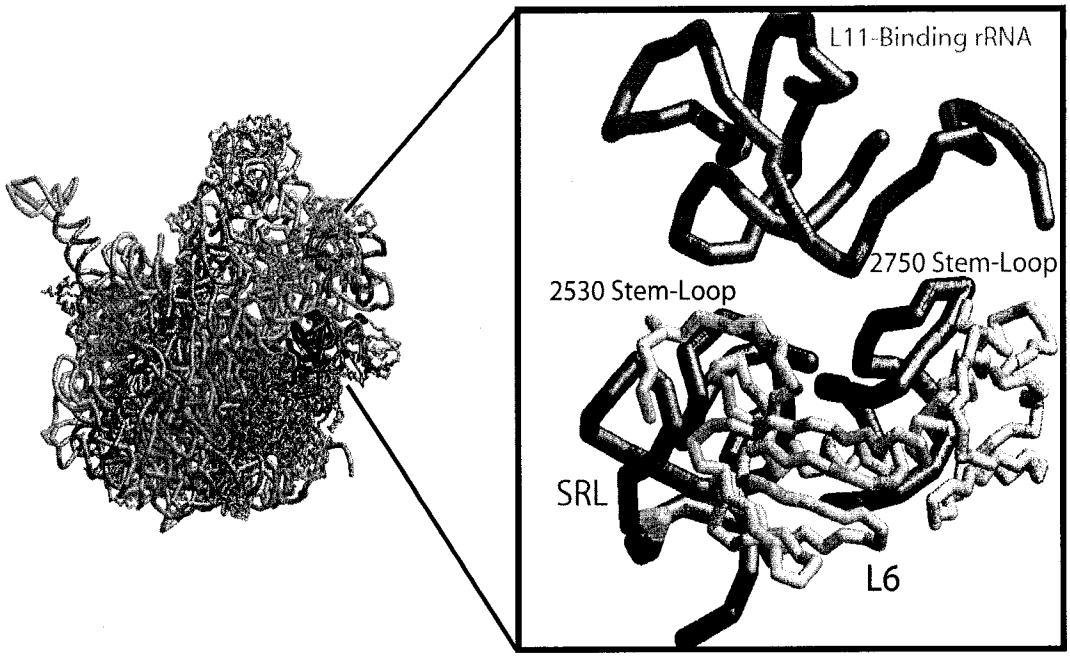

Figure 2.9 Crystal Structure of the 50S Subunit. Pictured is the crystal structure of the 50S subunit from *Deinococcus radiodurans* (180). On the left is the entire structure as seen from the subunit interface view (rRNA is in shown in orange backbone representation and ribosomal proteins are shown in grey backbone representation. The stem-loops identified in the probing studies are colored for clarity. Red, SRL; blue, 2530 stem-loop; green, L11-binding rRNA; purple, 2750 stem-loop. On the right is a blown-up view of the region around the SRL with the same coloring scheme and with the surrounding rRNA omitted for clarity. The position of the residue opposite the phenanthroline:Cu^{2+} complex when the derivatized probe is bound is colored yellow on the SRL. Residues that are cleaved by the bound, derivatized probe in each different region are colored black. The position of ribosomal protein L6 is shown in grey.

regions. Efficient cleavage of the three regions would be possible if the binding of the oligonucleotide induced the SRL to fold closer to the rRNA pocket formed between the 2530 loop, the 2750 loop and the L11-binding rRNA domain (Figure 2.9). Judging from the crystal structure of the 50S subunit, such folding would be prevented by the presence of ribosomal protein L6 and would only be possible if the L6 interaction with the SRL is disrupted by probe binding. As L6 interacts with residues in the terminal loop of the

SRL, it is possible that these interactions are disrupted, allowing the prescribed movement of the SRL.

A second possibility requires that binding of the oligonucleotide to the SRL induces changes in the structure of the rRNA in the regions cleaved by bound oligonucleotide, moving them closer to the bound probe. This possibility is supported by several previous studies. In one, the authors found that binding of the antibiotic thiostrepton to the L11-binding region induces a change in the structure of the 50S subunit that protects the SRL from the action of the ribotoxin, α-sarcin (234). Such protection could result from a thiostrepton-induced shift of the L11-binding domain toward the SRL region, sterically blocking the approach of the ribotoxin to the SRL. In another study, the depurination activity of the ribotoxin ricin at the SRL on large subunits from eukaryotic ribosomes induced structural changes in the stem-loop equivalent to the 2530 loop on prokaryotic ribosomes (258). This suggests potential conformational coupling between the SRL and 2530 stem-loop domain. However, no studies have been done that specifically link DNA oligonucleotide binding in the SRL to structural changes in these domains.

Alternatively, longer probing distances would result if the tethered chemical nuclease produces a species such as a hydroxyl radical that diffuses from the hybridized position of the probe and produces rRNA lesions outside of the range of the tether. Under anaerobic conditions, reduction of the phenanthroline:Cu^{2+} complex results in the production of hydrogen peroxide *in situ* (259), and the addition of exogenous peroxide enhances the cleavage reaction (3,237). These observations led to the suggestion that the hydrogen peroxide produced in the reaction or added exogenously oxidizes the reduced

Cu^+ chelated by phenanthroline, leading to the production of hydroxide anion and diffusible hydroxyl radicals (Eq. 2.1) (260).

$$OPCu^+ + H_2O_2 \longrightarrow OPCu^{2+} + {}^-OH + \cdot OH \quad \textbf{(Eq. 2.1)}$$

However, the authors of a kinetic study of the phenanthroline:Cu^+ reaction with hydrogen peroxide found that the rate of the reaction between the generated reactive species and the subustrate was much slower than those involving production of a hydroxyl radical (261), and significant evidence exists in favor of the formation of a high-valent copper-oxo species that remains chelated by phenanthroline (262-264).

Recently, we addressed the question of the production of a diffusible reactive species during the phenanthroline:Cu^{2+} reaction by comparing hybridized complementary oligonucleotide-directed cleavage of 16S rRNA by oligonucleotides with either tethered phenanthroline:Cu^{2+} or tethered EDTA:Fe^{2+}, a known producer of hydroxyl radicals (265). This paper is presented in this study in Appendix A. In this study, delocalized 16S rRNA cleavage mediated by the tethered EDTA:Fe^{2+} complexes suggested the involvement of a diffusible reactive species, while cleavage mediated by the tethered phenanthroline:Cu^{2+} complex was localized to the proximity of the tethered nuclease under normal reaction conditions. However, diffuse tethered phenanthroline:Cu^{2+}-mediated cleavage did occur with the addition of exogenous hydrogen peroxide when the reaction time was prolonged. The mechanism for the diffuse phenanthroline:Cu^{2+}-mediated cleavage with added peroxide and prolonged reaction times is unknown, but Muth *et al.* have suggested that, under these conditions, the tethered nuclease may cleave

the backbone of the hybridized DNA probe near the tethering point. Conceivably, this would produce a diffusible fragment of a few DNA nucleotides and the tethered nuclease that could explain the resulting diffuse cleavage pattern (266).

A final, and possibly more likely explanation for the discrepancy in the "reach" of the SRL-bound oligonucleotide is that the derivatized 5'-end of the oligonucleotide reversibly dissociates from the rRNA when bound to the SRL. This possibility is supported by the fact that our RNase H studies of probe binding do not detect formation of the rRNA:DNA duplex between the DNA oligonucleotide and positions A2654-C2658 on the SRL (Figure 2.5). If only the 5'-end of the probe hybridizes to the rRNA in the SRL, the length of the reach of the phenanthroline:Cu^{2+} complex would be increased by the flexible length of the five residues on the 3'-end of the probe. If we calculate this length on the basis of 3.4 Å per residue in a B-form DNA helix, it could add as much as 17 Å to the reach of the phenanthroline:Cu^{2+} complex, and it would make the anchor point for the probe the tip of the SRL around position G2659. This would place each region of the rRNA cleaved by the derivatized probe within the reach of the hybridized probe.

These probing results place the SRL and L11BR rRNA, two highly conserved regions of 23S rRNA that are separated by substantial distances in the secondary structure of 23S rRNA(Figure 1.9), in close proximity on the large subunit of prokaryotic ribosomes. Although this was one of the first biochemical studies that directly linked these two regions in the tertiary structure of the large subunit rRNA, publication of these results was precluded by the emergence of the high resolution x-ray crystal structures of the large subunit near the completion of the probing analysis.

Protection of the L11-Binding Region by Thiostrepton

Previous chemical modification protection probing of this domain indicated specific residues that were protected by thiostrepton binding (143). These included A1067, G1068, A1095, and A1070. Our study has uncovered three new residues, G1071, C1072, and A1073, that thiostrepton protects. In this case, binding of the antibiotic appears to change the structure of this region of the rRNA in such a manner as to make it less susceptible to cleavage by the Sarcin2654 probe bound at the SRL. It may either "tighten" the structure of the junction between the two stem-loops in the L11-binding region (Figure 1.10), or it may induce a shift in the position of the whole domain relative to the subunit.

Discovery of a potential structural change in the L11-binding domain upon thiostrepton binding prompted us to examine whether this structural change might be related to the function of the L11-binding rRNA on the ribosome. Our experiments to elucidate the role of the L11-binding rRNA in the function of the ribosome are detailed in Chapters 3 and 4.

Materials and Methods

Subunit Preparation

Ribosome were prepared from the RNase deficient *Esherichia coli* strain MRE600 using a protocol developed in our laboratory (267,268). A 250 mL culture of bacteria was used to inoculate 10 L of Luria broth at 37° C and was grown with agitation and aeration to early log phase (optical density of 0.5 at 600 nm). The culture was then concentrated on a Millipore pelican filtration harvester and pelleted by centrifugation at

10,000 rpm for 10 minutes at 4° C in a Sorvall GSA rotor. Concentrated bacteria were frozen at -80° C in preparation for isolation of ribosomal subunits.

For subunit isolation, 20 g of frozen bacterial cells were mixed with 30 g of sterile alumina and were ground at 4° C with a mortar and pestle for one hour. At the end of the grinding period, 20 mL of buffer (10 mM Tris-Cl, pH. 7.5, 0.5 M NH_4Cl, and 10 mM $MgCl_2$, 3 mM β-mercaptoethanol) was added to resuspend the grindate. The solution was then centrifuged at 10,000 rpm in a Sorvall SSW34 rotor at 4° C to remove cell debris and alumina. To remove smaller debris, the supernatant from the first centrifugation was centrifuged at 28,000 rpm in a Beckman Ti70 rotor at 4° C for 30 minutes. Ribosomes were pelleted from the supernatant by centrifugation at 60,000 rpm in a the Ti70 rotor at 4° C for 2.5 hours. The pellets were washed with 30/50 buffer (10 mM Tris-Cl, pH 7.5, 60 mM KCl, and 1.5 mM $MgCl_2$) and were resuspended in the same buffer (~4 hr at 4° C). The 28,000 rpm and 60,000 rpm centrifugation steps were repeated one extra time to remove residual debris.

To isolate 50S subunits, the pellets from the second 60,000 rpm centrifugation step were dissolved in 22.5 mL of 30/50 buffer with 5%, diethylpyrocarbonate (DEPC)-treated sucrose. The solution was loaded onto a Beckman Ti14 rotor with a linear 10-38% sucrose gradient in 30/50 buffer, a 100 mL overlay of 30/50 buffer, and a 50% sucrose cushion (30/50 buffer) for zonal centrifugation. After 4 hours of centrifugation at 45,000 rpm, the gradient was unloaded and the solution was monitored by UV absorbance at 280 nm for the appearance of 30S and 50S subunit peaks. The 50S subunits were recovered by pooling the appropriate, non-overlapping peak fractions and centrifuging them at 60,000 rpm in a Ti70 rotor at 4° C overnight, resupending the pellet

in cleavage buffer (20 mM HEPES, pH. 7.7, 60 mM NH_4Cl, 30 mM KCl, and 10 mM $MgCl_2$), and dialyzing the solution overnight in the same buffer with 2 buffer changes to remove residual sucrose. The isolated 50S subunits were aliquoted and stored at -80° C for later use in probing experiments. The concentration of the subunits was assessed by checking the UV absorbance of the sample at 260 nm and calculating the concentration using an extinction coefficient of 26.1

Synthesis of 3'-Phorphorothioate DNA Oligonucleotides

An 11-mer oligonucleotide (Sarcin 2654) was designed to be complementary to nucleotides 2654-2664 of 23S rRNA and contained the sequence shown in Table 2.1. It was synthesized with a 3'-phosphorothioate group and a 5'-hydroxyl group for tethering of 5-iodoacetamido-1,10-orthophenanthroline (5IOP) using phosphoramidite chemistry on an ABI 394 DNA/RNA synthesizer using the following procedure. A 3'-phosphate was incorporated using a 3'-phosphate control-pored glass (CPG) column (Glen Research; Sterling, Virginia) that was oxidized after the first step of synthesis using sulfurizing reagent (3H-1,2-benzodithiol-3-one 1,1dioxide) from the manufacturer (Glen Research). The normal base synthesis step was interrupted at the coupling stage, which was increased to 6 minutes. After coupling, the capping step was omitted and the oxidizing step was continued with sulfurizing reagent (Glen Research) replacing the normal oxidizer. Synthesis of the sequence: 3'-TCATGCTCTCC-5'-OH' was then carried out using normal phosphoramidite chemistry. The oligonucleotide was cleaved from the solid support without removal of the 5'-trityl group for further purification.

The full-length product was purified from smaller contaminating termination sequences using reversed-phase-HPLC and a 0.5 M ammonium acetate/100% acetonitrile

gradient. The peak containing the full-length oligonucleotide with the protecting trityl group was collected, lyophilized and resuspended in HPLC-grade water. Deprotection of the purified oligonucleotide by removal of the trityl protecting group involved treatment at 65° C in 25 mM NH_4OH/ethylamine solution for 10 minutes. After deprotection, the oligonucleotide was precipitated and resuspended in water to derivitization.

5IOP Modification of Oligonucleotides

For modification of the 3'-phosphorothioate oligonucleotide, 50 nmoles of 5-iodoacetamido-1,10-phenanthroline (5IOP) (Molecular Probes) in DMSO were added to 10 nmoles of 3'-phosphorothioate oligonucleotide (5'-P(S)-Sarcin2654) in a solution of 100 µL of 1:1 DMSO:HPLC-grade water. The reaction mixture was then incubated at room temperature in the dark for 60 minutes and was immediately lyophilized. The pellet was resuspended in 100 µL of a 0.5 M ammonium acetate and derivatized oligonucleotides were separated from underivatized oligonucleotides and excess 5IOP by reverse-phase HPLC on a 0.5 M ammonium acetate/100% acetonitrile gradient. Purified oligonucleotides were precipitated, resuspended in water, and the resulting concentration was determined by UV spectrophotometry and an extinction coefficient of 0.0854 $AU*pmole^{-1}$ plus the contribution of the attached phenanthroline (0.032 $AU*pmole^{-1}$). The derivatized oligonucleotide was stored at -80° C for later use in probing experiments.

PAGE and APM/PAGE Analysis of Derivatized Oligonucleotides

Gel electrophoresis analysis was used to determine the efficiency of the derivatization reactions. For this, 500 pmol of derivatized or underivatized oligonucleotides were dissolved in 5 µl of gel loading buffer (7 M urea, 20 mM EDTA, 0.05% xylene cyanol, 0.05% bromophenol blue) and loaded on a 15% acrylamide

denaturing gel with or without 0.01 $mg \cdot ml^{-1}$ [(N-acryloylamino) phenyl]mercuric chloride (APM was synthesized in our lab by G. Muth) and run for 20 minutes at 20 mA constant current on a 10 cm x 10cm x 0.5 mm gel (approximately 35 V/cm at the beginning of the run). Bands were visualized by staining with methylene blue. On an APM gel, molecules bearing a 5'- or 3'-thiol group are markedly retarded in their migration (5). Thus oligonucleotides bearing unreacted phosphorothioate groups display much slower migration relative to the same oligonucleotides that were successfully derivatized. Typically the derivatization with or 5IOP was essentially quantitative (see Figure 2.4).

5'-End Labeling of Derivatized Oligonucleotides

The derivatized DNA oligonucleotides were 5'-end labeled by utilizing the polynucleotide kinase reaction. For derivatization, 10 nmoles of derivatized DNA oligonucleotide was incubated with 30 units of T4 polynucleotide kinase (Amersham Biosciences) and 1 nmoles of [γ-^{32}P]-ATP (New England Biolabs-3000 Ci/mmol) in the reaction buffer supplied by the manufacturer. The mixture was incubated for 30 minutes at 37° C and the reaction was terminated by heating the solution to 65° C for 15 minutes. Unreacted ATP was removed from the solution using a G-25 biospin chromotagraphy column (Biorad).

Binding of Derivatized DNA Oligonucleotides to 50S Subunits

Binding reactions were carried out in 50 μL cleavage buffer by the addition of increasing concentrations (0.5-50 μM) of radiolabeled, derivatized DNA probes to a solution of 1 μM 50S subunits. The 50S subunits were pre-incubated to 37° C, probe was added, and incubation was continued for 15 minutes. Following the 15 minute

incubation, the subunit:probe reactions were placed on ice for 1 hour. After 1 hour on ice, the solutions were diluted to 1 mL with cold cleavage buffer and were immediately filtered over presoaked 0.45 μm nitrocellulose filters (Millipore) under vacuum. The filters were washed 3 times with cold cleavage buffer and dried under vacuum. When completely dry, the radioactivity that remained on the filters was quantified in liquid scintillant on a Packard scintillation counter. The percentage of 50S with bound was calculated from the predetermined amount of radioactivity per picomole of radiolabeled oligonucleotide probe. For competition experiments, increasing amounts of unlabeled Sarcin2654-phosphate probe (50-500 μM) were added to the subunit:probe (10 μM probe reaction) complex just prior to the incubation on ice and the experiments and analysis were carried out otherwise the same as above.

Probing 50S subunits with Complementary, Derivatized Oligonucleotides

Cleavage reactions with the phenanthroline-derivatized probe were carried out in 25 μL of cleavage buffer by combining 25 pmoles of 50S subunits with increasing amounts (2.5-20 μM) of derivatized Sarcin2654 probe in the presence of a concentration of $CuSO_4$ equal to that of the probe. When thiostepton (10 μM) was added, it was added to 50S subunits either before or after the introduction of derivatized probe and the solution was incubated at 37° C for 15 minutes to induce binding of the antibiotic to the subunits. The mixtures were incubated at 37° C for 15 minutes and placed on ice. Cleavage was induced by the addition of 1 mM mercaptopropionic acid (MPA) to the solution on ice and was allowed to continue for 1 hour. The cleavage reaction was quenched by the addition of 100 μL of precipitation buffer (70% ethanol, 8.4 mM NaOAc, pH 6.5, and 0.8 mM EDTA) followed by precipitation at -80° C for 15 minutes

and centrifugation at 13,000g for 25 minutes. The pellets were resuspended in extraction buffer (8.4 mM NaOAC, pH 5 and 5 mM EDTA) and extracted twice with an equal volume of water-saturated phenol (pH 4.3) and once with an equal volume of chloroform. After extraction, the rRNA was precipitated by the addition of 2.5 volumes of 95% ethanol and centrifuged at 13,000g for 25 minutes to pellet the rRNA. The pellets were resuspended in storage buffer (10 mM Tris-Cl, pH 7 and 5 mM EDTA) in preparation for primer extension analysis.

Primer Extension Analysis of Probing Templates

Primer extension analysis was carried out based upon the technique of Noller and co-workers (222). First, 0.5 pmoles of the template rRNA from the cleavage reactions was mixed with 3 pmoles of a DNA primer (17 nucleotide long oligonucleotide complementary to staggered regions of 23S rRNA) in 4.5 μL of hybridization buffer (50 mM HEPES, pH 7.0, 100 mM KCl) and the solution was heated to 90° C for 1 minute and cooled slowly to 45° C to allow annealing of the primer to the rRNA. To this solution was added 2 μL of extension mix containing extension buffer and deoxynucleotide triphosphates (dNTP's), dGTP, dATP, dCTP, and dTTP. The final concentrations for these components was 0.13 mM Tris-Cl (pH 7.5), 69.2 mM KCl, 32 mM $MgCl_2$, 2 mM dithiothreitol (DTT), 5.57 μM dGTP, 5.57 μM dATP, 5.57 μM dCTP, 0.29 μM dTTP, 11.4 μM [α-^{32}P]-dTTP and 3 units of AMV reverse transcriptase (Takara). To sequencing tubes, 1.5 μL of either 1.5 μM dideoxycytidine triphosphate (ddCTP) for indicating guanosine (G) residues or dideoxythymidine (ddTTP) for indicating adenosine (A) residues, was added with the extension mix. The tubes were incubated for 30 minutes at 42° C. Following extension, the tubes were chased by adding

1 μL of chase mix (1 mM of each dNTP) to each tube and 2 μL of 67 μM ddCTP or ddTTP to the G and A sequencing tubes respectively. The reactions were terminated by the addition of 75 μL of precipitation buffer (70% ethanol, 8.4 mM NaOAc (pH 6.5), and 0.8 mM EDTA) and were precipitated at -80° C for 15 minutes. The synthesized products were then pelleted by centrifugation at 13,000g for 25 minutes and were resuspended in 10 μL tracking dye (7 M urea, 0.025% xylene cyanol FF, 0.025% bromophenol blue in 1x Tris-Borate-EDTA buffer). 1.5 μL of the radiolabeled DNA transcripts in tracking dye were resolved on a denaturing (7M urea) 6% polyacrylamide gel (600 mm x 0.25 mm) by electrophoresis at 55W for appropriate times (1-3 hours depending on the primer used). The gel was transferred to Whatman 3MM filter paper, was dried under vacuum, and was exposed on x-ray film (typically 4-12 hours).

Chapter 3

Interaction of Thiostrepton and Elongation Factor-G with the Ribosomal Protein L11-Binding Domain

William S. Bowen[1], Natalya Van Dyke[2], Emanuel J. Murgola[2], J. Stephen Lodmell[1], and Walter E. Hill[1,3]

(A manuscript accepted for publication by the Journal of Biological Chemistry – January or February Edition)

Introduction

The region of the prokaryotic 50S ribosomal subunit associated with interactions of ribosome-dependent GTPase proteins such as elongation factors-G and -Tu (EF-G and EF-Tu), initiation factor-2 (IF2), as well as with interactions with release factors-1 and -2 (RF1 and RF2) during translation is referred to as the GTPase-associated center or region (GAR)(8). It contains three structural domains that are proximal on the 50S subunit: A pentameric complex ($L10.(L7/L12)_2$) that forms a protein stalk on the right shoulder of the 50S subunit (232,233); the highly conserved sarcin-ricin stem-loop domain (nt. 2646-2674 in *E. coli*) (81); and ribosomal protein L11 and its binding site on 23S rRNA (L11-binding domain-nt. 1051-1102 in *E. coli*), adjacent to the binding site of the pentameric complex. Ribosomal protein L11 and its binding domain on 23S rRNA (L11-rRNA complex) are involved in thiazole peptide antibiotic binding (thiostrepton and micrococcin) (143,176), have been implicated in binding of EF-G to the ribosome (71,72,201), and affect translation termination (153,269). Ribosomes lacking L11 are resistant to thiostrepton, show severely reduced levels of protein synthesis activity *in vitro*, and bind thiostrepton poorly relative to wild type ribosomes (270,271).

Thiostrepton has been found to inhibit most factor-dependent processes of GTPase proteins (e.g. see refs. (166,169); reviewed in (109)) and the functions of some non-GTPase factors (RF1 (272), RF2 (272), and stringent factor, RelA (273)) on the prokaryotic ribosome. Kinetic studies by Rodnina *et al.* indicated that thiostrepton binding to the L11-rRNA complex does not appear to interfere with factor binding or coupled GTPase activity on the ribosome. But, it inhibits EF-G turnover subsequent to GTP hydrolysis (169). However, recent biochemical analysis by Cameron *et al.*

indicated that thiostrepton and the related thiazole antibiotic, micrococcin, interfere directly with EF-G binding (166). Previous studies indicated that the effect of thiostrepton may be to prevent conformational transitions in either the RNA (274,275) or L11 (8,276) that are important for ribosome function. However, as thiostrepton appears to interact with both L11 and its 23S rRNA binding domain (73,172,276), it is not clear if a function of the protein or the rRNA is affected. Such apparently conflicting results emphasize a need for determining the structural basis and conformational requirements of the L11-rRNA domain that govern factor interactions during translation and its inhibition by thiostrepton.

With this in mind, we examined the effects on 23S rRNA structure, thiostrepton binding, and EF-G interactions in *Escherichia coli* mutants that lack functional endogenous L11 (153), mutants lacking L11 that were supplemented with an inducible plasmid bearing the entire L11 coding sequence (153), mutants bearing plasmids containing the coding sequence for C-terminal residues 68-142 of L11 (152), or mutants bearing a control plasmid without the L11 coding sequence (Table 3.1). Important structural changes were identified by using chemical modification techniques and by comparing the results from the mutant ribosomes in the presence and absence of thiostrepton with results from ribosomes from the isogenic parent strain (Table 3.1) and from ribosomes from which the ribosomal proteins had been extracted. To analyze the effects of the mutations on EF-G interactions with the ribosomes, we probed both pre- and post-translocation complexes of EF-G on the ribosome and compared the results for wild type and mutant ribosomes.

Our results revealed, not surprisingly, that the loss of ribosomal proteins induces extensive structural destabilization of the entire thiostrepton domain. Also, when all proteins except L11 are present, the L11-binding domain on the 50S subunit becomes conformationally flexible, but not on those ribosomes retaining only the C-terminal domain of L11. Both L11 and thiostrepton binding to rRNA on the 50S subunit induce significant tertiary structure changes in the L11-binding region. Thiostrepton-induced structural changes were proximal to the presumed thiostrepton binding site (141,143,277) and suggest that antibiotic binding may induce a tightening of the L11-rRNA junction and structural changes near the site of factor interactions that would interfere with factor binding to ribosomes. Finally, probing results in the presence of EF-G showed significant differences in the interactions of the factor with wild type and mutant ribosomes in the factor binding domains in the pre- and post-translocation states, revealing that the L11-stabilized structure of the rRNA is critically important for EF-G interactions in the post-translocation state.

Table 3.1. Strains Used for Isolation of 70S Ribosomes with Ribosomal Protein L11 Mutations

Strain	Name	Relevant Genotype	Ref. #
NVD001	wild type (wt)	wt L11 chromosomal gene (*rplK*)/pΔCAT (control plasmid)	(153)
NVD002	$L11N^{-}$	Δ*rplK*/pL11 (pΔCAT expressing 76 amino acid CTD of L11)	(152)
NVD003	$L11^{-/+}$	Δ*rplK*/pL11 (pΔCAT expressing wt L11)	(153)
NVD005	$L11^{-}$	Δ*rplK*/pACYC177 (control plasmid)	(153)

Experimental Procedures

L11 Mutant Strains- Bacterial strains used in the study were derived from *E. coli* K-12 (Table 3.1). Chromosomal L11 gene (*rplK*) knockout mutants of *E. coli* carrying plasmids for inducible (P_{tac} promoter) in vivo expression of the entire L11 protein from *E. coli* ($L11^{-/+}$) (153) or harboring a plasmid encoding the sequence for inducible expression of the C-terminal domain (residues 68-142) of L11 ($L11N^{-}$) were described previously (152). The L11 knockout mutant carrying a control plasmid without the L11 gene ($L11^{-}$) was constructed as described (153) but in an ampicillin resistance background (pACYC177). The strain without the L11 knockout, but harboring a control plasmid (pΔCAT) (153) was utilized as wild type for these studies.

Isolation of Mutant Ribosomes and Extraction of rRNA- *E. coli* strains harboring wild type, $L11N^{-}$, and $L11^{-/+}$ ribosomes were grown in 1 mM IPTG and 7 μg/mL tetracycline and the strain harboring $L11^{-}$ ribosomes in 1 mM IPTG and 100 μg/mL ampicillin ($L11^{-}$). Ribosomes from each strain were purified from frozen cells essentially as described (268,278). After isolation, $L11^{-}$, $L11N^{-}$, $L11^{-/+}$ and wild type ribosomes could not be distinguished upon sucrose gradient centrifugation or analytical ultra-centrifugation (data not shown), indicating that mutant ribosomes assembled normally. Naked rRNAs were prepared by phenol-chloroform extraction as described (265). Prior to probing, ribosomes (25 picomoles) were activated by incubation for 15 minutes at 37°C in 20 mM Hepes (pH 7.6), 5 mM MgOAc, 100 mM KCl, and 1 mM DTT ($H_{50}M_5K_{100}D_1$) buffer with or without the addition of thiostrepton in DMSO to the desired final concentration (1% DMSO). Controls were made 1% in DMSO.

Chemical Probing- Chemical probing with dimethyl sulfate (DMS), 2-keto-3-ethoxybutyraldehyde (kethoxal), or 1-cyclohexyl-3-(2-morpholinoethyl)-carbodiimide metho-p-toluenesulfonate (CMCT) were carried out in a manner adapted from Christensen *et al.* (279): 1 μL of 1:10 dilution of DMS in EtOH, 50 μl of 42 mg/mL CMCT in 1X-$H_{50}M_7K_{100}D_1$ buffer, or 5 μL of 40 mg/mL kethoxal in 20% EtOH was added to samples followed by incubation for 5 min. for DMS samples, 30 min. for DMCT samples, or 10 min. for Kethoxal samples respectively at 37°C. The samples were precipitated and phenol-chloroform extracted in preparation for use as templates for reverse transcriptase primer extension and PAGE analysis (240,280). Probing of thiostrepton titrations was carried out in the same manner as above with the addition of increasing amount of antibiotic in 100% DMSO (final concentration of DMSO was 2% in reactions to aid thiostrepton solubility at higher concentrations).

Purification of EF-G from E. coli- His_6-tagged EF-G on a pET24b-fusA plasmid was a generous gift of K. Lieberman and H.F. Noller and was over-expressed in *E. coli* strain BL21(DE3) by growing in LB with 30 μg kanamycin at 37°C to late log phase, inducing expression with the addition of 1 mM IPTG, and growth for 4 more hours. Cells were harvested by centrifugation and frozen for storage. His_6-EF-G was isolated as described (80,281) with the following modifications: (1) cell lysis was performed by grinding 10 g of frozen cells with 20 g of baked alumina; (2) EF-G bound to a Ni-NTA column was washed with 25 mL of buffer containing 10 mM imidazole (pH 8) before elution of protein.

Binding of EF-G Complex to 70S Ribosomes- Increasing concentrations of 70S ribosomes in 50 µl 1X-$H_{50}M_7K_{100}D_1$ buffer were incubated at 37°C for 10 min. with 0.5 µg/µl poly-U mRNA (Sigma) followed by the addition of $tRNA^{Phe}$ to 1.5 µM and incubation at 37°C for 10 min. To these pre-translocation complexes were added fusidic acid to 0.2 mM, [α-(^{32}P)]-GTP (Amersham) to 0.5 mM, and EF-G to 2 µM, followed by incubation at 37°C for 10 min. Subsequently, 45 µl of the reaction were filtered through 45 µm nitrocellulose filters and washed with 1 ml of ice-cold 1X-$H_{50}M_7K_{100}D_1$ buffer. Percent of ribosomes with bound EF-G complex was quantified by scintillation counting of washed filters and calculation of the concentration of retained radioactive signal from GDP in complex on ribosomes relative to controls incubated in the absence of ribosomes.

Probing EF-G-Ribosome Complexes- Fusidic acid or GDPNP-stabilized EF-G-Ribosome complexes were constructed in a manner similar to Moazed and Noller (72). Briefly, 0.5 µM 70S wild type or mutant ribosomes in 1X-$H_{50}M_7K_{100}D_1$ buffer were incubated for 10 min. at 25°C with 5 µg of poly-U mRNA (Sigma), followed by 10 min at 25°C with 1.5 µM of deacylated $tRNA^{Phe}$ from *E. coli* (Sigma). To these complexes were added either 0.5 mM GDP and 0.2 mM fusidic acid (Sigma) or 0.5 mM GDPNP (Sigma), followed by addition of EF-G to 2.5 µM and incubation at 25°C for 10 min. The complexes were probed with DMS, Kethoxal, and CMCT as above with minor deviations; probing temperature was 25°C and no DMSO was added to the reactions. Preparation of rRNA and primer extension analysis for probing reactions was as above for thiostrepton experiments.

Results

Chemical Probing of L11 Mutant Ribosomes

To determine whether the loss or truncation of L11 induced the loss of other ribosomal proteins, particularly the adjacent pentameric complex (L10.(L7/L12)$_2$) (141,232,282), from ribosomes, we compared the reactivities of several nucleotides in the region associated with pentameric complex binding, including C1044, A1046, G1047, A1050, G1110, A1111, and G1112. These reactivities did not differ between the wild type and mutant (L11N$^-$ and L11$^-$) ribosomes (Fig. 3.1a-c, lanes 2-6; Fig. 3.1). Importantly, the reactivity of nucleotide A1046, previously shown to interact directly with L10 upon pentameric complex binding (179,180), did not change in the L11$^-$ or L11N$^-$ ribosomes. These results corroborate previous results using two-dimensional SDS-PAGE analysis (152), that showed all proteins present except L11.

When all proteins were extracted from the rRNA, the reactivity of C1044, A1046, A1048, C1109, G1110, A1111, and G1112, as well as several residues on both sides of the lower D helix and throughout the entire rRNA domain differed markedly from the reactivities found for wild type and mutant ribosomes (Fig. 3.1a-d). The regional changes are presumably due to the loss of pentameric complex (L10.(L7/L12)$_2$) and ribosomal proteins L16, L13, L6, L36 interactions (178-180).

The reactivities of residues in the L11-binding region in L11$^-$and L11N$^-$ mutant ribosomes were clearly different from those on wild type ribosomes. The nucleotides in the L11-binding region that had altered reactivities on L11$^-$ ribosomes included those residues possibly involved in direct interactions with the protein (A1088, U1082, U1061,

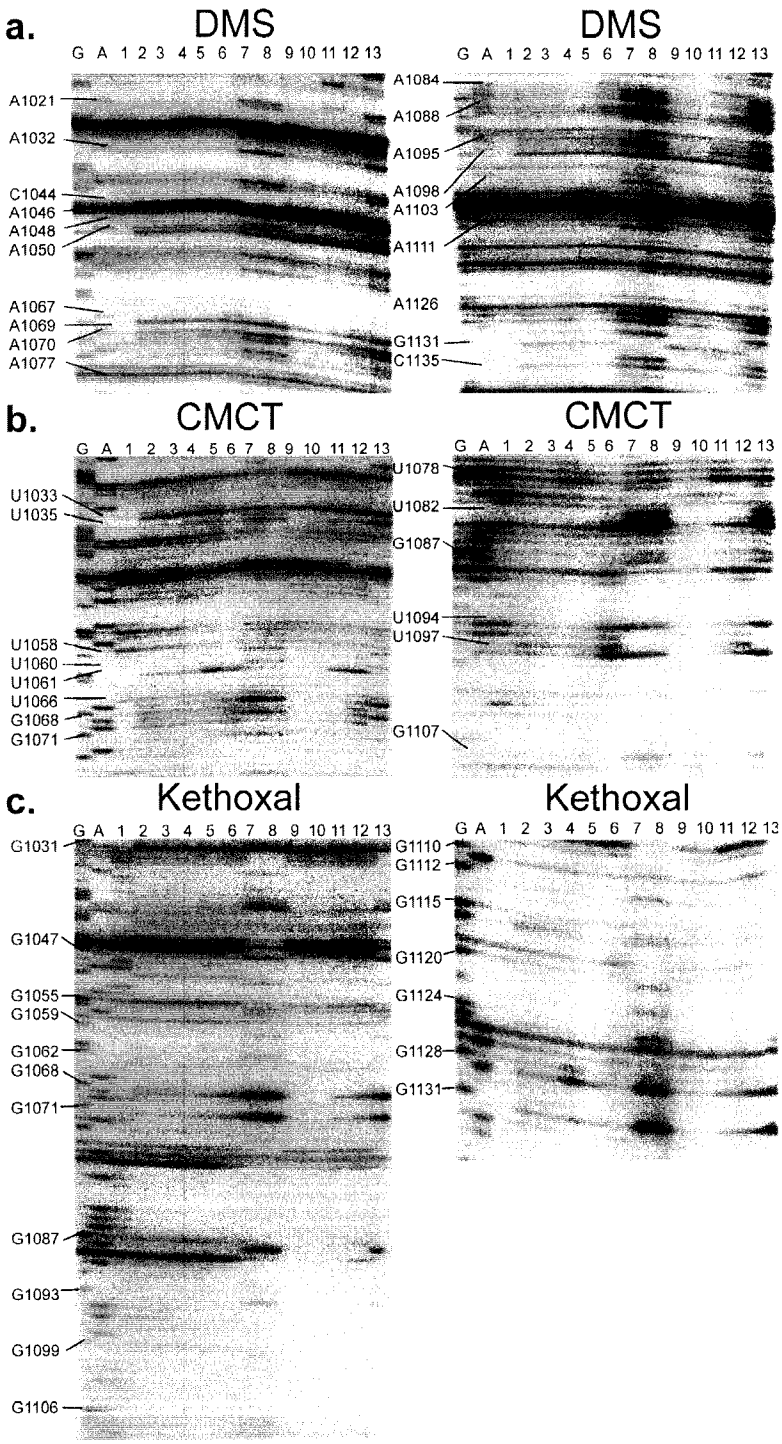

(Figure 3.1 Legend – Following Page)

Figure 3.1. Chemical Probing of Wild Type and Ribosomal Protein L11 Mutant Ribosomes. Conditions and probing techniques as described in Materials and Methods. (G and A): sequencing lanes; Lanes: (1) wild type 70S ribosomes without modification; (2) wild type 70S ribosomes probed without added DMSO (wt/c); (3) wild type 70S ribosomes (wt); (4) ribosomes from the L11$^-$ strain in which L11 was supplied by expression in vivo from a plasmid (L11$^{-/+}$); (5) ribosomes from L11$^-$ strain in which the C-terminal domain (residues 76-142) was supplied by expression in vivo from a plasmid (L11N$^-$); (6) ribosomes from the L11$^-$ strain (L11$^-$); (7) extracted rRNA from 70S ribosomes without added DMSO; (8) extracted rRNA from 70S ribosomes; (9) wild type ribosomes in the presence of 5 μM thiostrepton; (10) L11$^{-/+}$ ribosomes in the presence of 5 μM thiostrepton; (11) L11N$^-$ ribosomes in the presence of 5 μM thiostrepton; (12) L11$^-$ ribosomes in the presence of 5 μM thiostrepton; (13) extracted rRNA in the presence of 5 μM thiostrepton. Fig. 3.1a, DMS probing; Fig. 3.1b, CMCT probing; Fig. 3.1c, Kethoxal probing. The labels indicate the positions of the bases on the sequencing lanes. Modifications at the indicated bases prevent incorporation of the complementary nucleotide by the reverse transciptase and, therefore, bands appear one position below the modified base (representing a transcriptase product one base shorter.)

and A1070) (8,136), and also those potentially involved in tertiary interactions that stabilize the rRNA structure (U1066, G1068, G1071, U1083, A1089, U1094 and U1097) (274).

Interestingly, probing of L11N$^-$ ribosomes revealed only two nucleotides for which changes in reactivity could be traced exclusively to truncation of the N-terminal domain of L11. Nucleotide U1061 became hyper-reactive to CMCT in the absence of the N-terminal domain of L11, but displayed reactivity only slightly greater than that of wild type ribosomes for L11$^-$ ribosomes (Fig. 3.1b). This could be explained if U1061 is exposed in the rRNA structure stabilized by the C-terminal domain of L11, but is partially buried when the structure shifts in response to the absence of L11. Nucleotide A1070 became more reactive to DMS both in L11N$^-$ and L11$^-$ ribosomes (Fig. 3.1a). Changes in reactivity on L11$^-$ and L11N$^-$ ribosomes were not found outside of the L11-binding region of the rRNA.

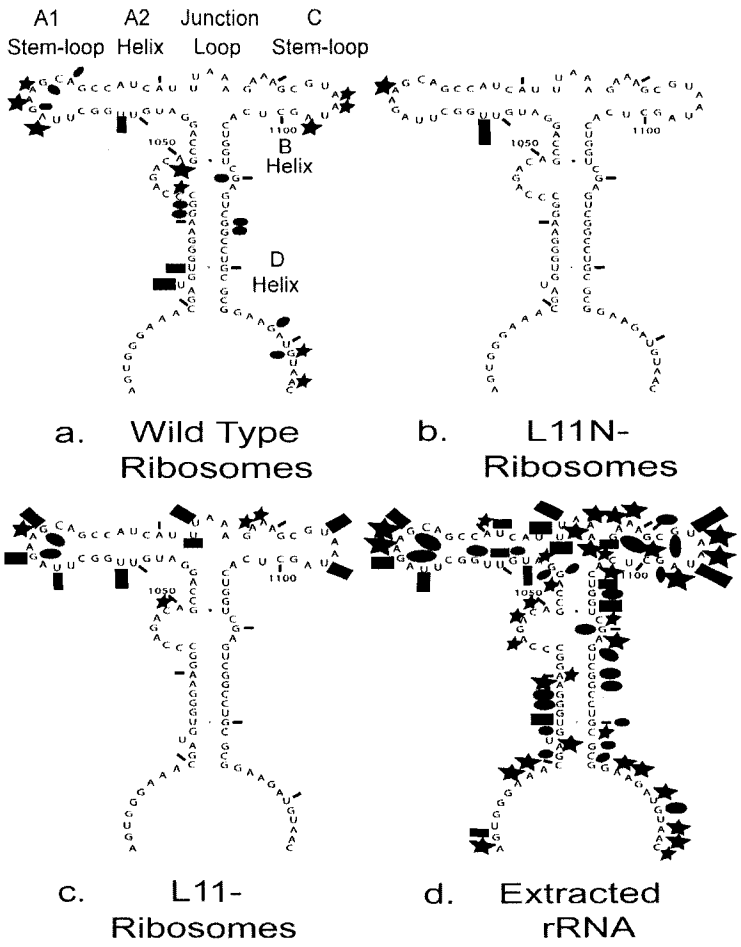

Figure 3.2. Chemical Modification Protection in the L11-Binding Region. Secondary structure maps of 23S rRNA in the L11-binding region showing the changes in reactivity to chemical probes, relative to wild type ribosomes, of nucleotides on L11N$^-$, L11$^-$ ribosomes, and phenol/chloroform-extracted rRNA. Star = DMS reactivity; Bar = CMCT reactivity; Oval = Kethoxal reactivity. The size of the symbols is proportional to the reactivity of the nucleotide to modifiers. Domains are labeled in Figure 3.2a according to the convention of Laing and Draper (283). The structure is derived from the Comparative RNA Web Site (www.rna.icmb.utexas.edu) (6).

Thiostrepton Interactions with Mutant Ribosomes

Chemical probing in the presence of thiostrepton on wild type ribosomes indicated protections at several residues previously associated with binding of the antibiotic (141,143), and at several additional sites (Table 3.2), including U1061

(CMCT), G1071 (Keth/DMS), and U1097 (CMCT). Probing of L11N$^-$ ribosomes, L11$^-$ ribosomes, and the extracted rRNA from ribosomes (Fig. 3.1, lanes 11-13) revealed only partial protection for L11N$^-$ ribosomes (~40-50% protection relative to wild type at most residues) and L11$^-$ ribosomes (~10-20%), and less than 10% protection for extracted rRNA relative to wild type in the presence of thiostrepton under the probing conditions. This is consistent with previous studies that showed a profound reduction in the affinity of thiostrepton for 23S rRNA versus intact ribosomes (176,275). Therefore, we

Table 3.2. Thiostrepton Protections of rRNA in Wild Type and Mutant 70S Ribosomes

rRNA Nucleotide	Reagent	% Protection[a] by Thiostrepton		
		70S(WT)	70S(L11N-)	70S(L11-)
U1061[b]	CMCT	40 ± 7	37 ± 6	3 ± 4
A1067	DMS	42 ± 5	21 ± 4	14 ± 4
G1068	Kethoxal	53 ± 14	24 ± 5	11 ± 5
A1070	DMS	56 ± 6	26 ± 5	(2 ± 3)[c]
G1071[b]	DMS	19 ± 3	16 ± 3	(1 ± 6)[c]
G1071[b]	Kethoxal	22 ± 6	20 ± 5	17 ± 6
A1095	DMS	44 ± 13	17 ± 5	14 ± 5
U1097[b]	CMCT	18 ± 4	1 ± 6	0 ± 4

a - % Protection is relative to ribosomes incubated without thiostrepton but otherwise treated in the same manner in parallel experiments. Values shown are for wild type and mutant ribosomes in the presence of 5 μM thiostrepton. Corrections for background and standard deviation are as described in the Figure 3.3 legend. CMCT, 1-cyclohexyl-3-(2-morpholinoethyl)-carbodiimide metho-p-toluenesulfonate; DMS, dimethyl sulfate; Kethoxal, 2-keto-3-ethoxybutyraldehyde; WT, wild type ribosomes; L11N-, 70S ribosomes with only the C-terminal domain residues 68-142 of ribosomal protein L11 present; L11-, ribosomes lacking the entire L11 protein. **b** – Novel protections revealed in this study. **c** – parentheses indicate an increase in reactivity relative to controls in response to added thiostrepton.

anticipated saturation of thiostrepton protection near wild type levels for mutant ribosomes probed in the presence of higher levels of antibiotic. However, protection levels on mutant ribosomes never reached the levels of wild type ribosomes. This may be explained if antibiotic binding on wild type ribosomes is dependent upon interactions with the N-terminal domain of L11 (276,277), and, therefore, the binding interaction differs for mutant ribosomes.

Although many of the residues protected by thiostrepton on wild type ribosomes were at least partially protected on L11N$^-$ ribosomes and L11$^-$ ribosomes, several residues (U1061, U1097, and A1070) did not appear to be (Fig. 3.1, lanes 11-12). This may be attributable to an interaction between the N-terminal domain of L11 and the rRNA upon thiostrepton binding, as is suggested in the crystal structure of the L11-rRNA complex (8) (see also Fig. 3.6b) To test this, we added increasing amounts of thiostrepton to wild type and mutant ribosomes and probed them with modifiers as above.

The results from a representative experiment for protection at A1067 are shown in Figure 3.3. In most cases, wild type ribosomes were protected more than mutant ribosomes at a given concentration of thiostrepton, saturating above 5 μM (Fig. 3.3). Both U1061 and A1070 are protected by thiostrepton on wild type and L11N$^-$ ribosomes. However, that protection is completely lost on L11$^-$ ribosomes. Nucleotide U1097 is the only residue that is protected by thiostrepton on wild type ribosomes, but that is not protected on either L11N$^-$ or L11$^-$ ribosomes. This indicates that tightening of the L11-rRNA junction probably occurs only near the proximal apices of the A1 and C stem-loops of the rRNA and the N-terminal domain of L11 (Fig. 3.6b).

EF-G Interactions with Mutant Ribosomes

As the L11-binding region of the 70S ribosome is known to participate in binding of translation elongation factors, we undertook to study the effects of the L11 deletion

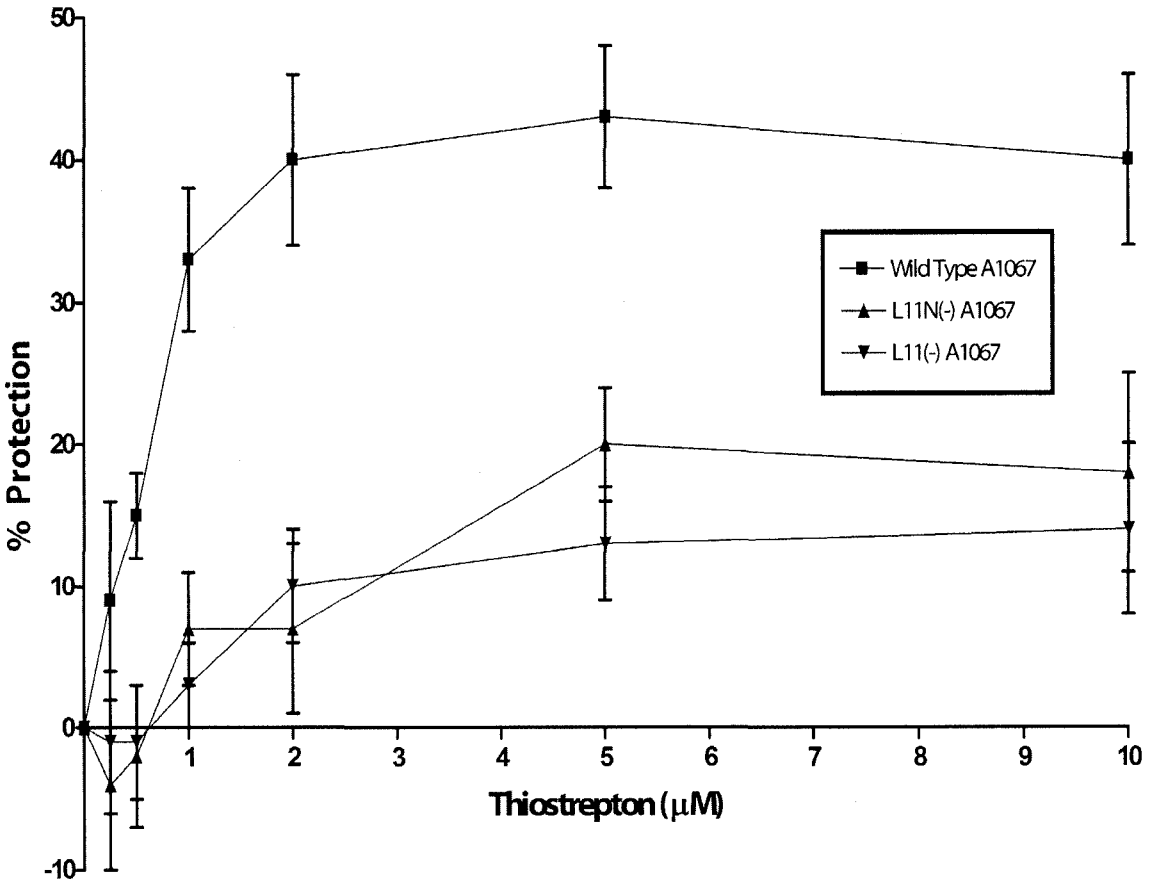

Figure 3.3. Protection of rRNA Residue A1067 by Thiostrepton Binding to the Ribosomes. (a), Wild type or ribosomes with deletions or truncations of ribosomal protein L11 were incubated with increasing concentration of thiostrepton, were probed with DMS, Kethoxal, or CMCT, and were analyzed for the protection of residues from chemical modification. % Protection is relative to ribosomes incubated without thiostrepton but otherwise treated in the same manner in parallel experiments. Standard deviations (3 independent experiments/2 ribosome preparations) are represented as error bars and are calculated based on the differences in intensity between bands in modification lanes with and without the addition of thiostrepton, corrected for differences in the lane intensities in the L11-binding rRNA region of the phosphorimager scans. The graph shows a representative experiment for protections at A1067. Results for other residues protected by thiostrepton binding are listed in Table 3.2.

and truncation mutations on the interactions of EF-G with ribosomes. To do this, we utilized two approaches. First, we used fusidic acid, an antibiotic that binds to the EF-G-GDP-ribosome complex and prevents dissociation of EF-G from the ribosome following GTP hydrolysis, stalling the complex in a post-translocation intermediate state (284). Second, we used guanosine 5'-[ß,γ-imido]triphosphate (GDPNP), a non-hydrolyzable nucleotide analog that binds EF-G, prevents coupled GTP hydrolysis on the ribosome, and stalls the ribosome complex in a pre-translocation intermediate state (80,285). By adding EF-G along with each of these components to translocation-competent wild type or mutant ribosomes (70S + poly-U mRNA + tRNA), we were able to compare the interactions of EF-G with the factor binding domains of the large ribosomal subunit in both the pre- and post-translocation states.

Several residues in the L11-binding region (Table 3.3) showed changes in reactivity to chemical modifiers upon the addition of the EF-G complexes to wild type and mutant ribosomes. A previous report identified A1067 and A1069 as residues that are protected upon binding of EF-G to wild type ribosomes (72). Our probing identified protection at A1067 for both fusidic acid-stabilized and GDPNP-stabilized complexes (Fig. 3.4b, Table 3.3). The reactivity of U1061 was increased in the presence of the EF-G-GDP-fusidic acid complex (Fig. 3.4a), and U1097 showed a slight increase in reactivity on wild type ribosomes upon the addition of the fusidic acid, but not the GDPNP-stabilized complex (Fig. 3.4c).

L11N$^-$ ribosomes showed protection at a level similar to wild type at A1067 for both the fusidic acid and GDPNP-stabilized complexes (Fig. 3.4b). However, L11N$^-$ ribosomes were not protected at U1061 or U1097 in the presence of either complex (Fig.

3.4a,c), suggesting that the N-terminal domain of the protein is required to protect these residues on wild type ribosomes prior to EF-G interactions. Residue A1067 was not significantly protected in L11$^-$ ribosomes by the fusidic acid-stabilized or the GDPNP-stabilized-complexes (Fig. 3.4b). This result correlates well with our results from the EF-G binding study (Fig. 3.5) that show little binding of the EF-G-GDP-fusidic acid complex to L11$^-$ ribosomes relative to L11N$^-$ and wild type ribosomes. Similarly, U1061, A1070, and U1097 did not show changes in reactivity on L11$^-$ ribosomes for either complex (Fig. 3.4a-c).

We did not see protections at A1069 on any of the combinations of ribosomes and EF-G complexes used in this study (Fig. 3.4b). This is in contrast to the results of Moazed *et al.* (72) that described a small but significant protection by EF-G at this position. The possible reasons for this difference include the alternative buffers (specifically 10 mM Mg^{2+} versus 5 mM Mg^{2+} in our reactions) and probing temperatures (0°C versus 25°C in our reactions). It is possible that lower Mg^{2+} concentrations or higher temperatures may induce destabilization of complexes by increasing the off-rate of bound factors, leading to increased reactivity to chemical modifiers. However, the level of protection at the many of the other residues protected by EF-G complexes is comparable between the two studies, indicating that the interaction at A1069 may be particulary sensitive to environmental conditions.

When we probed another element of the GTPase-associated region, the sarcin-ricin stem-loop, a short stem-loop with the apex around nucleotide A2660 of 23S rRNA, we discovered a significant distinction (Fig. 3.4d-e, Table 3). First, wild type and L11N$^-$ ribosomes were protected to a similar extent at G2655, A2660, and G2661 by the EF-G-

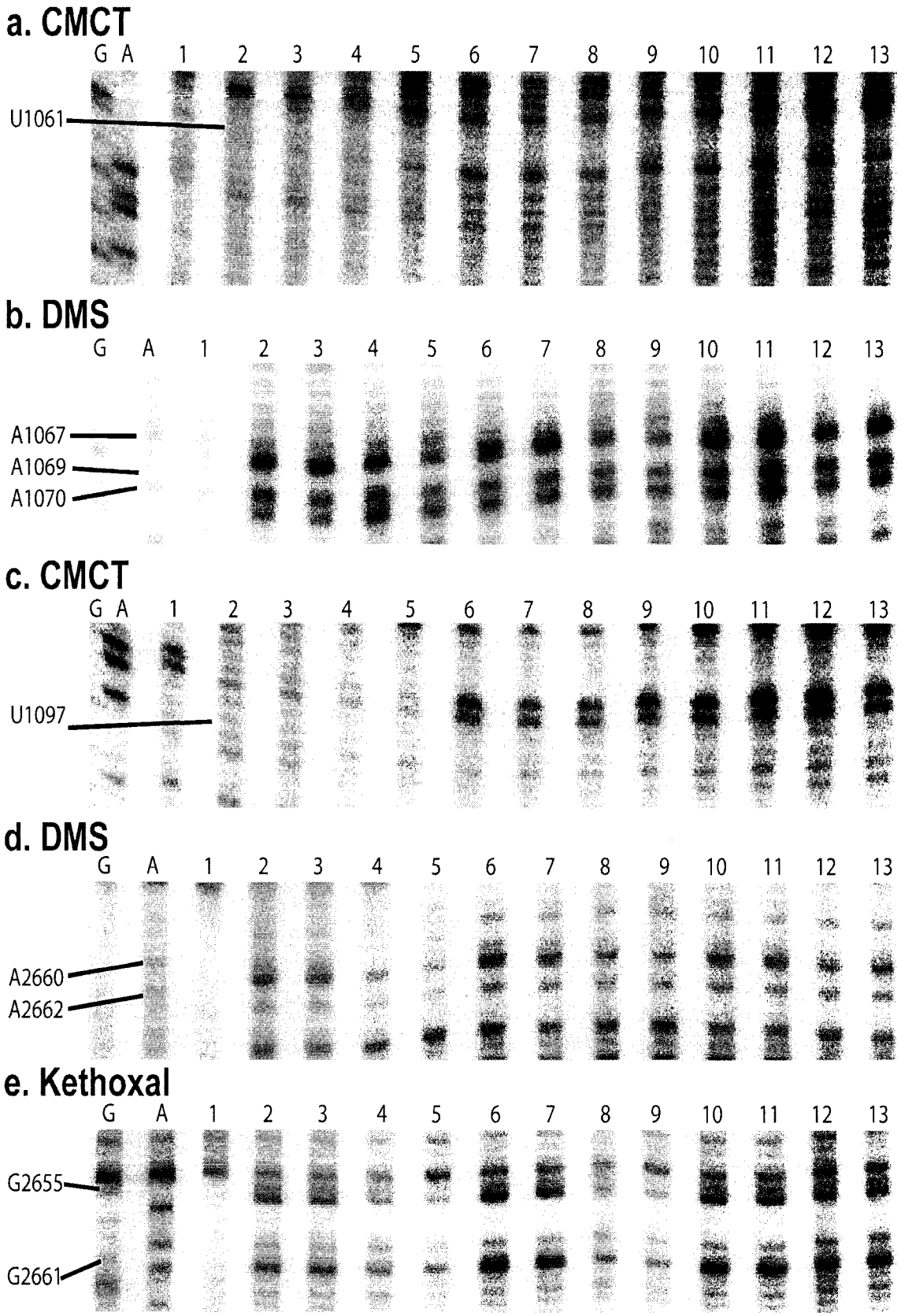

(Figure 3.4 Legend – Following Page)

Figure 3.4. Interactions of EF-G with the L11-Binding Region of rRNA. Complexes of wild type and mutant ribosomes with either EF-G-GDPNP or EF-G-GDP-fusidic acid were probed with DMS, Kethoxal, and CMCT. Fig. 3.4a: G and A sequencing lanes; (1) control without chemical modifier; (2) wild type 70S ribosomes with chemical modifier; (3), wild type 70S ribosomes + poly-U mRNA + $tRNA^{Phe}$; (4), wild type 70S + poly-U mRNA + $tRNA^{Phe}$ + EF-G-GDPNP; (5) wild type 70S + poly-U mRNA + $tRNA^{Phe}$ + EF-G-GDP-Fusidic Acid; (6), L11N$^-$ 70S ribosomes with chemical modifier; (7), L11N$^-$ 70S ribosomes + poly-U mRNA + $tRNA^{Phe}$; (8), L11N$^-$ 70S + poly-U mRNA + $tRNA^{Phe}$ + EF-G-GDPNP; (9), L11N$^-$ 70S + poly-U mRNA + $tRNA^{Phe}$ + EF-G-GDP-Fusidic Acid; (10), L11$^-$ 70S ribosomes with chemical modifier; (11), L11$^-$ 70S ribosomes + poly-U mRNA + $tRNA^{Phe}$; (12), L11$^-$ 70S + poly-U mRNA + $tRNA^{Phe}$ + EF-G-GDPNP; (13), L11$^-$ 70S + poly-U mRNA + $tRNA^{Phe}$ + EF-G-GDP-Fusidic Acid. Modifications at the indicated bases prevent incorporation of the complementary nucleotide by the reverse transciptase and, therefore, bands appear one position below the modified base (representing a transcriptase product one base shorter.)

Table 3.3. EF-G Protections of rRNA in Wild Type and Mutant 70S Ribosomes

rRNA Nucleotide	Probing Reagent	% Protection[a] by EF-G-GDPNP			% Protection by EF-G-GDP-FA		
		70S WT	70S L11N-	70S L11-	70S WT	70S L11N-	70S L11-
U1061	CMCT	2 ± 6	5 ± 8	5 ± 9	(27 ± 6)[b]	4 ± 1	6 ± 9
A1067	DMS	17 ± 5	23 ± 7	8 ± 6	41 ± 8	32 ± 9	4 ± 8
A1069	DMS	3 ± 6	(7 ± 6)[b]	9 ± 12	(4 ± 8)[b]	10 ± 9	8 ± 9
U1097	CMCT	(4 ± 6)[b]	2 ± 7	7 ± 7	(15 ± 5)[b]	(4 ± 12)[b]	9 ± 7
G2655	Kethoxal	43 ± 9	37 ± 7	15 ± 10	57 ± 8	49 ± 8	3 ± 8
A2660	DMS	53 ± 7	24 ± 5	19 ± 7	46 ± 5	49 ± 5	(3 ± 6)[b]
G2661	Kethoxal	36 ± 10	44 ± 8	13 ± 8	52 ± 9	56 ± 6	1 ± 5

a - % Protection is relative to the reactivity of ribosomal residues in the absence of added EF-G (see **Experimental Procedures** for complex constituents). Values are an average of 3 experiments. Corrections for background and standard deviation are as described in the Figure 3.3 legend. **b** – parentheses indicate an increase in reactivity relative to controls in response to complex binding. CMCT, 1-cyclohexyl-3-(2-morpholinoethyl)-carbodiimide metho-p-toluenesulfonate; DMS, dimethyl sulfate; Kethoxal, 2-keto-3-ethoxybutyraldehyde; GDPNP, guanylyl-5'-imidodiphosphate; WT, wild type; L11N-, 70S ribosomes with only the C-terminal domain residues 68-142 of ribosomal protein L11 present; L11-, ribosomes lacking the entire L11 protein; EF-G, elongation factor-G.

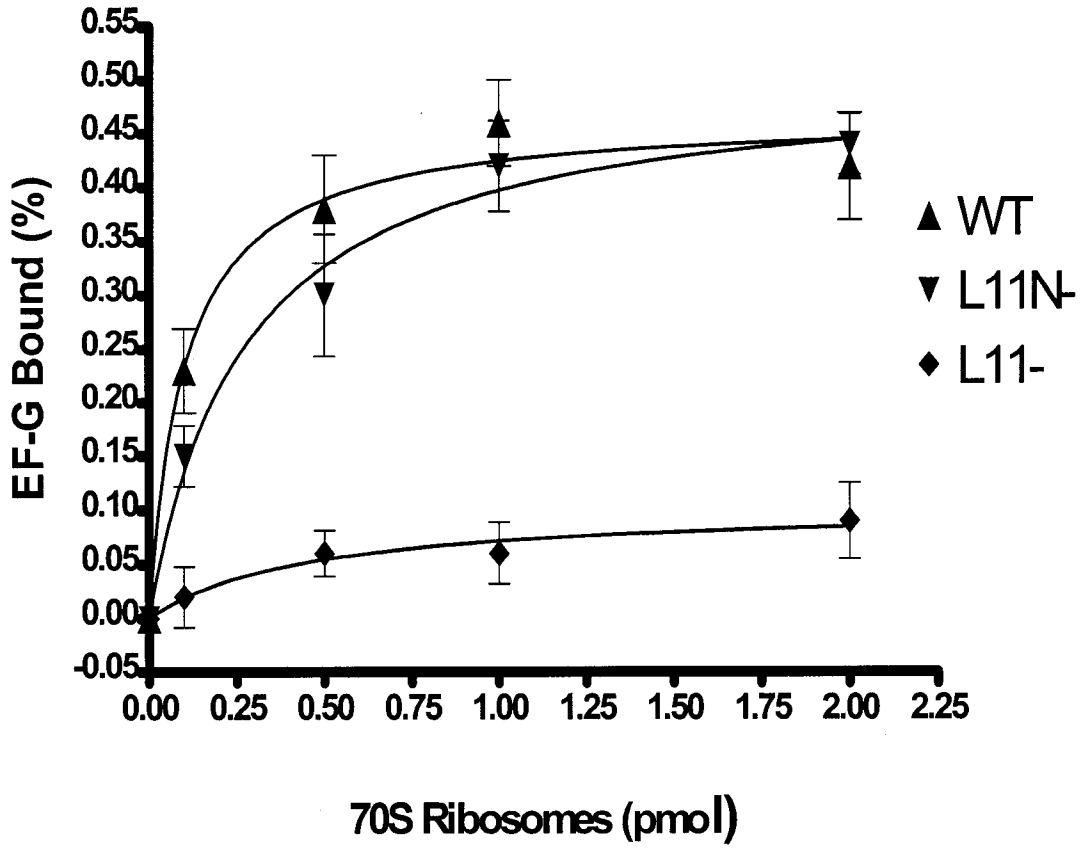

Figure 3.5. Binding of EF-G to Wild Type and L11 Mutant Ribosomes. Binding of EF-G-GDP-fusidic acid (as % of ribosomes with bound complex relative to controls without added ribosomes) was quantified by filtering complexes of increasing concentrations of wild type or mutant ribosomes with poly-U mRNA (0.5 μg/μl), $tRNA^{Phe}$ (1.5 μM), EF-G (2 μM), [α-(^{32}P)-GTP] (0.5 μM), and fusidic acid (0.2 mM) through nitrocellulose filters and scintillation counting of radioactivity left on the filters (see experimental procedures for details). Results are an average of ≥2 experiments with standard deviations for experiments are shown. WT, wild type 70S ribosomes; L11N$^-$, 70S ribosomes with only the C-terminal domain (residues 68-142) of ribosomal protein L11 bound; L11$^-$, 70S ribosomes lacking L11.

GDPNP complex and the EF-G-GDP-fusidic acid complex (Fig 5d-e). In contrast, L11$^-$ ribosomes were protected to a very limited extent by the EF-G-GDPNP complex, and were not protected above background by binding of the fusidic acid-stabilized complex (Fig. 3.4d-e). This suggests that the GDPNP- and fusidic acid-stabilized complexes interact poorly to ribosomes in the absence of L11.

As L11$^-$ ribosomes were not protected by the EF-G-GDP-fusidic acid complex in either the L11-binding domain or the sarcin-ricin domain, we reasoned that L11$^-$ ribosomes may not effectively bind the complex in the post-translocation state. Therefore, we utilized filter-binding analysis to determine the extent of binding of radiolabeled EF-G-GDP-fusidic acid complex on wild type and mutant ribosomes. Figure 3.5 illustrates that wild type and L11N$^-$ ribosomes bind the complex to similar extents, while binding to L11$^-$ ribosomes is only slightly above background levels. As the only difference between L11N$^-$ and L11$^-$ ribosomes is the presence of the C-terminal domain, the results further establish the importance of this domain of L11 for EF-G binding in the post-translocation state.

Discussion

Modulation of Structure in the L11-Binding Domain

The results of this study suggest that L11 binding stabilizes key tertiary interactions in the rRNA structure around the L11-binding domain. For instance, nucleotides G1071 and A1089 involved in two important base triple interactions (G1071:G1091:C1100; A1089:A1090:U1101 (8,136)), became reactive in the absence of L11. In addition, bases U1066, U1083, and U1094, each involved in a U-turn motif (286), became reactive on L11$^-$ ribosomes. Finally, G1068 and A1096 became reactive in ribosomes lacking L11. G1068, in the A1 stem-loop, normally interacts with the phosphate backbone of A1096 in the C stem-loop, stabilizing the juxtaposition of the two stem-loops (8).

L11 binding also protected A1088 and U1082 from chemical modification. The A1088:U1060 reverse-Hoogsteen base pair is a universally conserved feature of this rRNA domain and probably stabilizes the long-range interactions of the A1 and C helices. The reverse-Watson-Crick U1082:A1086 base pair closes the short junction loop and participates in a ribose zipper-minor groove interaction that stabilizes the interaction between the junction loop and the B helix (8). Taken together, these results indicate that L11 binding to the rRNA combines stabilization of key tertiary interactions with stabilization of the rRNA backbone fold, a strategy that has also been documented for another ribosomal protein, S15 (216).

Our results for L11$^-$ and L11N$^-$ ribosomes indicate that the rRNA in the L11-binding region becomes conformationally flexible only in the absence of the entire L11 protein, and not when the C-terminal domain is present. Therefore, the results do not support the model in which reversible dissociation of the N-terminal domain of L11 governs a functional transition in the structure of the associated rRNA (275). But, the results do favor a model in which the N-terminal domain of L11 modulates direct interactions of L11 with factors (71,276), while the C-terminal domain stabilizes the conformation of the L11-binding rRNA. This would explain why nucleotides U1061 and A1070, which are packed against Gln-12 and Lys-10 at the junction of the L11 N-terminal domain and the L11-binding rRNA (Fig. 3.6c), become hyper-reactive in L11N$^-$ mutants.

Thiostrepton Interactions in the L11-Binding Domain

Many protections from thiostrepton binding occur in the binding cleft between the proximal apices of the A1 and C stem-loops of the rRNA (Fig. 3.6a). However, the

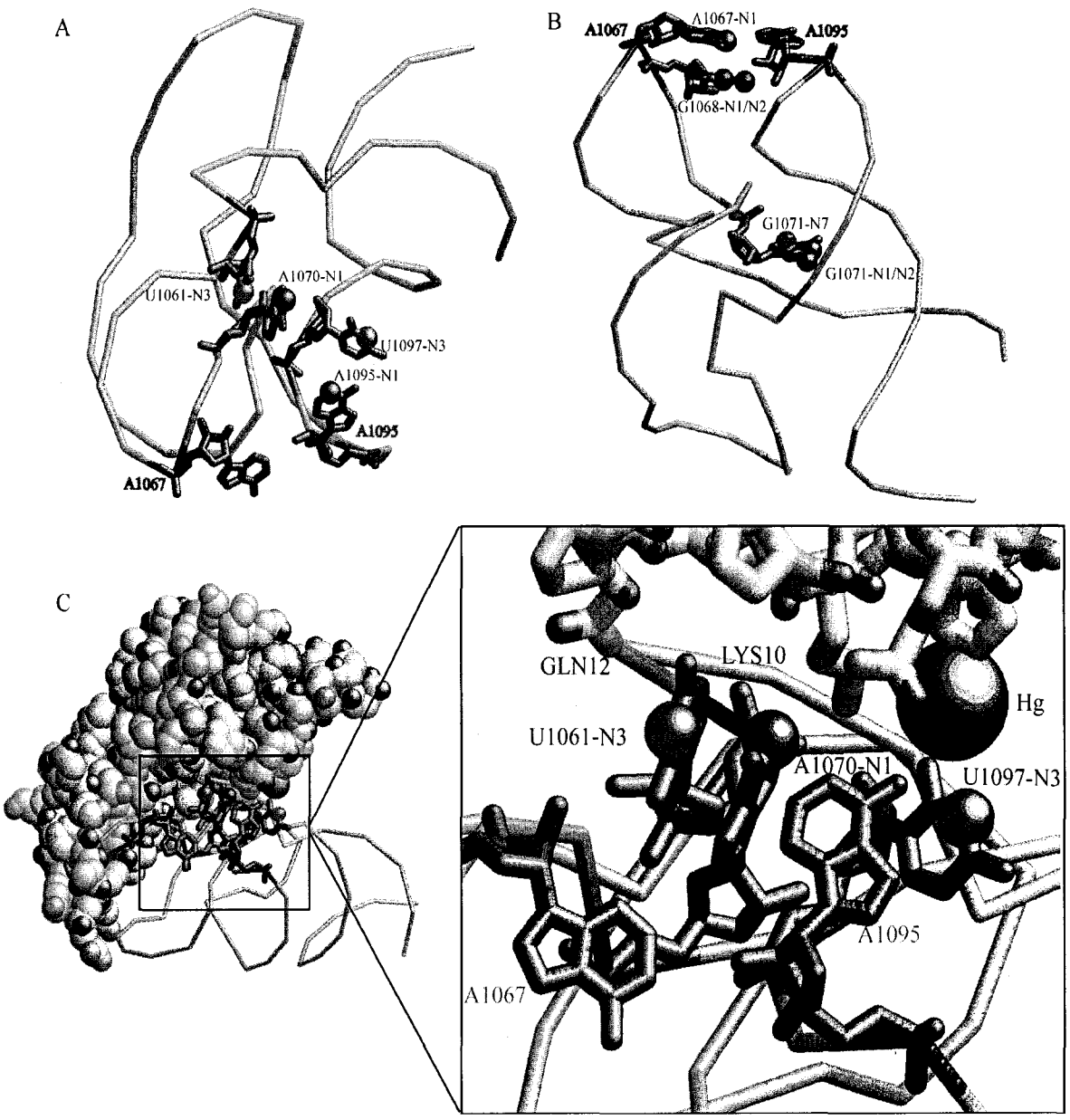

Figure 3.6. Chemical Modification Protection of rRNA by Thiostrepton Shown on the Crystal Structure of the rRNA Fold (Protein Data Bank: 1MMS (8)). (A) Protections on the top face of the L11-binding domain rRNA in the cleft between the A1 and C stem-loops. Blue = previously identified protections; green = novel protections from this study. (Residue numbers (*E. coli* numbering) and atom positions are labeled). (B) Protections on the bottom face (opposite side of structure shown) of the L11-binding domain rRNA. (B) Potential interactions of rRNA bases with residues from the N-terminal domain of L11 (N-terminal residues shown in wireframe for clarity, and the coloring and labeling are as in A and B). A mercury ion, present in the crystal structure, suggest a potential ion mediated interaction between U1097 and the L11. Figures made using RASMOL (4).

known thiostrepton protection at A1070 and novel protections found in this study (U1061 and U1097) suggested that thiostrepton binding may induce a tightening of the junction between the rRNA and the N-terminal domain of L11. However, by titrating thiostrepton to saturating concentrations in the probing reaction, we discovered that only the protection of U1097 was specifically dependent upon the presence of the N-terminal domain of L11. As the concentration of thiostrepton was increased, U1061 and A1070 became protected on L11N$^-$ ribosomes, but not on L11$^-$ ribosomes. Therefore, protection of these two residues is dependent upon the presence of only the C-terminal domain of L11. As the C-terminal domain of L11 in known to responsible for binding and stabilization of the rRNA structure in the L11-binding region (142), we propose that only this stabilized structure of the L11-binding domain presents A1070 and U1061 in the orientation necessary for antibiotic interactions. Conversely, thiostrepton binding to the rRNA may induce a conformational change around U1061 and A1070 that protects these residues from modification. This protection does not occur in the absence of L11, or at least the C-terminal portion of L11.

Additional changes in reactivity induced by thiostrepton involve residues adjacent to but probably outside of the binding site. The changes in reactivity of G1071, part of a crucial base triple at the junction of the four helices (Fig. 3.2a) that stabilizes the rRNA fold (274), changes at U1061 and A1070 and several thiostrepton-induced reactivity changes on the rRNA surface opposite the L11 interaction (Fig. 3.6b), suggest that either

A recent NMR study described docking of thiostrepton onto the crystal structure of the L11-binding rRNA (277). The authors postulated that the likeliest direct interactions of thiostrepton with 23S rRNA are with residues A1067, A1095, and A1096

at the apices of the A1 and C stem-loops (Fig. 3.6a). This provides further evidence that the distal surfaces of the rRNA must both be indirectly but significantly altered by antibiotic binding. These alterations could be substantial enough to account for the effect of the antibiotic on factor interactions.

Interactions of EF-G with the L11-Binding Domain

The evidence outlined above provides important insight into the function of the L11-binding domain of large subunit rRNA. Although it has long been suspected that this domain forms part of the factor binding site or GTPase-associated domain on the large subunit, little is known about the structural requirements for this function. Previous reports suggested that EF-G may undergo GTPase-associated conformational changes on the ribosome in the process of stimulating translocation of tRNAs from the peptidyl (P) site to the exit (E) site and acceptor (A) site to the P site (135,287). Such changes would probably require distinctive modes of interaction with the ribosome in the pre- and post-translocation states.

Our results corroborate data from a recent report (80) that described increases in EF-G protections from hydroxyl radicals in the L11-binding domain rRNA following translocation and GTP hydrolysis (fusidic acid-stalled complex). In our study, protection of A1067 in this domain is 50% higher in the presence of this complex versus the pre-translocation (GDPNP-stalled) complex. This difference may be associated with a shift in domain V of EF-G towards the L11-binding domain following translocation seen in recent cryo-electron microscopic studies (135,287). The present study also provides evidence that the N-terminal domain of L11 probably reversibly dissociates from the L11-binding rRNA in a step following translocation. Nucleotide U1061, a residue

closely associated with the N-terminal domain of L11 in an x-ray crystal structure of the ribosomal fragment containing L11 and the L11-binding domain rRNA (8), becomes reactive to chemical probes both in L11N⁻ mutants and when EF-G is stalled on the ribosome in complex with GDP and fusidic acid (Fig. 3.2, 3.5). However, this reactivity is not evident on ribosomes lacking bound EF-G-GDP-fusidic acid, nor on ribosomes

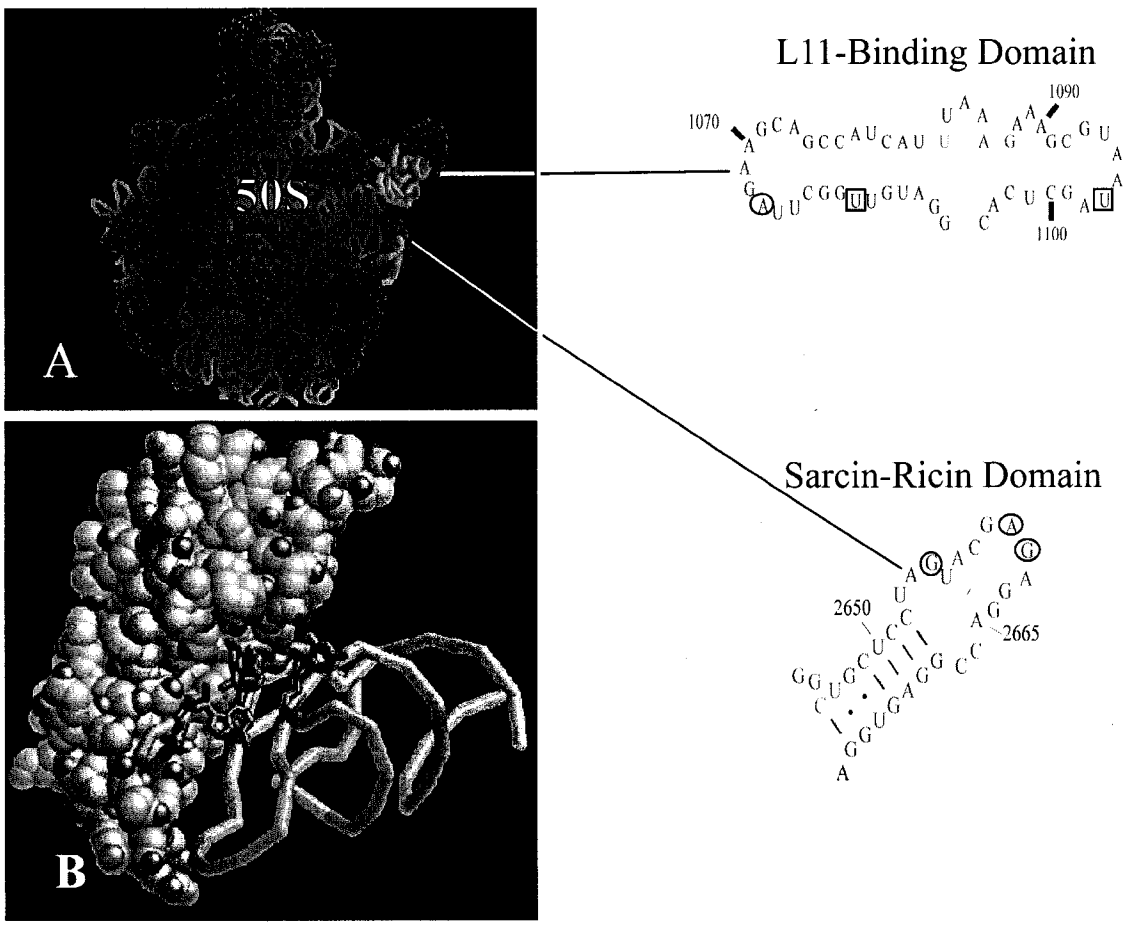

Figure 3.7. Protection of rRNA Residues upon EF-G binding. (a) Location of L11-binding domain and sarcin-ricin domain on 50S subunit of *Haloarcula marismorui* . Secondary structure of the two domains is shown blown up to indicate the chemical modification protections from EF-G-GDP-fusidic acid complex binding that are absent on ribosomes lacking ribosomal protein L11. Circles = modification protection; Squares = modification enhancement. (b) Location of the residues in the L11-binding domain of wild type ribosomes that show a change in chemical modification when EF-G is bound. Red = A1067; purple = U1061; green = U1097. Figures made using RASMOL (4) and derived from the L11-rRNA crystal structure (8).

with EF-G bound in the pre-GTPase state (EF-G-GDPNP). A similar change is postulated from the results of a cryo-electron microscopic study of the same complex (71).

Our results with mutants of ribosomal protein L11 suggest that stabilization of the post-translocation state is acutely dependent upon a specific structure of the L11-binding domain rRNA that is stabilized by its interaction with the C-terminal domain of L11 (Fig. 3.7). Only ribosomes with the C-terminal domain present are able to form substantial post-translocation complexes. Protections of rRNA in the sarcin-ricin domain by the pre-translocation complex are also reduced significantly (Figure 3.4; A2660, G2655, G2661) on ribosomes lacking L11, suggesting that the structure of the L11-binding domain is involved in stabilization of the pre-translocation state as well. Previously it was also suggested that the proximal L10-binding domain in the region around the A1050 internal loop (Fig. 3.2) may also be associated with pre-translocation complex formation (80). The significance of these structural transitions is not fully understood. Changes in the conformation of EF-G on the ribosome are postulated to induce changes in ribosome structure that drive the process of translocation (287). The structural basis of these conformational changes and concomitant structural changes at the molecular level will be the subject of future studies.

Acknowledgments

We would like to thank Martha J. Rice and Stephen George for technical assistance, Scott Hennelly for purification of EF-G, and Klas Hedenstierna and Letizia Brandi for critical reading. This research is supported by U.S.N.I.H grant GM35717 to W.E.H and GM21499 to E.J.M.

Chapter 4

Functional Studies on Mutants of Ribosomal Protein L11

Introduction

Previous studies on ribosomes lacking ribosomal protein L11 indicated that, in the absence of the protein, *in vitro* translation decreased greater than 50% (288). In addition, the EF-G-dependent GTPase activity of the mutant ribosomes was reduced significantly. The ribosomes used in the previous study were isolated from a strain of *Bacillus megaterium* by selection for resistance to thiostrepton, an antibiotic believed to bind in the L11-binding rRNA domain of the large ribosomal subunit (172,176). The results of these studies prompted us examine the effects on *in vitro* translation and GTPase activity of a chromosomal L11 gene (*rplK*) knockout mutation in *Escherichia coli* ($L11^-$) (153). To further understand the role of L11, we also examined the translation and GTPase activities of the same L11 knockout mutant that expressed the C-terminal domain of L11 *in vivo* from a recombinant plasmid vector ($L11N^-$) (152). The C-terminal domain of L11 is believed to anchor the protein to its binding site on 23S rRNA, while the N-terminal domain of L11 has been found to regulate the interaction of RF-1 with ribosomes during translation termination (152), and the factor RelA-dependent synthesis of guanosine tetra- and pentaphosphate (ppGpp and pppGpp) (155,157). Guanosine pentaphosphate is known as the "stringent factor" due to its role in regulating the response of bacteria to conditions of amino acid starvation.

Our study of the L11 mutants included a comparison of the growth rates of mutant strains with wild type *E. coli*, a comparison of the *in vitro* translation rates of L11 mutant ribosomes in the presence or absence of translation elongation factors with the rates of translation for wild type ribosomes, and a comparison of the ribosome/EF-G- dependent

GTP hydrolysis rates for L11 mutant ribosomes with the rates of hydrolysis for wild type ribosomes.

Significant growth defects were found for both ribosomal protein L11 mutant strains with ribosomes lacking the C-terminal domain of L11 and mutants lacking the entire L11 protein. To elucidate the possible cause of the growth defects, we studied ribosomes from the mutants strains in an *in vitro* translation system that specifically analyzes the elongation stage of translation, translation of poly-uridylic acid (poly-U) synthetic mRNA. This system does not require factor-dependent formation of initiation complexes and does not favor factor-dependent translation termination, as it encodes neither start nor termination codons. The results from *in vitro* translation assays performed in the presence or absence of translation elongation factors, EF-G and EF-Tu, suggested that both $L11^-$ and $L11N^-$ mutant ribosomes primarily have a defect in EF-G-dependent functions during the elongation stage of translation.

Finally, to help uncover what aspect of EF-G was most significantly affected by mutations in L11, we analyzed the rates of EF-G/ribosome-dependent GTP hydrolysis on the wild type and L11 mutant ribosomes. As L11 and the L11-binding rRNA have previously been linked to factor-dependent GTP hydrolysis on the ribosome, we hypothesized that the defect of the L11 mutant ribosomes *in vitro* translation is related to a defect in the rate of EF-G-dependent GTP hydrolysis. Ribosome-dependent hydrolysis of GTP in the GTP-binding domain of EF-G is believed to occur following the transfer of the nascent peptide from P- to A-site tRNA during the process of EF-G-dependent translocation of A- and P-site tRNA to the P- and E-sites respectively (49). Mutations in L11 have previously been shown to affect EF-G-dependent GTP hydrolysis (288). In our

analysis, differences in the rates of GTP hydrolysis for the wild type and mutant ribosomes suggested that the presence of L11, and specifically the N-terminal domain of L11, may affect the turnover of EF-G on the ribosome. The defect in EF-G turnover on mutant ribosomes caused by the L11 mutations, therefore, may be a factor that contributes to slower translation rates. The effect could also account for the slow growth phenotype of the L11 mutant strains. The significance of these results and the potential for future experiments are discussed.

Results

Growth Characteristics of L11 Mutant Strains

Previous studies on the effect of L11 mutations on the growth of bacteria have been done on strains that were isolated by selection for thiostrepton resistance. These studies showed a dramatic increase in the doubling time for strains harboring ribosomes that lacked L11 (152,288). As part of our characterization of the L11 mutant strains, therefore, we compared the growth of the wild type (wt) *Esherichia coli* strain with that of the knockout $L11^-$ mutant and knockout mutants in which either the entire L11 protein ($L11^{+/-}$) or the C-terminal domain (76 amino acids) of the L11 protein ($L11N^-$) were supplied by *in vivo* expression from a plasmid. Table 4.1 shows calculated doubling times for the four strains tested at three different temperatures. The use of three different temperatures allowed us to analyze the temperature dependence of the growth lesions in the L11 knockout strains.

The values for growth of the L11 mutants in Table 4.1 compared favorably with those found by our collaborators (152) for many of the same strains, with one minor exception. In our study, the $L11^{+/-}$ strain grows slightly but reproducibly slower than the

Table 4.1. Growth Characteristics of L11 Mutants		
[a]Strain	[b]Genotype	[c]Doubling Time (minutes)
wild type (wt) (31° C) wild type (wt) (37° C) wild type (wt) (43° C)	wild type L11 chromosomal gene (*rplK*)/pΔCAT (control plasmid)	33 ± 5 25 ± 4 38 ± 2
L11N$^-$ (31° C) L11N$^-$ (37° C) L11N$^-$ (43° C)	Δ*rplK*/pL11 (pΔCAT expressing 76 amino acid CTD of L11)	47 ± 5 49 ± 7 54 ± 4
L11$^{-/+}$ (31° C) L11$^{-/+}$ (37° C) L11$^{-/+}$ (43° C)	Δ*rplK*/pL11 (pΔCAT expressing wt L11)	41 ± 3 36 ± 4 42*
L11$^-$ (31° C) L11$^-$ (37° C) L11$^-$ (43° C)	Δ*rplK*/pACYC177 (control plasmid)	145 ± 8 166 ± 6 ---------

[a]L11$^{-/+}$, strain lacking L11 gene but replaced *in vivo* on a plasmid; L11N$^-$, strain lacking the N-terminal domain of L11; L11$^-$, strain lacking L11 gene.
[b]Listed are the genotypes of the chromosomal L11 gene and the plasmid with which the strains are transformed for *in vivo* expression of all or part of ribosomal protein L11.
[c]Values are calculated from growth curves based upon absorbance measurements of cultures over time.
*Only one experiment performed

wild type strain at all temperatures, while their study indicated similar rates of growth between the wild type and this strain. Also notable is the lethal phenotype of the L11$^-$ strain when grown at 43° C. Interestingly, growth of this strain at 37° C was not lethal and was only slightly slower than at 31° C. The wild type and L11$^{+/-}$ strains showed only slight decreases in growth rates at the higher and lower temperatures. Also, the L11N$^-$ strain showed levels of growth inhibition at 31° C and 43° C similar to those for the wild type and L11$^{+/-}$ strain. Therefore, the lethal phenotype at high temperature (43° C) applies only when expression of the entire L11 protein is prevented.

In Vitro Translation Studies on L11 Mutant Ribosomes

To attempt to understand the functional consequences of the L11 deletion mutations, we carried out *in vitro* translation assays utilizing ribosomes isolated from

each of the L11 mutant strains. A colleague in our lab had previously begun work on this aspect of the L11 mutants (289). He found that the L11$^-$ and L11N$^-$ strains were inhibited relative to wild type in the extent of translation over a 30 minute time course. We wished to expand upon his analysis to provide further characterization of the effects of the mutations on the rates of protein synthesis. Specifically, we looked at the elongation stage of translation. As L11 has been linked to the function and interactions of elongation factors, we hypothesized that mutations in L11 would deleteriously affect factor-dependent functions during the elongation phase of translation.

As previous work has shown that ribosomes lacking L11 have defects in the initiation (168) and termination (152,153) stages of translation, we devised a strategy to also look at the effects of the mutations on the elongation stage. In order to look at this stage separately, we took advantage of a well-known method to subvert the initiation and termination stages in the *in vitro* translation assays as noted above. First, we utilized an mRNA analog, polyuridylic acid (poly-U), that does not have an initiation codon (AUG) and does not require normal translation initiation factors (IF1, IF2, IF3) to assemble an initiation complex at the start of translation (290). Instead, we formed initiation complexes with a tRNA analog with a blocked amino group, N-acetyl-Phe-tRNA^{Phe} (N-Ac-Phe-tRNA^{Phe}). N-Ac-Phe-tRNA^{Phe} was used as it can form an initiation complex without the potential for residual polymerization occurring in the absence of translation factors. Second, poly-U mRNA does not have a stop codon (UAG, UAA, or UGA), and therefore is not a substrate for translation termination by release factors RF1, RF2, and RF3. Therefore, translation with poly-U does not terminate normally.

This translation method allowed us to analyze specifically the effects of L11 mutations on the elongation phase of translation. One disadvantage of the poly-U system, however, is that ribosomes can initiate at any place along the poly-U message. Therefore, it was important to concentrate our analysis on the initial "burst" or linear phase of poly-U translation, before a significant percentage of translating ribosomes become stalled at the terminus of the mRNA, affecting the rate calculations.

Formation of Translation Initiation Complexes

To begin our analysis, we first determined the efficiency of formation of the initiation complex on each of the ribosome mutants. To do this, we incubated ribosomal subunits isolated from each of the mutant strains (wild type, $L11^{+/-}$, $L11N^{-}$, and $L11^{-}$) with poly-U mRNA and radiolabeled N-Ac-Phe-$tRNA^{Phe}$ and calculated the amount of initiation complex from the amount of radioactivity retained after passing the complexes

Table 4.2. Formation of N-Ac-Phe-$tRNA^{Phe}$ Initiation Complexes on L11 Mutant Ribosomes

[b]Strain	[a]Percent of Ribosomes Forming Initiation Complexes with Nac-Phe-$tRNA^{Phe}$
Wild Type	38 ± 7%
$L11^{-/+}$	31 ± 10%
$L11N^{-}$	40 ± 9%
$L11^{-}$	23 ± 6%

[a]Values are calculated from two separate experiments adjusted to control for the retention of Nac-^{3}H-Phe-$tRNA^{Phe}$ on filters in incubation without ribosomes added.
[b]$L11^{-/+}$, strain lacking L11 gene but replaced *in vivo* on a plasmid; $L11N^{-}$, strain lacking the N-terminal domain of L11; $L11^{-}$, strain lacking ribosomal protein L11.

over nitrocellulose filters that retain ribosomes or complexes but do not retain unbound N-Ac-Phe-tRNA^{Phe}. Table 4.2 shows the levels of radiolabeled tRNA that form initiation complex on each of the L11 mutant ribosomes.

As Table 4.2 illustrates, ribosomes from most of the strains were able to form initiation complexes to comparable extents with N-Ac-^{3}H-Phe-tRNA^{Phe}. The L11^{-} strain was the only strain that showed a marginally reduced ability to form the complex. This is a factor that had to be considered in interpreting the results of translation assays.

Poly-U Translation on L11 Mutant Ribosomes

In our first test of the function of the L11 mutant ribosomes we compared the rates of translation on a poly-U mRNA template that is driven by translation factors supplied from a cytosolic fraction of *E. coli*. This cytosolic fraction (S100) is prepared by differential centrifugation of the lysate from disrupted *E. coli* cells (see **Materials and Methods** for details) and contains initiation factors, elongation factors, termination factors, and tRNA synthetases (to "charge" tRNA with amino acyl groups). Ribosomes were initiated by incubating 50S and 30S subunits with poly-U mRNA and N-Ac-Phe-tRNA^{Phe}. Ribosomal 30S subunits purified from mutant or wild type strains were used in combination with 50S subunits from each strain to determine if the L11 mutations might also affect the activity of 30S subunits from those strains. To initiated ribosomes was added a mixture of tRNA^{Phe} and a system to replenish the supply of GTP from GDP produced by factor-dependent hydrolysis during translation. This system consisted of ATP, phosphoenolpyruvate and pyruvate kinase (291). S100 was immediately added to this mix to begin translation. Figure 4.1 displays a time course for synthesis of poly-Phe in this translation system, and the calculated initial rates are listed in Table 4.3.

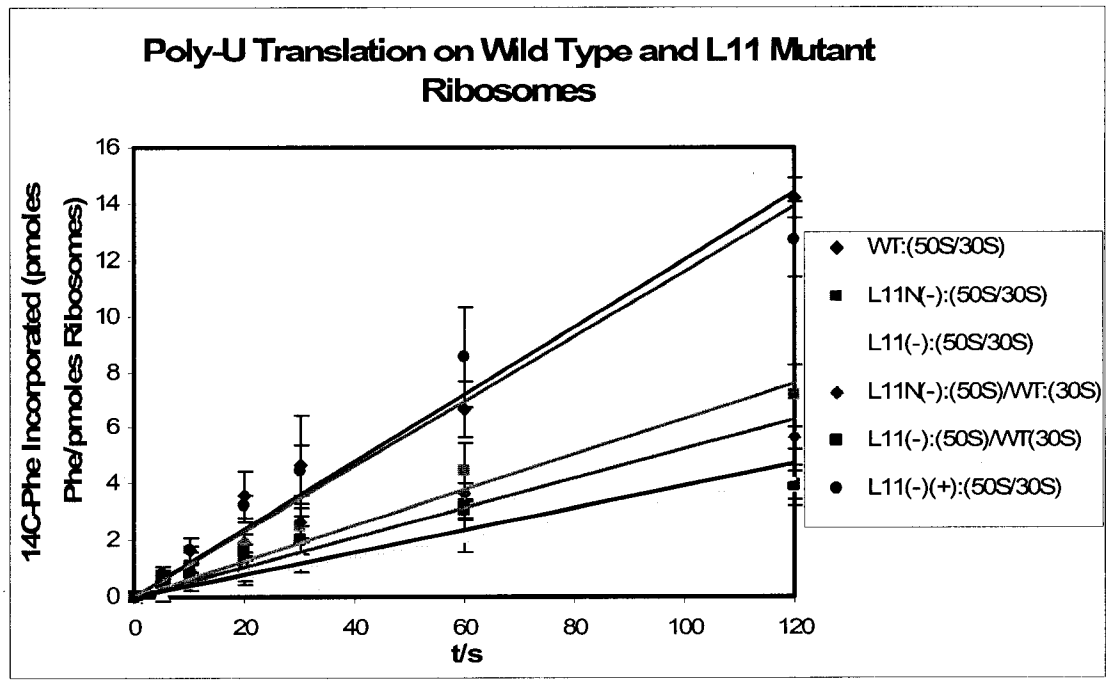

Figure 4.1. Initial rates of poly-U Translation for Ribosomes with Subunits Purified from Wild Type or L11 Mutant Strains. Experiments were carried out as described in the text and **Material and Methods**. Incorporation of acid-precipitatable poly-(^{14}C)Phe was measured by scintillation counting portions of the translation mix over 120 seconds. The results are averages of two separate experiments with the standard deviation shown. Ribosomal 50S subunits from L11 mutant strains were used in translation experiments with 30S subunits either from the same strain or from the wild type strains as a control. WT, wild type; L11N$^-$, ; L11N$^-$, subunits from a strain lacking the N-terminal domain of L11; L11$^-$, subunits from a strain lacking the entire L11 protein.

Ribosomes formed from wild type and L11$^{-/+}$ subunits consistently translated the poly-U message at a higher rate than those formed from subunits from mutant ribosomes or from combinations of 50S subunits from mutants and 30S subunits from wild type strains. The average rate of translation for the wild type strain was almost twice that of ribosomes with L11N$^-$ 50S subunits and three times that of ribosomes with L11$^-$ 50S subunits. Ribosomes with L11N$^-$ 50S subunits translated at rates above those of with L11$^-$ 50S subunits. Part of this difference, however, may be attributable to the smaller number of ribosomes capable of forming initiation complexes on L11$^-$ ribosomes (Table 4.2).

Table 4.3. Poly-U Translation by Wild Type and L11 Mutant Ribosomes	
[b]Ribosome Subunit Composition (50S/30S)	[a]14C-Phe Incorporation (picomoles/picomole ribosomes/sec)
Wild Type (50S/30S)	0.24 ± .04
L11N$^-$ (50S/30S)	0.13 ± .01
L11N$^-$ (50S)/Wild Type (30S)	0.12 ± .02
L11$^-$ (50S/30S)	0.08 ± .02
L11$^-$ (50S)/Wild Type (30S)	0.07 ± .01
L11$^{-/+}$ (50S/30S)	0.23 ± .03
[a]Values were calculated from averages of two experiments as shown in Figure 4.1 for each combination of subunits. [b]L11N$^-$, strain lacking the N-terminal domain of L11; L11$^-$, strain lacking ribosomal protein L11.	

"Factor-Free" In Vitro Translation on L11 Mutant Ribosomes

Our poly-U translation experiments confirmed that the L11 mutant ribosomes have a defect in the elongation phase of translation. To determine if the defect is due to elongation factor-dependent functions, we chose to test the ability of ribosomes from each strain to synthesize poly-phenylalanine (Phe) in a system in the absence of elongation factors. It is well known that ribosomes can carry out translation, albeit at severely reduced levels, in the poly-U translation system in the absence of factors. Therefore, we used this system to test whether any effects of the mutations on translation elongation were due to a specific effect related to factor activity on the ribosome. The results from the "factor-free" translation experiments are shown in Figure 4.2. They illustrate the levels of production of acid-precipitatable poly-Phe after 2 hours of *in vitro* translation. Factor-free translation showed a linear increase over two hours for each strain, allowing us to estimate the rates of translation over this range (Table 4.4). Translation rates on wild type ribosomes in this system were not significantly above the

levels for ribosomes with L11N⁻ 50S subunits. However, ribosomes with L11⁻ 50S subunits translated at levels significantly lower than both wild type and L11N⁻ ribosomes.

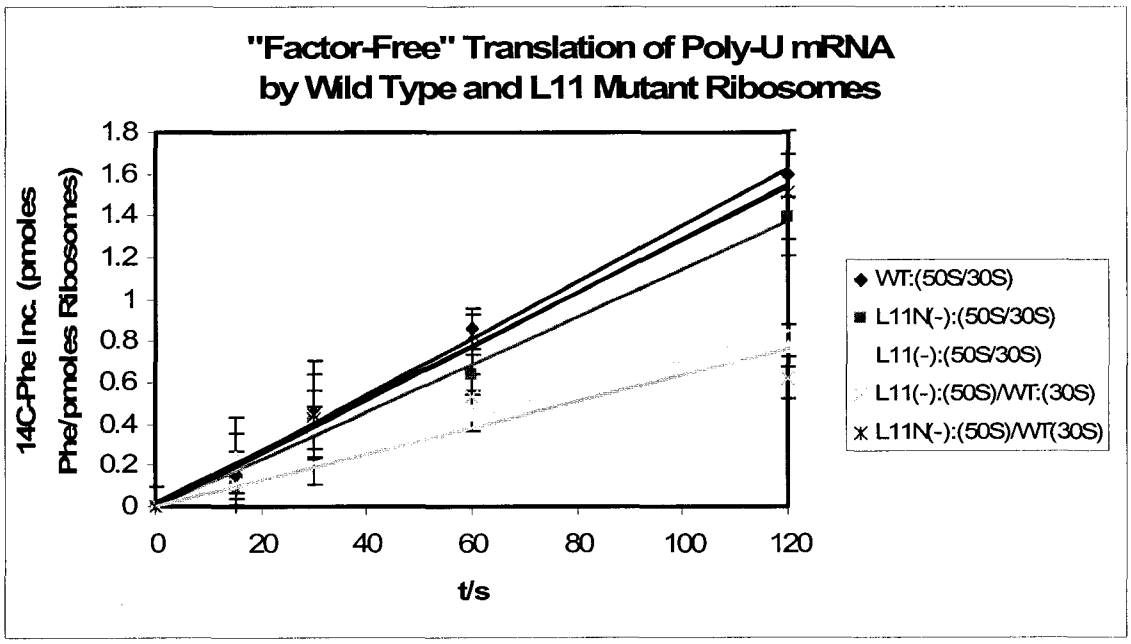

Figure 4.2. "Factor free" Translation with a Poly-U mRNA Template. Translation of poly-^{14}C-phenylalanine (Phe) was carried out under the conditions outlined in the Materials and Methods section at the end of the chapter. Incorporation of acid-precipitatable poly-(^{14}C)Phe was measured by scintillation counting portions of the translation mix over 2 hours of incubation. Ribosomal 50S subunits from L11 mutant strains were used in translation experiments with 30S subunits either from the same strain or from the wild type strains as a control.The subunit composition of the ribosomes used in translation are listed in the legend. WT = wild type; L11N(-) = 50S subunits lacking the N-terminal domain of L11; L11(-) = 50S subunits lacking the entire L11 protein.

Again, it is possible that the lower rates for ribosomes with L11⁻ 50S subunits reflect the decreased capacity of these ribosomes to form initiation complexes. These results indicate that, at least for ribosomes with L11N⁻ 50S subunits, the defect in translation is primarily related to elongation factor functions.

"Factor Free" Translation on L11 Mutants in the Presence of Elongation Factors

Next we wished to know if the reduced poly-U translation levels of the factor-free translation system could be improved by the addition of elongation factors. We added

EF-G and EF-Tu separately, or added both together to factor-free translations to ascertain the effect on the rates of elongation. As our earlier data had indicated that the defect in factor-dependent poly-U translation was related to factor functions, we expected to find that the addition of elongation factors would significantly improve translation on wild type ribosomes would not significantly improve translation on ribosomes with L11

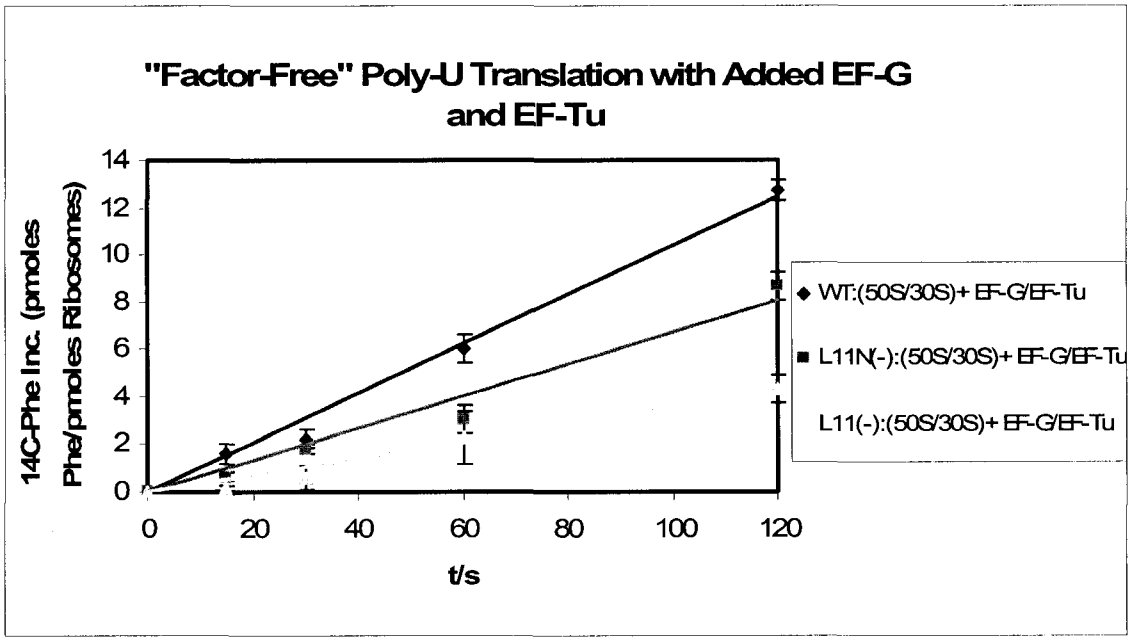

Figure 4.3. "Factor free" Translation with a Poly-U mRNA Template in the Presence of Added Elongation Factors. Translation of poly-^{14}C-phenylalanine (Phe) was carried out under the conditions outlined in the Materials and Methods section at the end of the chapter. Incorporation of acid-precipitatable poly-(^{14}C)Phe was measured by scintillation counting portions of the translation mix over 2 hours of incubation. The subunit composition of the ribosomes used in translation are listed in the legend. WT = wild type; L11N(-) = 50S subunits lacking the N-terminal domain of L11; L11(-) = 50S subunits lacking the entire L11 protein; EF-G, elongation factor-G; EF-Tu, elongation factor-Tu.

mutant 50S subunits. As Figure 4.3 and Table 4.4 illustrate, the rate of translation on wild type ribosomes was improved almost 15-fold on wild type ribosomes by the addition of EF-G and EF-Tu , while the rate of translation on L11N$^-$ ribosomes and L11$^-$ ribosomes was improved approximately 10-fold.

While the differences for wild type and L11 mutant ribosomes in factor-free translation with added elongation factors agree with the magnitude of the differences seen in normal factor-dependent poly-U translation, the addition of EF-G and EF-Tu does not increase the rates of translation to levels approaching that in the poly-U system with added S100. In fact, the rates are almost two orders of magnitude lower than in the "factor-free" system with added elongation factors. We can only speculate on this large

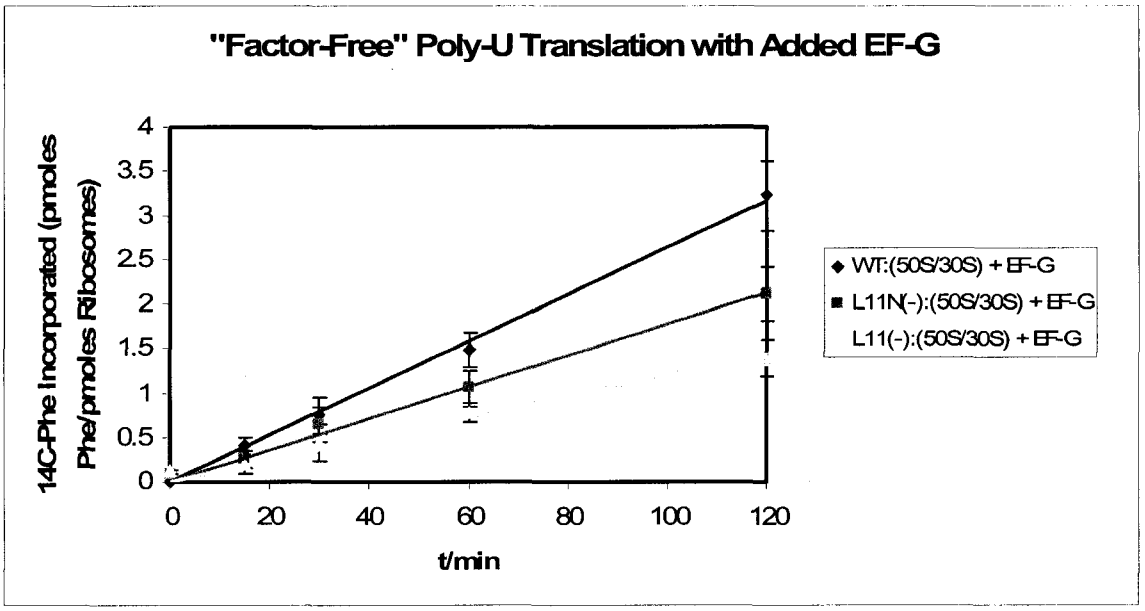

Figure 4.4. "Factor free" Translation with Added Elongation Factor-G. Translation of poly-^{14}C-phenylalanine (Phe) was carried out under the conditions outlined in the **Materials and Methods** section at the end of the chapter. The incorporation of poly-^{14}C-Phe was as described in Figure 4.3 The subunit composition of the ribosomes used in translation are listed in the legend. WT = wild type; L11N(-) = 50S subunits lacking the N-terminal domain of L11; L11(-) = 50S subunits lacking the entire L11 protein; EF-G, elongation factor-G.

difference in the two systems (see discussion below). Also, the differences in translation with added elongation factors between wild type and L11 mutant ribosomes do notdistinguish between the effects of added EF-G and EF-Tu on translation. Therefore,

we sought to elucidate these effects by adding the factors separately to factor-free translation systems.

The effects on "factor-free" translation of the addition of EF-G or EF-Tu alone are shown in Figure 4.4 and are listed in Table 4.4 below. The addition of EF-G alone increases the rate of translation 4-fold over factor-free translation without added EF-G for wild type ribosomes, while it increases the rate for L11N$^-$ ribosomes about 2.7-fold and

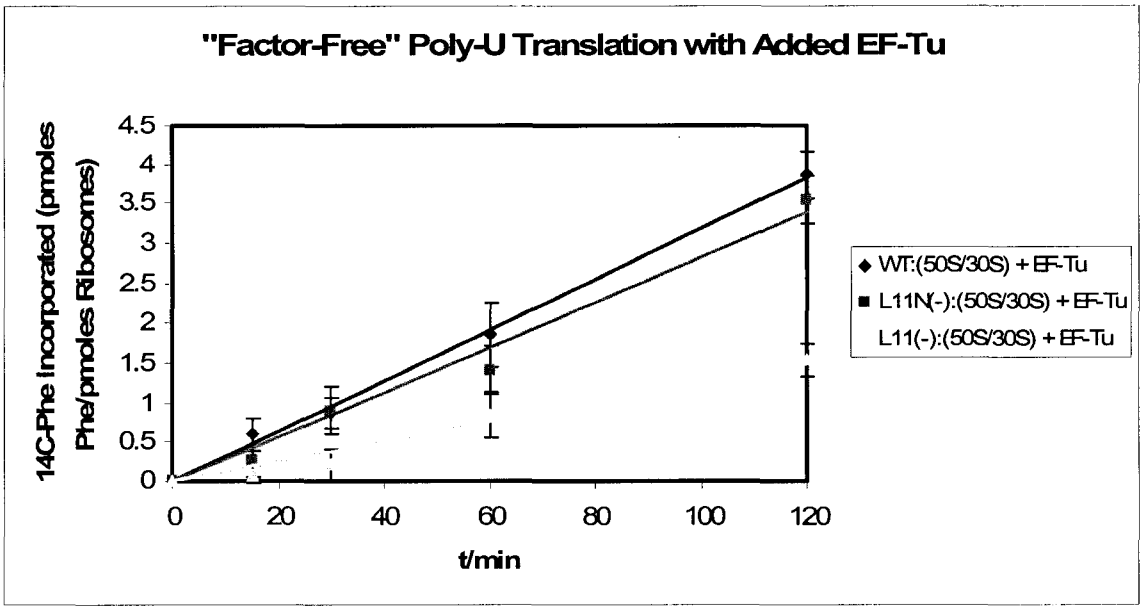

Figure 4.5. "Factor free" Translation with Added Elongation Factor-Tu. Translation of poly-^{14}C-phenylalanine (Phe) was carried out under the conditions outlined in the Materials and Methods section at the end of the chapter. The incorporation of poly-^{14}C-Phe was as described in Figure 4.3 The subunit composition of the ribosomes used in translation are listed in the legend. WT = wild type; L11N(-) = 50S subunits lacking the N-terminal domain of L11; L11(-) = 50S subunits lacking the entire L11 protein; EF-Tu, elongation factor-Tu.

the rate for L11$^-$ ribosomes 2-fold. The addition of EF-Tu to the system increased translation rates on all ribosomes greater than 4-fold. The fact that EF-G does not increase translation on L11$^-$ and L11N$^-$ ribosomes to the same extent as wild type ribosomes, while EF-Tu increases translation to a similar extent for wild type and mutant

Table 4.4. "Factor-Free" Poly-U Translation without/with Added Elongation Factors				
	No Factor	+ EF-Tu	+ EF-G	+ EF-Tu/EF-G
[c]Ribosome Subunit Composition (50S/30S)	[a]Rate/([b]Fold Decrease Relative to Wild Type)	[a]Rate/([b]Fold Decrease Relative to Wild Type)	[a]Rate/([b]Fold Decrease Relative to Wild Type)	[a]Rate/([b]Fold Decrease Relative to Wild Type)
Wild Type (50S/30S)	0.014 ± .004/(1)	0.064 ± .008/(1)	0.053 ± .005/(1)	0.21 ± .03/(1)
L11N$^-$ (50S)/Wild Type (30S)	0.011 ± .002/(1.4)	-------	-------	------
L11N$^-$ (50S/30S)	0.013 ± .003/(1.1)	0.056 ± .005/(1.1)	0.035 ± .009/(1.5)	0.13 ± .02/(1.6)
L11$^-$ (50S)/Wild Type (30S)	0.006 ± .002/(2.3)	--------	-------	------
L11$^-$ (50S/30S)	0.006 ± .003/(2.3)	0.025 ± .006/(2.6)	0.012 ± .004/(4.4)	0.071 ± .017/(3.0)

[a]Rate values are in **picomoles ^{14}C-Phe incorporated/picomoles ribosomes/min** and were calculated from an average of 2 experiments.
[b]Fold decrease was determined by calculating the ratio of wild type to L11 mutant translation rates.
[c]L11N$^-$, strain lacking the N-terminal domain of L11; L11$^-$, strain lacking ribosomal protein L11.

ribosomes, indicates that the defect in elongation on the L11N$^-$ ribosomes may be primarily due to a defect in the interaction and/or function of EF-G with these ribosomes.

EF-G-Dependent GTP Hydrolysis by L11 Mutant Ribsomes

As the *in vitro* translation analysis indicated a decrease in the activity of EF-G during elongation in L11 mutant ribosomes, we analyzed one aspect of EF-G function, the hydrolysis of GTP that occurs during translocation on the ribosome. Hydrolysis of GTP in the GTP-binding domain of EF-G is believed to occur following the transfer of the nascent peptide from P- to A-site tRNA during the process of EF-G-dependent translocation of A- and P-site tRNA to the P- and E-sites respectively.

As L11 and the L11-binding rRNA are linked to the other elements of the GTPase-associated region (GAR), we hypothesized that the effect of the L11 mutations on EF-G-dependent functions on the ribosome might be a result of a defect in either the

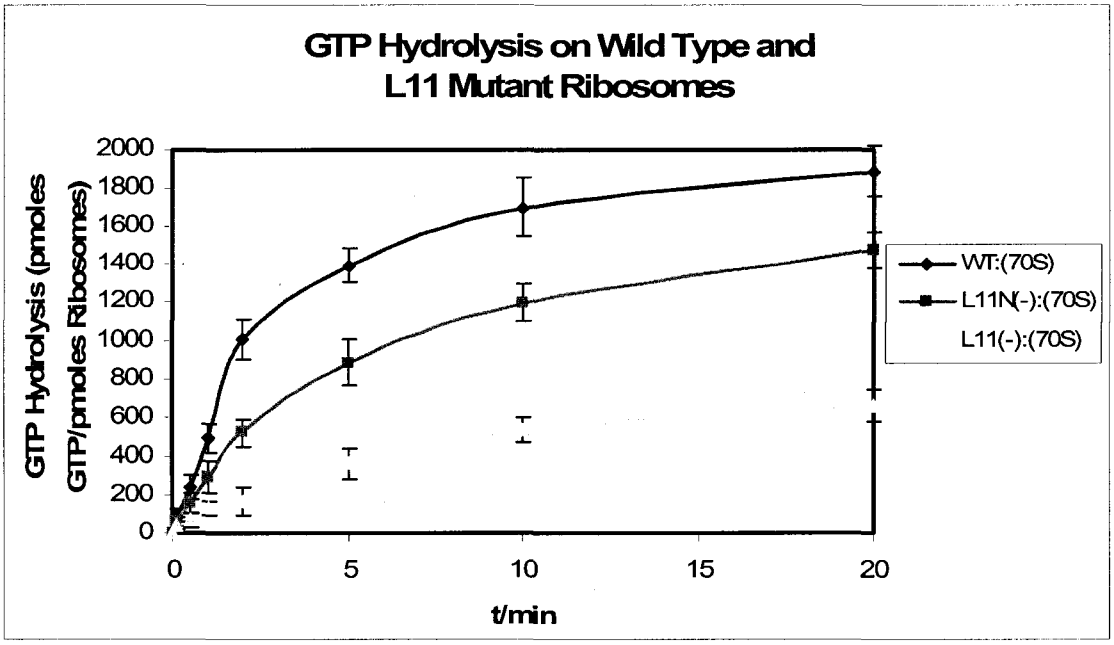

Figure 4.6. EF-G-Dependent GTP Hydrolysis on Wild Type and L11 Mutant 70S Ribosomes. GTP hydrolysis assays were carried out under the conditions outlined in the Materials and Methods section at the end of the chapter. The levels of GTP hydrolyzed at different time points were calculated from the ratios of the intensities of bands representing radiolabeled (α-^{32}P)-GDP and (α-^{32}P)-GTP when portions of reactions were separated by thin-layer chromatography, and are an average of two separate experiments. The ribosomes used in the assays are listed in the legend. WT = wild type; L11N(-) = 70S ribosomes lacking the N-terminal domain of L11; L11(-) = 70S ribosomes lacking the entire L11 protein.

activation of GTPase activity or a defect in the turnover of the factor on the ribosome. To test this, we compared the EF-G-ribosome-dependent GTPase activity of the wild type and mutant ribosomes. Figure 4.6 illustrate the EF-G-dependent GTP hydrolysis rates of wild type and L11 mutant ribosomes in the presence of a stoichiometric ratio of EF-G to ribosomes. The rate of hydrolysis in this system gradually decreases with time as the

GTP is consumed in the assay. However, the rates are relatively linear over the first two minutes. Therefore, we calculated the initial rates of GTP hydrolysis from the first two minutes of data and compared the values for wild type and L11 mutant ribosomes (Figure 4.7 and Table 4.5).

In this system, with a stoichiometric ratio of EF-G added to ribosomes, EF-G-dependent GTP hydrolysis was significantly reduced relative to wild type ribosomes on both L11N$^-$ and L11$^-$ ribosomes. The initial rate of hydrolysis for L11N$^-$ ribosomes is around one-half that of wild type ribosomes, while that for L11$^-$ ribosomes is only one-fifth that of wild type ribosomes (Table 4.5).

If the L11 mutations cause a defect in the turnover of EF-G on the ribosome, we would expect to see the rates of GTP hydrolysis on L11 mutant ribosomes fall relative to wild type ribosomes when conditions favor high turnover of the factor. This proved to be true in our analysis. When a sub-stoichiometric (catalytic) ratio of EF-G to ribosomes was used in the GTP hydrolysis assays (Figure 4.8), we saw an even greater inhibition of the rate of GTP hydrolysis relative to wild type ribosomes on L11N$^-$ and L11$^-$ ribosomes. These conditions that favor an increase in turnover of EF-G on ribosomes led to initial rates of approximately one-third relative to wild type rates for L11N$^-$ ribosomes and approximately one-ninth relative to wild type rates for L11$^-$ ribosomes (Table 4.5). The results favor the interpretation that turnover of EF-G is somehow inhibited in the absence of at least the N-terminal domain of L11. However, the even greater inhibition of GTP hydrolysis on L11$^-$ ribosomes relative to L11N$^-$ ribosomes with both stoichiometric and

catalytic amounts of EF-G suggests that another aspect of EF-G function on the ribosome, possibly EF-G binding or EF-G-dependent translocation, may also be inhibited on the ribosome in the absence of the entire L11 protein.

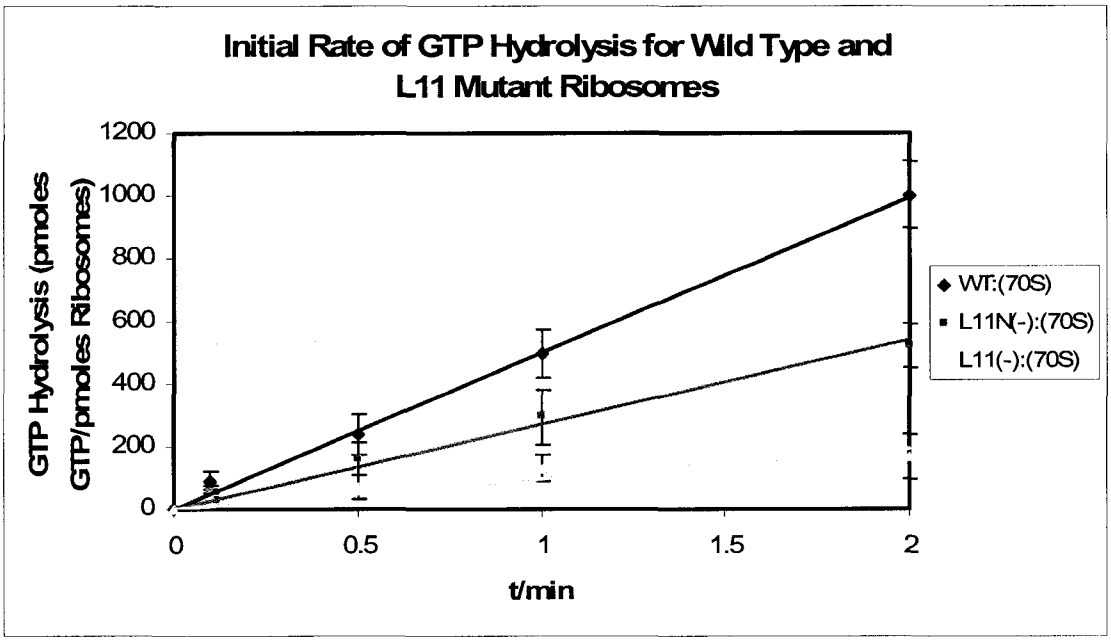

Figure 4.7. Initial Rates of EF-G-Dependent GTP Hydrolysis on Wild Type and L11 Mutant 70S Ribosomes. The figure illustrates the hydrolysis rates in the first two minutes of the assay from Figure 4.6 and the initial rates calculated from the linear fits of the data are listed in Table 4.5. WT = wild type; L11N(-) = 70S ribosomes lacking the N-terminal domain of L11; L11(-) = 70S ribosomes lacking the entire L11 protein.

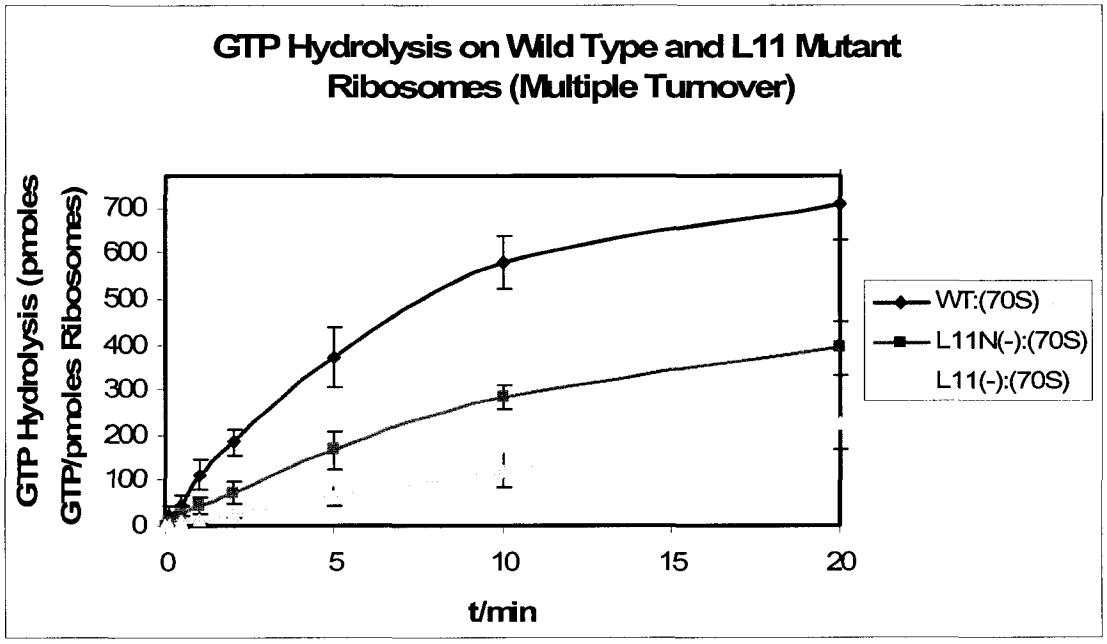

Figure 4.8. EF-G-Dependent GTP Hydrolysis with Catalytic Levels of EF-G. The levels of GTP hydrolysis were calculated as described in Figure 4.6. The values are averages of two experiments.

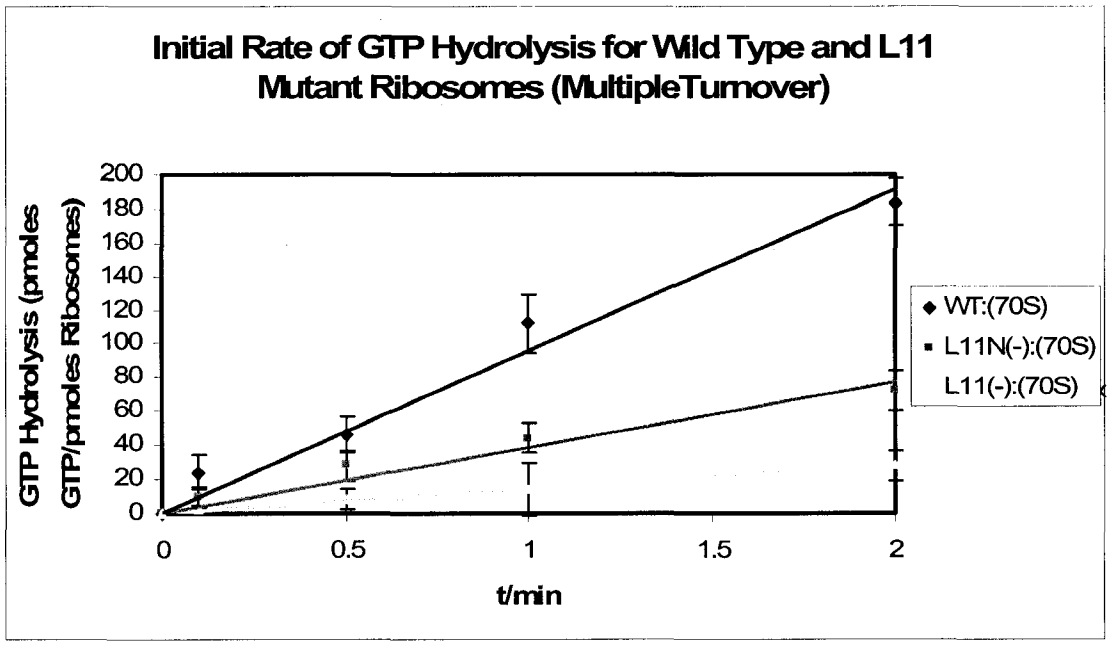

Figure 4.9. Initial rates of EF-G-Dependent GTP Hydrolysis with Catalytic Levels of EF-G. The figure illustrates the hydrolysis rates in the first two minutes of the assay from Figure 4.8 and the initial rates calculated from the linear fits of the data from two separate experiments are listed in Table 4.5. WT = wild type; L11N(-) = 70S ribosomes lacking the N-terminal domain of L11; L11(-) = 70S ribosomes lacking the entire L11 protein.

Table 4.5. EF-G-Dependent GTP Hydrolysis on Wild Type and L11 Mutant Ribosomes	
[b]Ribosome Strain	[a]GTP Hydrolysis (pmole GTP/min/pmole ribosome)
GTP Hydrolysis with a Super-Stoichiometric Ratio of EF-G to Ribosomes	
Wild Type (70S)	1051 ± 44
L11N$^-$ (70S)	538 ± 51
L11$^-$ (70S)	193 ± 26
GTP Hydrolysis with a Sub-Stoichiometric Ratio of EF-G to Ribosomes	
Wild Type (70S)	192 ± 17
L11N$^-$ (70S)	77 ± 19
L11$^-$ (70S)	21 ± 9

[a]Initial rates of GTP hydrolysis were calculated from Figure 4.7 and 4.9 using the method described in Figure 4.6. Values are an average of two or greater separate experiments.
[b]70S Ribosomes from the following strains were assayed: Wild type; L11N$^-$, strain lacking the N-terminal domain of L11; L11$^-$, strain lacking ribosomal protein L11.

Discussion

The functional analysis described above indicated a significant defect in growth rate, *in vitro* translation rate, and ribosome/EF-G-dependent GTP hydrolysis for each of the ribosomal protein L11 mutant strains tested. In this section we discuss these results in the context of previous research and a model for the function of L11 during translation.

Growth Characteristics

The analysis of the growth characteristics of wild type and L11 mutant strains indicated that all strains with mutations in the gene for ribosomal protein L11 had at least a small reduction in growth rate relative to wildtype at all growth temperatures tested. The strain lacking the entire L11 protein (L11$^-$) was the most severely affected, while the strain with the C-terminal domain of L11 replaced on a plasmid (L11N$^-$) had an intermediate growth defect and the strain with the entire L11 protein replaced on a

plasmid had only a slight growth defect. Inducible expression of L11 on a plasmid rather than from the chromosomal locus probably subverts cellular regulation of the L11 gene. Normally, the synthesis of ribosomal proteins is coordinately regulated with the assembly of mature ribosomes, often by a feedback mechanism (292). For instance, the L11 operon contains the genes for L11 (*rplK*) and L1 (*rplA*). When L1 synthesis exceeds its use in ribosome biogenesis, it binds the mRNA leader of the L11 gene and translationally represses synthesis of both L11 and the downstream L1 gene (293). Therefore, expression of L11 on an inducible plasmid subverts this regulation mechanism, leading to over-expression of L11. As L11 has been found to be involved in the interactions with both release factor-1 (RF1) (152) and the stringent factor RelA on the ribosome, it is possible that over-expression of the protein could titrate these factors to some extent inside the cells. This may be the cause of the somewhat slower growth phenotype for the $L11^{+/-}$ strain.

The L11 mutant strains used in this study were produced by a gene replacement technique that resulted in the deletion of the coding sequence for 83 amino acids (40-122) of the L11 gene, but that did not disrupt the regulatory elements necessary for normal translation and regulation of L1 (153). Therefore, normal levels of L1 were produced in L11 knockout strains, as judged by their incorporation in cellular ribosomes (152). Table 4.1 also indicates a previously noted temperature-dependent lethality of the L11 knockout mutation. Van Dyke *et al* have previously reported the lethal effect of the knockout mutation in the $L11^{-}$ strain and attributed this to destabilization of the L11-binding rRNA in the absence of the C-terminal domain of L11 (153).

In Vitro Translation

In the poly-U *in vitro* translation system using the cellular S100 fraction, L11$^-$ and L11N$^-$ ribosomes had a significantly reduced rate of poly-U translation relative to wild type ribosomes. The system does not approach rates of synthesis estimated for *in vivo* translation or in an optimized system with purified translation factors, tRNA synthetases, and a GTP regeneration systems (~10 picomoles Phe incorporated per second) (294). The rates of poly-Phe synthesis are almost two orders of magnitude lower than this level. We can only speculate on this large difference in the two systems. It may be the combination of the stimulatory effects of the recycling of GTP to keep an optimal ratio of GTP to GDP for factor function and the effects of the recycling of amino-acylated tRNA^{Phe}. This may be due to our use of a less optimal buffer/ion system or less than optimal translation factor (elongation factors and tRNA synthetases) concentrations in the S100 fraction. However, our system was used with levels of S100 that provided the highest levels of poly-Phe synthesis in our analysis (data not shown).

In this translation system, L11$^-$ and L11N$^-$ had a significantly reduced rate of poly-Phe synthesis relative to wild type and L11$^{-/+}$ ribosomes. This inhibition of translation for L11$^-$ ribosomes is consistent with previous analysis of L11$^-$ ribosomes obtained as resistance mutations to the antibiotic thiostrepton (288). Some of the inhibition may have been due to the lower capacity of L11$^-$ ribosomes to form initiation complexes with N-Ac-Phe-tRNA^{Phe} that was observed. It is not clear why the L11$^-$ ribosomes would have a lower affinity for N-Ac-Phe-tRNA^{Phe} than wild type and L11N$^-$ ribosomes, as L11 and the L11-binding rRNA do not form part of the P-site tRNA binding pocket seen in the x-ray crystal structure of the ribosome/tRNA complex (99).

The same crystal structure model, however, indicated that the L11-binding rRNA may interact with a 23S rRNA stem-loop around nucleotide 2475 that forms part of the A-site tRNA binding at the base of its stem (99). It is possible that disruption of the L11-binding rRNA structure destabilizes this interaction and modulates the structure of proximal tRNA binding sites on the large subunit, leading to a lower affinity for tRNA. The L11N$^-$ mutant retaining the rRNA-binding C-terminal domain should not destabilize the structure of the L11-binding rRNA to the same extent (140), possibly explaining the differences in the affinities for N-Ac-Phe-tRNA^{Phe} for the two L11 mutants.

The fact that ribosomes formed from combinations of L11 mutant 50S subunits and wild type 30S subunits showed similar activities in the translation assays to those formed from 50S subunits and 30S subunits from mutant strains confirms that the mutations do not affect 30S function in translation. The inhibition of N-Ac-Phe-tRNA^{Phe} binding noted above for L11$^-$ mutant ribosomes, however, could also be a result of inhibition or destabilization of the association of 50S and 30S subunits in forming the initiation complex. L11$^-$ mutant 70S ribosomes were stable when purified from mutant strains, but could be destabilized by formation of the initiation complex. Interestingly, Naaktgeboren *et al.* previously found that thiostrepton binding in the L11-binding region impairs coupling of 50S and 30S in IF2-dependent formation of the initiation complex with mRNA and fMet-tRNA^{fMet} (295). It is tempting to speculate that these two phenomena are related. To clarify the issue of the stability of the initiation complex on the L11$^-$ mutant ribosomes it will be necessary in the future to carry out equilibrium centrifugation studies. Such studies would allow us to compare the affinities of the initiating tRNA for wild type and mutant ribosomes under equilibrium conditions.

EF-G/Ribosome-Dependent GTP Hydrolysis

GTP hydrolysis by EF-G on the ribosome has previously been linked to L11 and the L11-binding domain through research on the affects of the antibiotic thiostrepton that binds in the L11-binding domain, and by research on the affects of the L11 mutants selected for by resistance to thiostrepton. Thiostrepton binding inhibits EF-G dependent GTP hydrolysis either by inhibiting the interaction of EF-G with the ribosome (166), or by inhibiting the turnover of the factor on the ribosome (169). In thiostrepton resistance mutants of *Bacillus megaterium*, the absence of L11 was found to significantly reduce the level of EF-G-dependent GTP hydrolysis with stoichiometric ratios of EF-G added to hydrolysis reactions (288).

Several factors could lead to a decrease in GTP hydrolysis rates on the L11 mutant ribosomes. For instance, GTP hydrolysis would be reduced if the mutations cause a decrease in the affinity of the L11 mutants for the EF-G in the steps in translocation preceding GTP-hydrolysis. Our studies on the binding of EF-G to L11 mutant ribosomes in the post-GTP hydrolysis (fusidic acid stabilized) state in Chapter 3 (Figure 3.5) indicated that binding of EF-G was severely inhibited on L11$^-$ ribosomes, but not on L11N$^-$ ribosomes. In addition, our chemical modification probing studies on wild type and L11 mutant ribosomes showed that protection of 23S rRNA residues in both the L11-binding domain and the sarcin-ricin stem-loop (SRL) domain were reduced for L11$^-$ ribosomes in both the post-GTP hydrolysis (fusidic acid stabilized) and the pre-GTP hydrolysis (in the presence of the non-hydrolyzable GTP analog GDPNP) states (Table 3.3). It is likely, therefore, that the lower affinity of L11$^-$ ribosomes for EF-G contributes to the reduction in GTP hydrolysis for these ribosomes.

In these same assays, we did not detect inhibition of EF-G binding to L11N$^-$ ribosomes in the post-GTP hydrolysis state, and only one residue, A2660 in the SRL domain, was significantly less protected from chemical modification in the pre-GTP hydrolysis state relative to wild type ribosomes (Table 3.3). The data do not suggest that a decrease in affinity for EF-G on L11N$^-$ ribosomes contributes significantly to the decrease in GTP hydrolysis rates. In the future our analysis would benefit from an assay designed to test directly for binding of EF-G to ribosomes in the pre-GTP hydrolysis state. A defect at this stage in the EF-G interaction with the ribosome could explain some of the results we observed. Such an experiment could be undertaken by utilizing a radiolabeled, non-hydrolyzable GTP analog in binding reactions similar to those undertaken for the fusidic acid-stabilized (post-GTP hydrolysis) state of EF-G on the ribosome.

Differences in the rate of turnover of EF-G on the ribosome following GTP hydrolysis may also play a role in decreased rates of GTP hydrolysis on the L11 mutant ribosomes. In the present study, the rates of EF-G-dependent GTP hydrolysis on L11 mutant ribosomes were more severely reduced under conditions that favored increased turnover of the factor. The differences between GTP hydrolysis rates in the presence of stoichiometric and catalytic levels of EF-G on wild type and L11 mutant ribosomes found in this study do suggest that the decreases in the rate of turnover of the EF-G on the L11 mutant ribosomes could lead, at least in part, to a reduction in the rates of GTP hydrolysis on the mutant ribosomes. Further elucidation of the primary cause of the reduction of EF-G-dependent GTP hydrolysis rates on L11 mutant ribosomes would benefit from a more systematic kinetic analysis of the rates using an array of EF-G concentrations.

Also, it would be helpful compare the rates of GTP hydrolysis in multiple turnover reactions with the rates of single round GTP hydrolysis for wild type and mutant ribosomes. The assays utilized by the authors in this study are too slow to resolve single round GTP hydrolysis, but a strategy to test the rates in a stopped-flow kinetics device would help to resolve these differences.

The differences shown between the wild type and L11 mutant ribosomes for GTP hydrolysis agree well with the differences in "factor-free" translation with added EF-G in Table 4.4. Although the rates of EF-G-dependent GTP hydrolysis and elongation cannot be directly correlated, the data do suggest a link between the two phenomena. It is also tenuous to try to directly correlate the reductions in *in vitro* translation and EF-G-dependent GTP hydrolysis with the reductions observed in growth rates for the strains harboring the L11 mutant ribosomes. A reduction in the rate of the elongation stage of protein synthesis in bacteria, however, would almost certainly lead to reductions in growth rates.

Materials and Methods

Isolation of Wild Type and L11 Mutant 70S Ribosomes and Subunits

Isolation of 50S and 30S subunits from the wild type and L11 mutant strains was as described in Chapter 2 for MRE600 *Escherichia coli ribosomes*. To isolate 70S ribosomes, the same protocol was used with the following deviation: Instead of using 1.5 mM $MgCl_2$ in the isolation buffers, a concentration that favors stabilization of subunit in 70S complexes, (10 mM $MgCl_2$) was used in the differential and sucrose gradient centrifugation steps. An S100 fraction was purified from the initial cell lysate by collecting the supernatant after the first differential centrifugation (60,000 rpm in the

Ti70 rotor) step and dialyzing 3 times (4 hours each) against 2 L of 70S isolation buffer (10 mM Tris-Cl (pH 7.5), 60 mM KCl, and 10 mM $MgCl_2$) with dithiothreitol (DTT) added to a concentration of 2 mM and glycerol added to 10%. Aliquots (50 μL) of the final solution were frozen and stored at -80° C before use.

Formation of Ribosome Initiation Complexes with N-acetyl-Phe-tRNA^{Phe}

In reactions, 10 units (~10,000 pmoles) of purified tRNA^{Phe} (Sigma) in 500 μL of H_2O was amino-acylated with phenylalanine by the addition of 100 μL 10X HMK buffer (20 mM HEPES (pH 7.6), 10 mM $MgCl_2$, 100 mM KCl), 191 μL H_2O, 100 μL of S100 cell lysate fraction from *Esherichia coli* as a source of amino-acyl synthetase enzyme, 2 μL of 5 mg/mL pyruvate kinase (Sigma), 2 μL of 100 mM CTP, 25 μL of ATP, 25 μL of 100 mM phosphoenolpyruvate (PEP), 5 μL of 50 mM DTT, 20 μL of L-[^{14}C]-phenylalanine (Amersham), and 60 μL of 1 mM L-phenylalanine (Sigma). The solution was incubated for 30 minutes at 30° C followed by the immediate addition of 2 M potassium acetate (pH 5.4) to a final concentration of 0.3 M. Then, we added 1.3 mL of acidic (pH 4.3) phenol and the solution was shaken for 15 minutes on ice to extract the tRNA. The solution was then centrifuged at 3500 rpm for 5 minutes, the phenol-containing supernatant was removed, and 3.2 mL of cold 95% ethanol was added to precipitate the tRNA. The tRNA was precipitated at -20 ° C for at least 1 hour and then centrifuged at 8500 rpm for 30 minutes. Following centrifugation, the supernatant was removed, the tRNA pellet was dried by centrifugation under vacuum (spinvac), and the pellet was resuspended 2 mL of 0.3 M potassium acetate (pH 5.4). The solution precipitated twice more using the procedure outlined above and the final pellet was resuspended in HMK buffer. Approximately 2 nmoles of amino-acylated tRNA was

recovered after the reaction based upon UV spectroscopy (195 $M^{-1}cm^{-1}$ extinction coefficient at 257.6 nm).

^{14}C-Phe-tRNA^{Phe} was N-acetylated by the addition to 400 µL ^{14}C-Phe-tRNA^{Phe} of 400 µL of 2 M potassium acetate (pH 5.0) and 40 µL of acetic anhydride added in 8 µL aliquots over 60 minutes. The reaction was precipitated twice with the addition of a 2X volume of cold 95% ethanol, incubation at -20 ° C and centrifugation at 8500 rpm for 30 minutes. The final pellet was resuspended in 50 mM potassium acetate (pH 5.0) and N-Ac-[^{14}C]Phe-tRNA^{Phe} was separated from unacytelated ^{14}C-Phe-tRNA^{Phe} by phenyl superose HPLC. Approximately 1 nmoles of N-Ac-[^{14}C]Phe-tRNA^{Phe} was recovered after the reaction based upon UV spectroscopy (195 $M^{-1}cm^{-1}$ extinction coefficient at 257.6 nm).

Binding of N-Ac-[^{14}C]Phe-tRNA^{Phe} to wild type and mutant ribosomes was assayed by nitrocellulose filtration. Poly-U mRNA (20 µg) (Sigma), 25 pmoles of 50S subunits, and 40 pmoles of 30S subunits were mixed in HMK buffer and incubated at 37° C for 15 minutes. To this solution was added 35 pmoles of N-Ac-[^{14}C]Phe-tRNA^{Phe}, the volume was adjusted to 50 µL with HMK buffer, and incubation was continued for 30 minutes at 37° C, followed by incubation on ice for 10 minutes. The solutions were diluted to 1 mL with cold HMK buffer and were immediately filtered over presoaked 0.45 µm nitrocellulose filters (Millipore) under vacuum. The filters were washed 3 times with cold HMK buffer and dried under vacuum. When completely dry, the radioactivity that remained on the filters was quantified in liquid scintillant on a Packard scintillation counter. The percentage of ribosomes with bound Nac-^{14}C-Phe-tRNA^{Phe} was calculated

from the predetermined amount of radioactivity per picomole of radiolabeled tRNA, corrected for background retention on the filters.

Poly-U Translation

Poly-U translation was carried out on 70S ribosomes formed from wild type and L11 mutant 50S and 30S subunits in the following manner. A ribosome mix of 25 μL was made containing 1X HMK buffer with 2 mM DTT, 25 pmoles of 50S subunits, 40 pmoles of 30S subunits, 20 μg of poly-U mRNA (Sigma) and 35 pmoles of N-Ac-Phe-$tRNA^{Phe}$ and was incubated for 15 minutes at 37 ° C. Meanwhile, a factor mix of 25 μL was made containing 1X HMK buffer with 2 mM DTT, 2 mM ATP, 5 mM GTP, 100 mM PEP, 5 μg of pyruvate kinase (Sigma), 1 mM L-[^{14}C]-phenylalanine at around 5 c.p.m/pmol (Amersham), and 5 μL of S100 fraction. The two solutions were mixed to start the translation and tubes were incubated for the desired time at 37 ° C. Translation was stopped by the addition of 25 μL of 450 mM potassium hydroxide and a portion of the translation mixture was spotted on filter paper (Whatman). Poly-[^{14}C]Phe peptides on filter paper were precipitated in 10% trichloroacetic acid (TCA) for 30 minutes at room temperature. [^{14}C-Phe] on excess [^{14}C]Phe-$tRNA^{Phe}$ in the reactions was hydrolyzed by placing the filters in boiling 5% TCA for 5 minutes. The filters were washed three times with room temperature 5% TCA, once with a 1:1 diethyl ether:ethanol solution, and once with a diethyl ether-only solution. The filters were dried for 30 minutes and the amount of acid-precipitatable poly-Phe peptide remaining was quantified by liquid scintillation counting, corrected for background in reactions without added ribosomal subunits. The quantity of acid-precipitatable poly-[^{14}C]Phe synthesized was calculated from the predetermined amount of radioactivity per picomole of [^{14}C]Phe added to reactions.

"Factor-Free" poly-U translation assays were carried out in the same manner as normal poly-U translation with the following deviations. S100 fraction or [^{14}C]Phe were not added to the factor mix. Instead, 1 mM [^{14}C]Phe-tRNA^{Phe} was added as a source of amino-acylated tRNA. When elongation factors (EF-G or EF-Tu or both) were added to the "factor-free" system, they were added to the factor mix to a final concentration of 0.1 μM.

EF-G/Ribosome-Dependent GTP Hydrolysis

GTP hydrolysis assays were carried out in the following manner. First, 25 pmoles of 70S ribosomes were incubated in 1X HMK buffer for 15 minutes at 37 ° C. To the ribosomes was added either 25 pmoles of EF-G for stoichiometric assays or 5 pmoles of EF-G for sub-stoichiometric assays and the volume was adjusted to 49 μL with 1X HMK buffer. To this mixture was added 1 μL of 125 mM [α-^{32}P]GTP mix (~10 cpm/pmole) to start the hydrolysis reaction. After the specified times, the reactions were stopped by the addition of 25 μL of a solution of 25% formic acid/5% TCA. The reactions were centrifuged at 8000 rpm for 10 minutes and aliquots were spotted on the bottom of polyethyleneimine cellulose TLC plates (J.T. Baker Chemical Co). The plates were dried and run in a covered chamber for 2.5 hours in a solution of 0.75 M Tris, 0.45 HCl, and 0.5 M LiCl. After chromatography, the plates were dried and radioactivity was quantified on phosphorimager plates using the supplied software. The amount of GTP hydrolyzed was calculated from the ratio of radioactivity in spots identified as [α-^{32}P]-GDP relative to the that remaining in [α-^{32}P]GTP spots for each TLC lane. The values were corrected for [α-^{32}P]-GDP present in reactions without EF-G or ribosomes added

and for the levels of GTP hydrolyzed in reactions with only EF-G added at each time point (uncoupled GTP hydrolysis).

Chapter 5
Summary and Conclusions

Introduction

In this study we have we have investigated the structure and function of the complex of ribosomal protein L11 and the L11-binding region (L11BR) of rRNA, a region of the large subunit of the prokaryotic ribosome involved in translation factor interactions during protein synthesis. The complex is part of the GTPase-associated region (GAR), a loosely defined combination of large subunit ribosomal elements that have been linked to ribosome-coupled GTP hydrolysis by the translational GTPase factors; IF2, EF-G, EF-Tu, RF3, and RRF. The elements include an rRNA element protected by factor binding to the large subunt, the sarcin/ricin stem-loop (SRL), a protein stalk on the large subunit that includes ribosomal protein L10 and two dimers of proteins L7 and L12 ($L10.(L7/L12)_2$) that is believed to be involved in GTPase activation, and the L11/L11BR complex.

Localization of the L11-Binding Region in the GTPase-Associated Region of the Large Subunit

Proximity and Dynamics of Elements in the GTPase-Associated Region (GAR)

We began our study by investigating the relative positions of the GAR elements on the large subunit (Chapter 2). As all these elements interact with translation factors, we postulated that, although distal in the secondary structure of the large subunit (Figure 1.9), they might be proximal to each other in the tertiary structure of the rRNA. By localizing a chemical nuclease to the SRL to probe surrounding rRNA, we found that the

L11/L11BR complex is within 25 Å of this stem-loop. As the L10.$(L7/L12)_2$ stalk binds to the large subunit at the base of the L11-L11BR (3), we reason that all of the GAR elements are probably proximal in the tertiary structure of the large subunit.

The results in Chapter 2 provided evidence of the proximity of several large subunit rRNA elements to the SRL. The elements include the stem-loop around 23S rRNA residue 2530, the stem-loop around 23S rRNA residue 2750, and the L11BR of 23S rRNA around residue 1070. The recent publication of high resolution crystal structures of large subunits allows us to interpret these results in relation to factor-dependent functions during translation on the ribosome. As illustrated in Figure 5.1, the SRL (red), the L11/L11BR complex (grey and green respectively), the 2530 stem-loop (blue), and the 2750 stem-loop (purple), are localized in one corner of the large subunit. The SRL and L11/L11BR complex are situated to interact with adjacent sites on EF-G. The L10.$(L7/L12)_2$ stalk interacts with the rRNA stem that supports the L11BR but is flexible and was not resolved in the subunit crystal structure (1,6). The 2750 stem-loop runs parallel to the SRL and the tip of this stem-loop interacts with the lower stem of the L11BR. The proximity of this element to both the SRL and L11BR puts it in a unique position to serve as a possible bridge between these two functional elements. Our structural probing suggested that this element may be flexible on the large subunit, and this flexibility could conceivably account for the coupling of conformational changes that have been seen between the SRL and L11BR in response to either thiostrepton binding in the L11BR (7) or the activity of the ribotoxins on the SRL (8).

The 2530 stem-loop (Figure 5.1, blue) also runs parallel to the SRL in the large subunit crystal structure model. The tip of the stem-loop nestles against the tip of the

SRL stem-loop. The two structures also are in close proximity and possibly interact with an rRNA internal loop around nucleotide A2565 (Figure 5.1, yellow). At the opposite end of this rRNA structure is the 2550 stem-loop, a loop consisting of conserved residues that is believed to form part of the A site tRNA binding pocket in the peptidyl transferase center. The proximity of these elements and the flexibility of the 2530 stem-loop indicated from the present study suggests a possible functional link between the SRL and the peptidyl transferase center. The mechanism for EF-G-stimulated translocation of tRNAs could include a step in which association of EF-G with the SRL or a conformational change in the factor following GTP hydrolysis induces a conformational change in the 2530 stem-loop that is transduced to the peptidyl transferase center through the 2565 internal loop and 2550 stem-loop. This model could, in part, account for the "unlocking" or destabilization of the tRNA binding elements of the peptidyl transferase center that would be necessary for translocation of P and A site tRNA across the ribosome to occur. Recently, Wilson *et al.* observed differences in the protection pattern of the SRL from hydroxyl radical cleavage when EF-G is in the pre- and post-translocation states (9), providing further evidence that EF-G modulates the structure of the SRL. The effects in the SRL suggested that EF-G interacts weakly with the SRL before mRNA translocation and strongly and more extensively with this stem-loop following mRNA translocation. The combination of our probing studies of the GAR and these recent observations provide evidence for a structurally-linked and dynamic region of the large subunit that may serve to transduce the signal from EF-G for translocation.

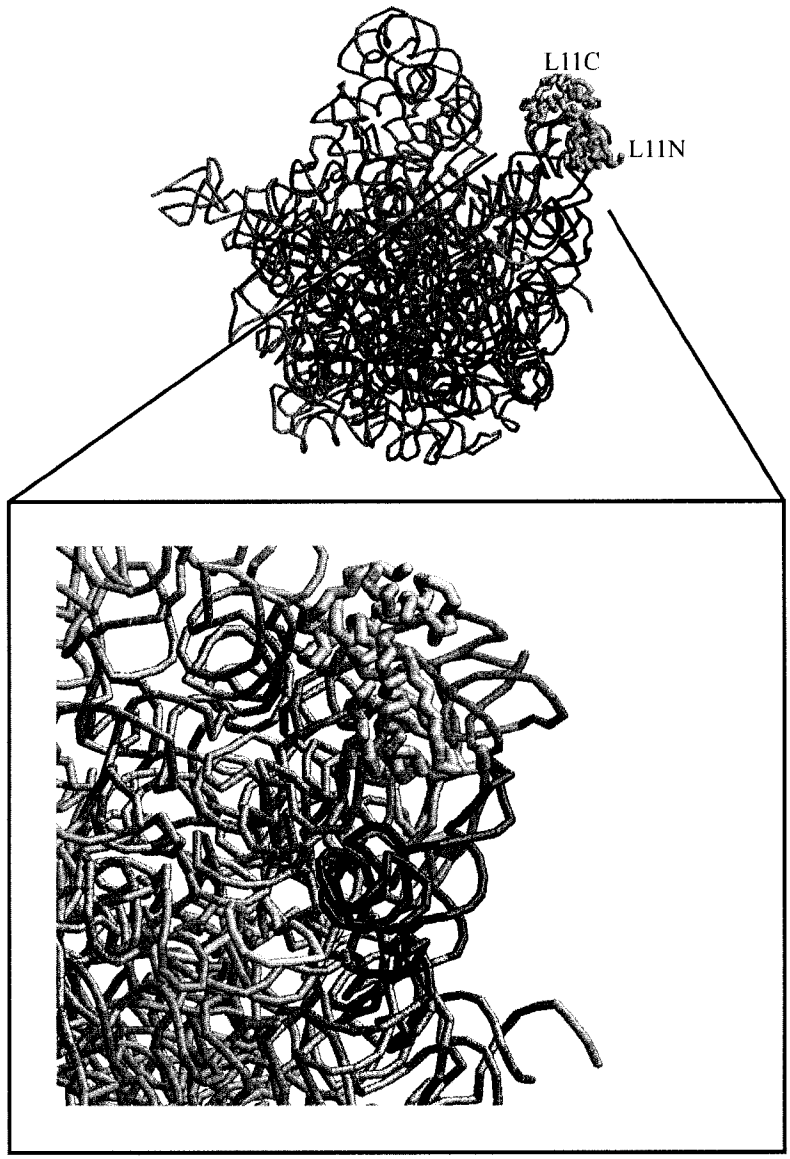

Figure 5.1. GTPase-Associated Region (GAR) on the Large Subunit of the Prokaryotic Ribosome. The elements of the GAR identified in this study are highlighted on the crystal structure model of the large subunit from *Deinococcus radiodurans* (1). The possible functional implications of the proximal elements are described in the text. Orange, rRNA backbone of large subunit; red, SRL; green, L11BR; purple, 2750 stem-loop; blue, 2530 stem-loop; yellow, rRNA structure containing the internal loop around nucleotide A2565 and the 2550 stem-loop; grey, protein backbone model of ribosomal protein L11. L11C, C-terminal domain of L11; L11N , N-terminal domain of L11.

Structural Dynamics and EF-G Interactions of the L11-Binding Region

Thiostrepton and EF-G do not cause extensive conformational changes in the L11BR

Chemical nuclease probing from the SRL also revealed a possible conformational change that occurs in the L11BR in response to binding of the antibiotic thiostrepton. This observation led us to hypothesize that the L11BR may shift between more than one functionally important conformation during translation on the ribosome, including one conformation that could be unproductively trapped by the antibiotic. To approach this question, we used small, diffusible chemical probes to further investigate the structural dynamics of the L11BR when thiostrepton binds in the domain (Chapter 3).

As a result of this analysis, we found that the binding of thiostrepton to the L11BR induces structural changes outside of the thiostrepton binding cleft that probably include tightening of the interaction between L11 and the L11BR. It has been postulated that when thiostrepton binds in the L11BR it "traps" one conformation of the L11BR, thereby preventing a conformational change in the rRNA that is induced by EF-G interactions and is necessary for stimulating translocation (10). The structural changes we observed were outside of the purported thiostrepton binding site (11,12), suggesting that thiostrepton binding modulates the structure of the domain. The changes, however, were localized to only a limited number of residues. Therefore, it is unlikely that thiostrepton binding modulates a significant conformational change of the entire L11-binding domain.

As ribosomal protein L11 also binds the rRNA in this domain, we expanded the research in Chapter 3 to investigate if the status of L11 binding on the large subunit affects the structure of the L11BR. We postulated that the status of L11 may regulate a

possible functionally important conformation of the L11BR. Specifically, we hypothesized that the N-terminal domain of might act as a molecular switch, inducing structural changes in the L11BR by reversibly dissociating from the rRNA in response to antibiotic or translation factor interactions. To help answer this question, we probed wild type and L11 mutant ribosomes to compare the structures of wild type ribosomes with those lacking the entire L11 protein ($L11^-$) and those lacking just the N-terminal domain of L11 ($L11N^-$).

We found that the structure of the L11BR is conformationally flexible only when ribosomes lacked the entire protein and not when they lacked only the N-terminal domain. Our analysis does not support a model in which the dissociation of the N-terminal domain of L11 causes a conformational switch in the L11-binding domain during translation. Our evidence does supports a model that suggests that the C-terminal domain is primarily responsible for binding of L11 to rRNA and stabilization of the rRNA structure, while the N-terminal domain is only tenuously associated with the L11BR (13). The absence of the L11 N-terminal domain only affects the accessibility of a few isolated L11BR residues thought to be involved in direct interactions with the domain.

Similarly, our results (Chapter 3) suggested that EF-G binding to the L11-binding rRNA does not cause extensive conformational changes in the L11BR. The limited number of residues protected when EF-G was bound to ribosomes in the pre- or post-translocation state could be explained by direct interactions between the factor and the rRNA.

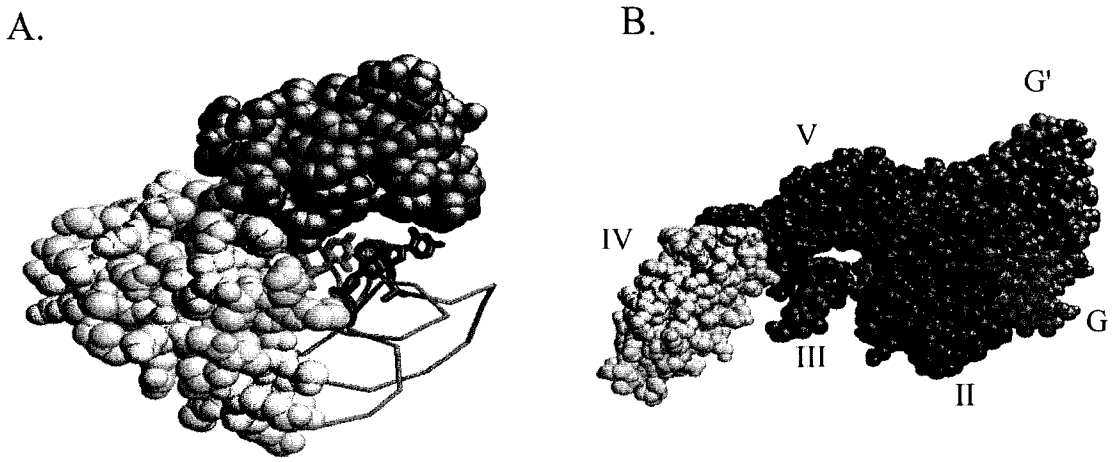

Figure 5.2. Structures of the L11/L11-Binding rRNA Complex and Translation Factor EF-G. (A) Complex of L11 and the L11-binding region of rRNA (L11BR) (2) with the protein in spacefill and rRNA in backbone model . The N-terminal domain of L11 is highlighted in grey and the C-terminal domain is highlighted in yellow. Residues of the L11BR with changes in reactivity associated with possible movements of the N-terminal domain of L11 are shown in distinct colors: U1061, green; A1070, blue; U1097, red. (B) Domain structure of EF-G (4) in spacefill model with the domains labeled and distinguished by color.

The Role of the L11 N-Terminal Domain in Translation

Thiostrepton protected nucleotides U1061, A1070, and U1097 in the L11BR, and the positions of of these residues relative to ribosomal protein L11 (Figure 3.6) suggest that binding of thiostrepton may "tighten" the interaction of the N-terminal domain of L11 with the L11BR. As binding of EF-G in the post-translocation state increased the reactivity of U1061 and U1097 to chemical probes, it is possible that EF-G disrupts the interaction of the N-terminal domain of L11 with the L11BR in the post-translocation state. This possibility is supported by a low-resolution cryo-electron microscopic study that suggests that domain V of EF-G intrudes into the cleft between the 23 S ribosomal RNA and the N-terminal domain of L11 in the post-translocation state, causing the N-

terminal domain to move and inducing the formation of an interaction between the G' domain of EF-G and this domain (14). Figure 5.2 illustrates the tenuous interaction between L11 and the domains of EF-G believed to be involved in interactions with the L11BR and L11.

The results described in Chapter 3 also suggest that L11 mutant ribosomes lacking L11 interacted with EF-G at a significantly reduced level relative to wild type ribosomes in either the pre- or post-translocation states. As the C-terminal domain is believed to stabilize the structure of the L11BR, it follows that the integrity of L11BR structure is necessary for the interaction of EF-G with the ribosome in both the pre- and post-translocation states. Alternatively, the interaction of EF-G with the L11/L11BR domain may require an interaction of the factor with specific residues in the C-terminal domain of L11.

Taken together, the evidence suggests a model in which EF-G interacts primarily with the SRL in the pre-translocation state. After ribosome/EF-G-dependent GTP hydrolysis, the conformation of EF-G shifts to one that favors a more extensive interaction with the the L11/L11BR domain. The conformational change in EF-G could be part of the mechanism for triggering the "unlocking" of the A and P site tRNA for translocation to occur on the large subunit, and it may involve transduction of the EF-G signal from the SRL to the peptidyl transferase center through elements of the GAR.

Further, an interaction of EF-G with the L11BR and N-terminal domain of L11 after GTP hydrolysis and translocation could serve to destabilize pre-translocation interactions of EF-G with the ribosome. This would favor formation of the post-

translocation conformation of EF-G and could increase the efficiency of removal of EF-G before the next round of elongation.

A transition from the pre- to post-translocation state of EF-G on the ribosome is accompanied by the hydrolysis of GTP (5). As L11 mutant ribosomes lacking L11 were deficient in the formation of both pre- and post-translocation complexes, we postulated that these mutations would affect elongation factor-dependent translation elongation and the accompanying elongation factor GTP hydrolysis on the ribosome. *In vitro* translation assays (Chapter 4) on L11$^-$ mutant ribosomes revealed a significant reduction in the rate of elongation factor-dependent protein synthesis relative to wild type ribosomes. L11N$^-$ ribosomes suffered an intermediate defect in the *in vitro* translation studies. Further analysis revealed that this defect was predominantly related to a defect in the function of EF-G during elongation.

To ascertain if the defect in EF-G function was related to factor-dependent GTP hydrolysis on the ribosome, we carried out ribosome/EF-G-dependent GTP hydrolysis assays on wild type and mutant ribosomes. In the GTP hydrolysis assays, L11$^-$ and L11N$^-$ ribosomes showed a reduced rate of GTP hydrolysis relative to wild type ribosomes. Analysis of the rates of GTP hydrolysis under high turnover conditions for EF-G suggested that the reduction in the hydrolysis rates for mutant ribosomes may be due to a defect in the turnover of the factor on the ribosome.

The results from functional assays support and expand our model for the role of L11 in elongation developed above. In this model, ribosomes lacking the N-terminal domain of L11 do not stabilize the post-translocation state of the ribosome as efficiently as wild type ribosome. This would result in a delay in the transition from the pre- to

post-translocation state of EF-G on the ribosome and may also reduce the efficiency of removal of EF-G from ribosome after translocation, delaying a transition into the next stage of elongation.

The study presented here greatly expands out understanding of the functions of the ribosomal protein L11 and the L11BR on the large subunit of prokaryotic ribosomes. The data do not support a role for a conformational change in the L11BR during translocation, as little evidence could be found for significant structural changes induced either by a change in the interaction of the L11BR with the N-terminal domain of L11 or by an interaction with EF-G. Instead, the L11BR appears to serve as a static but important scaffold for the interaction of EF-G with the ribosome in the post-translocatio state.

Our evidence does suggest that the N-terminal domain has a prominent role in stimulating the turnover of EF-G on the ribosome following GTP hydrolysis. Relatedly, we found that the antibiotic thiostrepton probably tightens the interaction of the L11BR with the N-terminal domain of L11, potentially preventing a functional conformational change in the protein in response to EF-G binding.

In the future, this study will benefit from several possible lines of investigation. First, the study of the function of the L11BR structure and its interactions with elongation factors could benefit from targeted mutations of the L11BR residues identified in the EF-G, L11, and thiostrepton interaction studies. Such studies may suggest the importance of specific residues in the L11BR for EF-G, L11, and thiostrepton interactions. Similarly, targeted mutational analysis could be used to identify the specific residues on the N-terminal domain of L11 that are related to antibiotic and factor binding.

A good place to start would be residues in the N-terminal domain of L11 that are closely associated with nucleotides in the L11BR (Gln-12, Lys-10). Finally, elucidating the specific stage of translocation inhibited by mutations in L11 will benefit from expanding the studies of ribosome/EF-G dependent GTP hydrolysis to include a systematic kinetic analysis of the process, including single-turnover analysis.

Appendix A

Comparison of rRNA Cleavage by Complementary 1,10-Phenanthroline-Cu(II)- and EDTA-Fe(II)-Derivatized Oligonucleotides

William S. Bowen, Walter E. Hill, and J. Stephen Lodmell

(A copy of a manuscript published by the authors in the Journal Methods: 25, 344-350 (2001)

METHODS 25, 344–350 (2001)
doi:10.1006/meth.2001.1246, available online at http://www.idealibrary.com on IDEAL®

Comparison of rRNA Cleavage by Complementary 1,10-Phenanthroline–Cu(II)- and EDTA–Fe(II)-Derivatized Oligonucleotides

William S. Bowen, Walter E. Hill, and J. Stephen Lodmell[1]

Division of Biological Sciences, University of Montana, Missoula, Montana 59812

The chemical nucleases 1,10-phenanthroline–Cu(II) and EDTA–Fe(II), have proven to be valuable tools for structural analysis of nucleic acids. Both have found applications in footprinting and directed proximity studies of DNA and RNA. Derivatives of each that provide for tethering to nucleic acid or protein are commercially available, allowing their widespread use for structural analysis of macromolecules. Although their applications are somewhat overlapping, differences in their cleavage mechanisms and chemical properties allow them to provide distinct and complementary structural information. The purpose of this study is to compare directly the cleavage patterns of tethered 1,10-phenanthroline–Cu(II) and EDTA–Fe(II) complexes within a similar experimental system. Here, the region surrounding nucleotide 1400 of 16S rRNA from *Escherichia coli* serves as a substrate for chemical cleavage directed by a derivatized complementary oligonucleotide. This region of rRNA is known to be involved in the decoding of mRNA during translation. The results of this study provide evidence in support of the mechanistic differences previously established for EDTA–Fe(II) and 1,10-phenathroline–Cu(II). The delocalized cleavage envelope produced by EDTA–Fe(II) cleavage suggests the involvement of a diffusible reactive species. On the other hand, rRNA cleavage induced by the tethered 1,10-phenanthroline–Cu(II) complex appears localized to the proximity of the chemical nuclease under normal conditions, although the production of an unknown diffusible species appears to occur during long reaction times.

Chemical nucleases represent a valuable class of tools for investigating nucleic acid structure and dynamics. The several chemical nucleases in current use offer a variety of target specificities and cleavage efficiencies (1, 2). Chemical nucleases present some advantages over conventional enzymatic nucleases in that they are smaller in size and thus can reach more sterically hindered regions of a macromolecule. In addition, chemical nucleases can be derivatized, allowing modulation of activity and/or specificity. Although many of the chemical cleavage reagents that have appeared in the literature over the past several years have been custom synthesized in the investigators' own laboratories, some of the reagents used as chemical nucleases are now commercially available. Two of these, the derivative of EDTA, *p*-bromoacetamidobenzyl-EDTA (BABE) complexed with Fe(II), and the derivative of phenanthroline, 5-iodoacetamido-1,10-phenanthroline (IoP) complexed with Cu(II), are in increasing use.

Several excellent reviews of the use of Fe–BABE and Cu–phenanthroline (Cu–oP) have recently been published and their respective protocols have been refined in individual systems (3–6). Our intention here is not to repeat those thorough works, but to determine what are the practical differences between the two techniques with respect to experimental methodology and interpretation of results. In this study, we conduct a side-by-side comparison of the cleavage efficiencies and specificities of Fe–BABE and Cu–oP under similar reaction conditions with respect to reducing agent [ascorbate or mercaptopropionic acid (MPA)] and the presence or absence of exogenously added hydrogen peroxide, which has the universal effect of increasing the robustness of the cleavage reaction.

We chose as our study system the 16S ribosomal RNA from the eubacterium *Escherichia coli*. We directed the chemical cleavage reagents toward a particularly interesting region of the 16S rRNA, the so-called decoding region, located around nucleotide 1400. This region of the 16S rRNA is known to play an active role during

[1] To whom correspondence should be addressed. Fax: (406) 243-4304. E-mail: lodmell@selway.umt.edu

1046-2023/01 $35.00

the mRNA–tRNA recognition process and it is exceptionally accessible to complementary DNA oligomer binding (7–13). We targeted our chemical nucleases to this region by tethering Fe–BABE or Cu–oP to an oligodeoxynucleotide complementary to the rRNA sequence in the vicinity of the decoding region (Fig. 1). Because the DNA oligomer to which we chemically joined the cleavage reagent remained constant, we were able to compare the cleavage patterns of the two reagents directly.

Several chemical and mechanistic features distinguish Cu–oP and Fe–BABE cleavage. First, the hydrophobic character of the 1,10-phenanthroline ring system (Fig. 1) may provide for reversible association of the coordination complex with accessible hydrophobic nucleobases. Partial docking in the minor groove or interactions with splayed bases could position the reactive species for oxidative attack on the ribose or deoxyribose, leading to direct strand scission (6, 14, 15). The structure and net negative charge of the Fe–BABE complex (Fig. 1) is not conducive to stable association with nucleic acids (16) and, therefore, is proposed to act in solution through the production of a diffusible radical species (17).

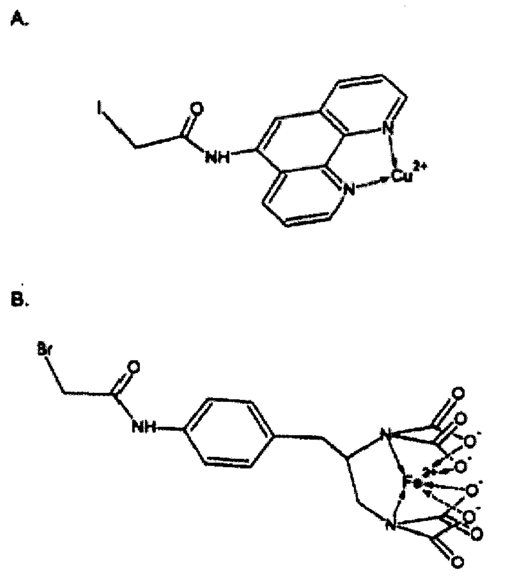

FIG. 1. Cleavage reagents used for oligonucleotide-directed cleavage reactions. The reagents are tethered to the 5′-phosphorothioate of the oligonucleotide via reaction at the substituted acetamido tether. (A) Derivatized 5-iodoacetamido-1,10-phenanthroline (IoP) with coordinated copper ion. (B) Derivatized 1-(P-bromoacetamidobenzyl)-EDTA (BABE) with coordinated iron ion.

Second, the proposed mechanisms for direct strand scission by Cu–oP and Fe–BABE are similar, but have distinctive characteristics. Cu–oP cleavage is believed to proceed via hydrogen atom abstraction from the ribose or deoxyribose, primarily at the C-1 position (18, 19). In this scheme (Fig. 2), a bound copper-oxo species forms on oxidation of the bound copper ion by endogenous or exogenous hydrogen peroxide. This reactive species, if positioned favorably, may abstract a hydrogen atom at C-1, leading to rearrangement and elimination to produce scission of the phosphodiester backbone. Because the reactive species is not diffusible (14), the tethered coordination complex must be oriented for specific binding adjacent to the C-1 position in the minor groove to initiate a cleavage event.

The mechanism for direct strand scission by Fe–BABE is believed to proceed via oxidation of the bound iron to produce a reactive species which may abstract a hydrogen atom from the ribose or deoxyribose. However, the reactive species is believed to be a diffusible hydroxyl radical with no requirement for docking of the BABE moiety to the nucleic acid (*20*). This scheme requires that the ribose or deoxyribose be solvent-accessible and that radical production occurs close enough to prevent solvent quenching of the radicals before abstraction can occur (5).

These chemical and mechanistic differences provide a framework for comparing directed cleavage using Cu–oP and Fe–BABE. Based on the requirement for specific docking of the Cu–oP complex in the minor groove of nucleic acids, and the less stringent proximity requirements of the Fe–BABE system, one would expect to see more robust cleavage patterns from Fe–BABE than from Cu–oP tethered to the same position. This difference would reflect the limitation of Cu–oP cleavage to targets within the tethered distance and binding of the Cu–oP complex to the nucleic acid in an orientation suitable for hydrogen atom abstraction. Fe–BABE cleavage, on the other hand, would be limited only by the solvent accessibility of the target ribose and the effective diffusion radius of the hydroxyl radicals in solution, estimated to be between 10 and 60 Å (21, 22).

DESCRIPTION OF METHODS

Preparation of 16S rRNA

The substrate for oligonucleotide-directed cleavage was 16S rRNA extracted from 30S ribosomal subunits of *E. coli*. The 30S ribosomal subunits were obtained from the ribonuclease deficient strain MRE600 by standard methods (e.g., 23). Subunits were extracted twice with an equal volume of water-saturated phenol

(pH 4.3), followed by one phenol–chloroform (24:24:1 phenol:chloroform: isoamyl alcohol) and one chloroform extraction. The rRNA was subsequently precipitated by the addition of 2.5 vol of ethanol and centrifuged for 25 min in a microfuge to precipitate. After the pellet was washed twice with cold 70% ethanol and dried in a vacuum concentrator, it was resuspended in H_2O, aliquoted, and frozen at −80°C for future use.

Synthesis of 5′-Phosphorothioate Oligonucleotide

A 21-nucleotide-long phosphorothioate-containing DNA oligomer, called 5′-P(S)-DEC1412 (oligonucleotides derivatized with phenanthroline and BABE are called Cu–oP-DEC1412 and Fe–BABE-DEC1412, respectively; see below), was designed to be complementary to nucleotides 1392–1412 in 16S rRNA. It was synthesized using standard phosphoramidite chemistry on an ABI 394 DNA/RNA synthesizer and included a 3′-phosphate group and a 5′-phosphorothioate group for tethering of BABE or IoP as follows. A 3′-phosphate CPG column (Glen Research) was used for incorporating the 3′-phosphate to prevent extension from cleavage probes during primer extension analysis. Synthesis of the sequence 5′-GGTGTGACGGGCGGTGTGTAC-3′ was carried out using normal phosphoramidite chemistry. The 5′-phosphorothioate was introduced with the use of a 5′-phosphorylating reagent (Glen Research) for the last step of the synthesis. The normal base synthesis step was interrupted at the coupling stage, which was increased to 6 min. After coupling, the capping step was omitted and the oxidizing step was continued with sulfurizing reagent (Glen Research) replacing the normal oxidizer. The oligonucleotide was then cleaved from the solid support and deprotected at 65°C in NH_4OH/ethylamine solution for 10 min. The product was then purified with reversed-phase HPLC using an ammonium acetate/acetonitrile gradient. Appropriate fractions were lyophilized and resuspended in HPLC-grade water to a concentration of 1000 pmol/μl.

BABE Modification of Oligonucleotide

We employed the method of Noller and co-workers (5, 21) with some modifications for derivatizing an oligonucleotide with BABE. In the first step, BABE (Dojindo, Gaithersburg, MD) was loaded with Fe^{2+} by mixing 10 μl of 10 mM BABE in DMSO with 10 μl of fresh 9 mM $Fe^{2+}(NH_4^+)_2(SO_4^{2-})_2 \cdot 6H_2O$. The mixture was incubated at room temperature for 60 min, lyophilized, and stored at −20°C. Attachment of BABE to the 5′-phosphorothioate on the oligonucleotide was accomplished by mixing 5000 pmol of purified 5′-phosphorothioate oligonucleotide with a lyophilized Fe(II)–BABE pellet from above (100 μmol), 2 μl of 400 mM potassium phosphate buffer (pH 8.5), and HPLC-grade water in a final volume of 20 μl. After vortexing and a brief centrifugation, the mixture was incubated at 37°C for 2 h. One microliter of 50 mM EDTA was added and incubation was continued for an additional 10 min to chelate remaining uncomplexed

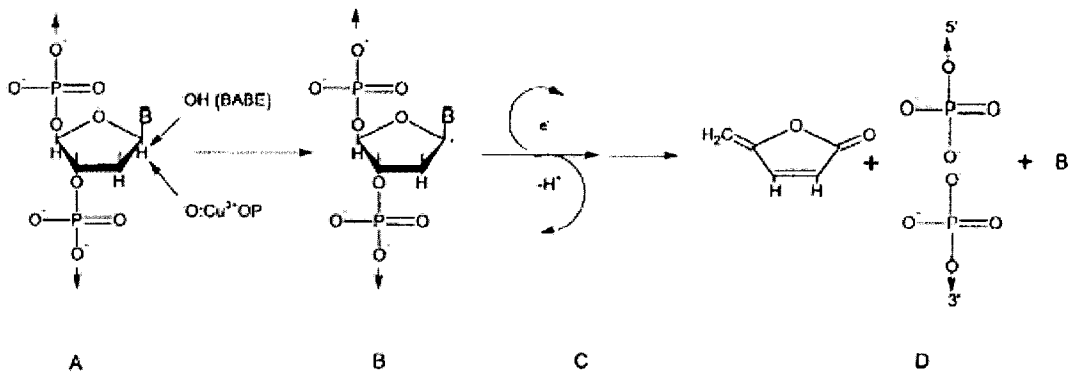

FIG. 2. General reaction scheme for chemical scission of DNA via hydrogen atom abstraction at C1 as proposed by Meijler *et al.* (26). The precise chemistry following abstraction by the metal-oxo species or hydroxyl radical remains uncertain for RNA, but probably follows similar chemistry. Abstraction at C4 can commonly occur with diffusible hydroxyl radicals, generating distinct scission products (27). (A) First step in strand scission mediated by hydrogen atom abstraction at C1 by either phenanthroline-coordinated copper-oxo species or diffusible hydroxyl radical. (B) Carbon-centered ribose radical formed from hydrogen atom abstraction. (C) Sequence of oxidation, rearrangement, and elimination of 3′- and 5′-phosphorylated strand fragments which is well defined for DNA, but which remains poorly defined for RNA. (D) Products of DNA strand scission: 5-methylene furanose, 3′ and 5′phosphorylated strand fragments, free nucleobase.

Fe^{2+}. Five microliters of 10 M ammonium acetate and 75 μl of HPLC-grade water were then added, followed by three water-saturated phenol (pH 4.3) and two chloroform extractions to remove unreacted Fe(II)–BABE complex. Three hundred microliters cold 95% EtOH was added and the mixture was incubated at −80°C for 25 min. The derivatized oligomer was recovered by centrifugation at 13,000*g* and 4°C for 25 min. The supernatant was carefully removed and the pellet was dried in a vacuum concentrator. The pellet was then resuspended in HPLC-grade water to a concentration of 25 pmol/μl for use in cleavage reactions.

IoP Modification of Oligonucleotide

Unlike Fe–BABE, the phenanthroline cleavage conditions do not require preloading of Cu^{2+}. For modification of the 5′-phosphorothioate oligonucleotide, 50,000 pmol of IoP in dimethyl sulfoxide (DMSO) was added to 5000 pmol of 5′-phosphorothioate oligonucleotide [5′-P(S)-DEC1412] in a solution of 1:1 DMSO:HPLC-grade water. The reaction mixture was then incubated at room temperature for 60 min and was immediately lyophilized. The pellet was resuspended in 100 μl of a 0.5 M ammonium acetate, HPLC-grade water solution and was extracted three times with water-saturated phenol (pH 4.3) and twice with chloroform. After the final extraction, 300 μl of cold 95% EtOH was added and the solution was precipitated at −80°C for 25 min. Finally, the solution was centrifuged at 13,000*g* at 4°C for 25 min, the supernatant carefully removed, and the pellet dried. The pellet was resuspended in HPLC-grade water to a final concentration of 25 pmol/μl for cleavage reactions.

PAGE and APM/PAGE Analysis of Derivatized Oligonucleotides

Gel electrophoresis analysis was used to determine the efficiency of the derivatization reactions. Five hundred picomoles of derivatized or underivatized oligonucleotide was dissolved in 5 μl of gel loading buffer (7 M urea, 20 mM EDTA, 0.05% xylene cyanol, 0.05% bromphenol blue), and loaded on a 15% acrylamide denaturing gel with or without 0.01 mg/ml [(*N*-acryloylamino)phenyl]mercuric chloride (APM; synthesized in-house by G. Muth)], and run for 20 min at 20-mA constant current on a 10 × 10-cm gel (approximately 35 V/cm at the beginning of the run). Bands were visualized by staining with methylene blue. On an APM gel, molecules bearing a 5′- or 3′-thiol group are markedly retarded in their migration (24). Thus oligonucleotides bearing unreacted phosphorothioate groups display much slower migration relative to the same oligonucleotides that were successfully derivatized. Typically the derivatization with BABE or IoP was essentially quantitative (see Fig. 3).

Cleavage of 16S rRNA

5′-Fe–BABE-DEC1412-directed cleavage of 16S rRNA

Cleavage reactions with the BABE-derivatized probe were carried out following the procedure of Joseph and Noller (5) with a few minor deviations. Reactions were set up by combining 25 pmol of derivatized probe with 4 μl of cleavage buffer [10×: 400 mM potassium cacodylate (pH 7.5), 200 mM $MgCl_2$, 750 mM KCl], 25 pmol extracted 16S rRNA, and brought to a final volume of 20 μl with HPLC-grade water. Control reactions omitted derivatized probe and substituted either underivatized probe, free cleavage reagent, or free metal ions (Fig. 4). The reactions were incubated at 42°C for 20 min and slow-cooled to room temperature to hybridize probe to 16S rRNA. Following binding, 1 μl of 100 mM reducing agent or 1 μl of 100 mM reducing agent plus 1 μl of 1% hydrogen peroxide were added immediately to the specified tubes by pipetting droplets onto opposite sides of the microfuge tubes and giving a pulse spin to initiate cleavage. The tubes were then incubated for either 5

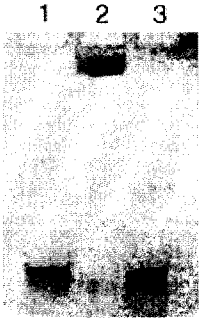

FIG. 3. Quantitation and separation of derivatized versus nonderivatized phosphorothioate-containing oligonucleotides on an APM gel. Five hundred picomoles of derivatized or underivatized oligonucleotide was dissolved in 5 μl gel loading buffer (7 M urea, 20 mM EDTA, 0.05% xylene cyanol, 0.05% bromphenol blue) and loaded on a 15% acrylamide denaturing gel with 0.01 mg/ml [(*N*-acryloylamino)phenyl]mercuric chloride. Bands were visualized by staining/destaining with methylene blue. Lane 1: 5′-Cu–oP-DEC1412; Lane 2: 5′-P(S)-DEC1412; Lane 3: Fe–BABE-DEC1412.

min at room temperature, 60 min on ice, or 2.5 h at both temperatures (Fig. 4). To quench the reactions, 300 μl cold 95% ethanol (EtOH) and 50 μl of 0.3 M sodium acetate were added to each tube and the tubes were placed in a dry ice/EtOH bath for 25 min. After centrifugation for 25 min at 13,000*g* and 4°C, the supernatant was carefully aspirated, the pellets were washed twice with cold 70% ethanol, then dried in a vacuum concentrator. The pellets were resuspended in 40 μl of HPLC-grade water and used for primer extension and gel electrophoresis analysis (5, 6, 10) to detect oligo-directed cleavage (Fig. 4).

Cu-oP-DEC1412-Directed Cleavage of 16S rRNA

Cleavage reactions with the phenanthroline-derivatized probe followed the same procedure as the BABE cleavages above. The main difference involved adding 1 μl of 200 μM $CuSO_4$ to the 25 pmol of oP-DEC1412 probe aliquot before setting up the reaction tubes. Construction of reactions and controls, cleavage reactions,

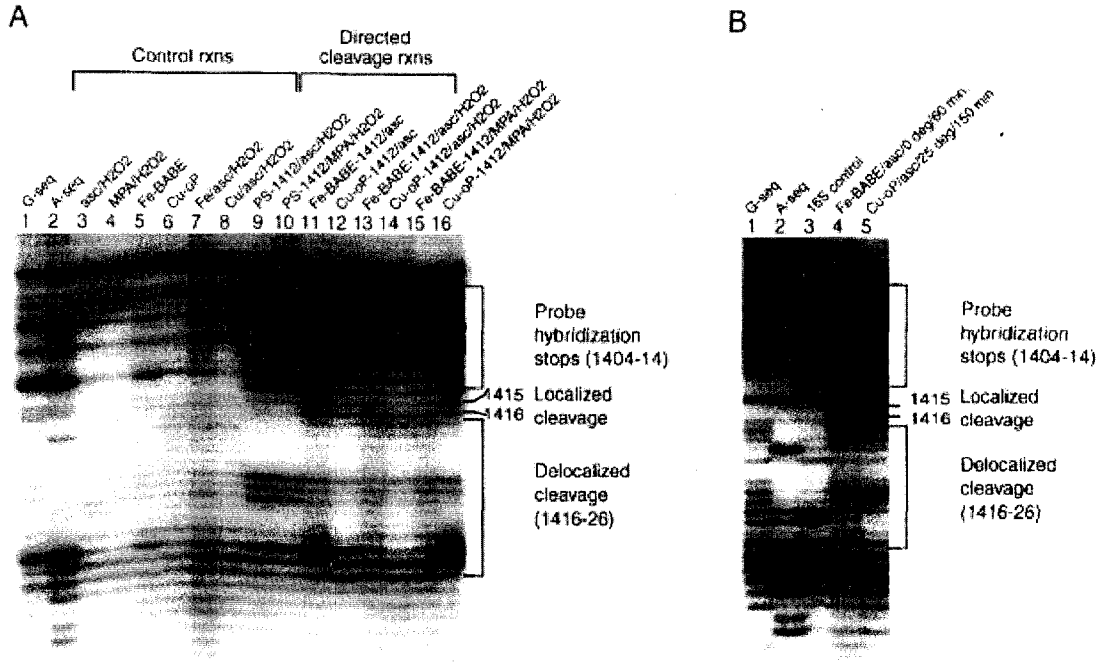

FIG. 4. (A) Example of Fe-BABE versus Cu-oP-mediated cleavage from the 1392–1412 oligonucleotide. Lane 1: G sequencing. Lane 2: A sequencing. Lanes 3–10: 25°C, 5-min cleavage control lanes with 1× cleavage buffer and the following control parameters: Lane 3: 16S rRNA (5 mM ascorbate, 0.05% H_2O_2); Lane 4: 16S rRNA (5 mM MPA, 0.05% H_2O_2); Lane 5: 16S rRNA with 125 pmol free Fe–BABE (5 mM ascorbate, 0.05% H_2O_2); Lane 6: 16S rRNA with 125 pmol free oP and 200 pmol $CuSO_4$ (5 mM ascorbate, 0.05% H_2O_2); Lane 7: 16S rRNA with 25 pmol $Fe^{2+}(NH_4^+)_2(SO_4^{2-})_2$ (5 mM ascorbate, 0.05% H_2O_2); Lane 8: 16S rRNA with 200 pmol $CuSO_4$ (5 mM ascorbate, 0.05% H_2O_2); Lane 9: 16S rRNA with 25 pmol underivatized 5′-P(S)-DEC1412 probe (5 mM ascorbate, 0.05% H_2O_2); Lane 10: 16S rRNA with 25 pmol underivatized 5′-P(S)-DEC1412 probe (5 mM MPA, 0.05% H_2O_2). Lanes 11–14: 25°C, 5-min cleavage lanes with 1× cleavage buffer and the following reagents: Lane 11: 16S rRNA with 25 pmol 5′-Fe–BABE-DEC1412 probe (5 mM ascorbate); Lane 12: 16S rRNA with 25 pmol 5′-oP-DEC1412 probe and 200 pmol $CuSO_4$ (5 mM ascorbate); Lane 13: 16S rRNA with 25 pmol 5′-Fe–BABE-DEC1412 probe (5 mM ascorbate, 0.05% H_2O_2); Lane 14: 16S rRNA with 25 pmol 5′-oP-DEC1412 probe and 200 pmol $CuSO_4$ (5 mM ascorbate, 0.05% H_2O_2). Lanes 15, 16: 0°C, 60-min cleavage reaction lanes with 1× cleavage buffer and the following reagents: Lane 15: 16S rRNA with 25 pmol 5′-Fe–BABE-DEC1412 probe (5 mM MPA, 0.05% H_2O_2); Lane 16: 16S rRNA with 25 pmol 5′-oP-DEC1412 probe and 200 pmol $CuSO_4$ (5 mM MPA, 0.05% H_2O_2). Probe hybridization stops: reverse transcriptase stops or RNase H cleavage induced by probe hybridization during primer extension. Localized cleavage: rRNA cleavage occurring within the estimated distance of the tethered nuclease, Fe–BABE or Cu–oP, from the 5′-end of the hybridized probe (20–30 Å). Delocalized cleavage: rRNA cleavage attributed to a diffusible reactive species. (B) Lane 1: G sequencing. Lane 2: A sequencing. Lane 3: 16S rRNA control. Lanes 4 and 5: reaction lanes with 16S rRNA, 1× cleavage buffer, and the following reagents (cleavage time and temperature indicated): Lane 4: 16S rRNA with 25 pmol 5′-Fe-BABE-DEC1412 probe (5 mM ascorbate, 60 minutes, 0°C); Lane 5: 16S rRNA with 25 pmol 5′-oP-DEC1412 probe and 200 pmol $CuSO_4$ (5 mM ascorbate, 2.5 h, 25°C).

incubations, quenching, precipitation, and analysis were otherwise the same as for the BABE reactions above. Results of both the Cu–oP and Fe–BABE cleavages are shown in Fig. 4.

TECHNICAL COMMENTS

Potential Free Metal Effects

Oligo-directed probing with Fe–BABE and that with Cu–phenanthroline are procedurally very similar. Some minor technical differences distinguish them, however. Free iron contamination in reactions can cause nonspecific cleavage, which must be distinguished from directed cleavage. The risk of nonspecific (nontethered) free iron cleavage is possible when performing Fe–BABE probing because some unliganded iron could potentially copurify with the Fe–BABE–oligonucleotide complex. Free copper ions are also redox reactive, but do not initiate extensive cleavage of the target RNA under the conditions employed (Fig. 4 and data not shown). The possibility of free metal contamination makes Chelex-treated buffers or HPLC-grade water desirable for either technique.

Chemical Reactivity of Linkers

When derivatizing the oligonucleotides, we found that the 5-iodoacetamido linker used for phenanthroline tethering was more reactive than the bromoacetamidobenzyl linker used in BABE tethering. Typically, the tethering reaction for BABE took 5 to 10 times longer than the 5-iodoacetamido-(1,10)-phenanthroline to go to completion at similar concentrations of oligo and nuclease. Increasing the concentration of Fe–BABE or IoP in the reactions can increase the yield of tethered probe, but also increases the chance of free (untethered) Fe–BABE or IoP contamination after purification.

rRNA Cleavage during Primer Extension

Note that the presence of the derivatized or underivatized oligonucleotide probe hybridized to the rRNA causes a strong stop during the primer extension (see Fig. 4, lanes 3–8 vs lanes 9 and 10). This can be explained by the reverse transcriptase that is engaged in the primer extension encountering the hybridized oligonucleotide, which results in reverse transcriptase pausing or dissociating. Alternatively, because reverse transcriptase itself has RNase H activity, it may cleave the rRNA at the site of the RNA/DNA hybrid.

Potential for Detachment of the Cleavage Reagent from the Oligonucleotide

The nucleolytic effects of these reagents are not limited to the target nucleic acid, but can potentially cleave off fragments of the complementary oligonucleotide used for directing cleavage. The predicted result would be a pattern of cleavage diffusion emanating from the position of complementarity, although under the reaction conditions described here, the expected contribution of this type of cleavage should be rather small.

RESULTS

Figure 4 shows results of the Fe–BABE and Cu–oP cleavage reaction comparisons. Derivatized-DEC1412-specific cleavage was observed as primer extension stops 3′ the probe binding region on the rRNA (nucleotides 1392–1412) and distinct from control lanes. A primer extension stop at a unique nucleotide position in experimental lanes is interpreted as a cleavage event at the nucleotide immediately 5′ to that position on the rRNA. Stops occurring directly at the region of probe binding (especially nucleotides 1408–1414) were attributed to pausing/stopping of reverse transcriptase or RNase H activity at the probe hybridization site, as discussed above.

Several features immediately stand out in the analysis of Fig. 4A. First, reactions that include Fe–BABE-DEC1412 (lanes 11,13,15) or Cu–oP-DEC1412 (lanes12,14,16) both provide robust rRNA cleavage at positions near the 5′ end of the rRNA-bound probe (nucleotides 1414–1416). However, the Fe–BABE-DEC1412 probe provides a significantly more delocalized cleavage pattern than lanes including Cu–oP-DEC1412 (lanes 12,14,16), both at room temperature (lanes 11–14) and at 0°C (lanes 15,16).

Second, the addition of exogenous hydrogen peroxide to Fe–BABE-DEC1412 reactions (lanes 13,15) results in an increase in the delocalization of cleavage when compared either with the reaction without added exogenous hydrogen peroxide (lane 11) or with those reactions that include Cu–oP-DEC1412 and exogenous hydrogen peroxide (lanes 14,16). The addition of hydrogen peroxide may increase the rate at which the reduced Fe(I)–BABE or Cu(I)–oP complex is oxidized to form the reactive species (25). However, this effect might be less pronounced in Cu–oP reactions in which the reduced complex is bound in the minor groove of the RNA, less accessible to solvent.

Figure 4B shows the results of running the reactions with Cu–oP-DEC1412 and ascorbate for an extended period (2.5 h) to determine whether cleavage intensity

would increase locally or if the overall pattern of cleavages might change. The results suggest that the low-intensity, localized cleavage seen with phenanthroline/ascorbate over short reaction times may be supplanted by less localized cleavage after 2.5 h in reactions containing ascorbate at 25°C (lane 5). This delocalized pattern resembles the typical pattern observed with BABE-DEC1412-directed cleavage, which is shown for comparison (lane 4). The BABE-DEC1412 cleavage is already robust at 60 min at 0°C; to obtain this pattern with Cu–oP-DEC1412 requires a longer incubation at higher temperature. Nevertheless, this result was somewhat unexpected inasmuch as the proposed RNA cleavage mechanisms of Cu–oP and Fe–BABE differ with respect to the diffusibility of the resultant reactive radical (14, 20). Based on these results we cannot rule out the involvement of a diffusible radical species in the ascorbate reaction with Cu–oP.

CONCLUDING REMARKS

Both Cu–oP and Fe–BABE are useful probes for investigating RNA structure, and their individual cleavage characteristics give them complementary roles in such studies. Overall, the cleavage attained using Fe–BABE is more robust, but owing to the generation of freely diffusible hydroxyl radicals, there is a concomitant reduction in the resolution of distance constraints. On the other hand, the mechanism of Cu–oP cleavage of RNA requires that the tethered Cu–oP partially intercalates into local RNA structure prior to cleavage. While this ensures that cleavage is strictly local under usual reaction conditions, some sites are more amenable to phenanthroline binding than others, thus varying cleavage intensity over the nucleotides that are within the tethered striking distance.

The charge and binding characteristics of each of the cleavage reagents are important factors for determining overall cleavage efficiency. Phenanthroline is more hydrophobic than the rather polar BABE moiety. Some environments are therefore better for binding one or the other. Indeed we encountered one case in which an oligonucleotide tethered to phenanthroline was capable of good binding to the rRNA, while the same oligonucleotide tethered to Fe–BABE did not bind well, and cleavage was attenuated (data not shown). Thus, when choosing a cleavage reagent, one must empirically determine which gives the best results with respect to differential binding of the tethered oligonucleotide as well as overall cleavage efficiency.

ACKNOWLEDGMENTS

We acknowledge Martha Rice for superb technical assistance. We also gratefully acknowledge helpful discussions on derivatization and cleavage using BABE with Simpson Joseph and Chuck Merryman. This work was supported by National Institutes of Health Grant GM35717 to W.E.H.

REFERENCES

1. Burrows, C. J., and Muller, J. G. (1998) *Chem. Rev.* **98**, 1109–1151.
2. Pogozelski, D. S., and Tullius, T. D. (1998) *Chem. Rev.* **98**, 1089–1107.
3. Hermann, T., and Heumann, H. (2000) *Methods Enzymol.* **318**, 33–43.
4. Hall, K. B., and Fox, (1999) *Methods.* **18**, 78–84.
5. Joseph, S., and Noller, H. (2000) *Methods Enzymol.* **318**, 175–190.
6. Muth, G. W., and Hill, W. E. (2001) *Methods* **23**, 218–232.
7. Gornicki, P., Nurse, K., Hellmann, W., Boublik, M., and Ofengand, J. (1984) *J. Biol. Chem.* **259**, 10493–10498.
8. Rinke-Appel, J., Junke, N., Stade, K., and Brimacombe, R. (1991) *EMBO J.* **10**, 2195–2202.
9. Weller, J., and Hill, W. E. (1994) *J. Biol. Chem.* **269**, 19369–19374.
10. Moazed, D., Van Stolk, B. J., Douthwaite, S., and Noller, H. F. (1986) *J. Mol. Biol.* **191**, 483–493.
11. O'Connor, M., Thomas, C. L., Zimmermann, R. A., and Dahlberg, A. E. (1997) *Nucleic Acids Res.* **25**, 1185–1193.
12. Bullard, J. M., van Waes, M. A., Bucklin, D. J., Rice, M. J., and Hill, W. E. (1998) *Biochemistry* **37**, 1350–1356.
13. Muth, G. W., Hennelly, S. P., and Hill, W. E. (2000) *Biochemistry* **39**, 4068–4074.
14. Sigman, D. S. (1990) *Biochemistry* **29**, 9097–9105.
15. Hermann, T., and Heumann, H. (1995) *RNA* **1**, 1009–1017.
16. Sigman, D. S., and Chen, C. H. (1990) *Annu. Rev. Biochem.* **59**, 207–236.
17. Tullius, T. D. (1988) *Nature* **332**, 663–664.
18. Kuwabara, M., Yoon, C., Goyne, T., Thederahn, T., and Sigman, D. S. (1986) *Biochemistry* **25**, 7401–7408.
19. Tronche, C., Goodman, B. K., and Greenberg, M. M. (1998) *Chem. Biol.* **5**, 263–271.
20. Pogozelski, W. K., McNeese, T. J., and Tullius, T. D. (1995) *J. Am. Chem. Soc.* **117**, 6428–6433.
21. Hellek, G. M., Marusak, R., Meares, C. F., and Noller, H. F. (1995) *Proc. Natl. Acad. Sci. USA* **92**, 1113–1116.
22. Que, B. G., Downey, K. M., and So, A. G. (1980) *Biochemistry* **19**, 5987–5991.
23. Tam, M. F., and Hill, W. E. (1981) *Biochemistry* **20**, 6480–6484.
24. Iglot, G. L. (1988) *Biochemistry* **27**, 3842–3849.
25. Marshall, L. E., Graham, D. R., Reich, K. A., and Sigman, D. S. (1981) *Biochemistry* **20**, 244–250.
26. Meijler, M. M., Zelenko, O., and Sigman, D. S. (1997) *J. Am. Chem. Soc.* **119**, 1135–1136.
27. Henner, W. D., Rodriguez, L. O., Hecht, S. M., and Haseltine, W. A. (1983) *J. Biol. Chem.* **258**, 711–713.

REFERENCES

1. Tortura, G. J., Funke, B.R., and Case, C.L. (2002) *Microbiology: An Introduction*, Pearson Education, New Jersey
2. Alberts, B., Johnson, A., Lewis, J., Raff, M., Roberts, K., and Walter, P. (1994) *Molecular Biology of the Cell*, 4 Ed., Garland Science, New York
3. Muth, G. W., Hennelly, S. P., and Hill, W. E. (2000) *Biochemistry* 39(14), 4068-4074
4. Sayle, R. A., and Milner-White, E. J. (1995) *Trends Biochem Sci* 20(9), 374
5. Igloi, G. L. (1988) *Biochemistry* 27(10), 3842-3849
6. Cannone, J. J., Subramanian, S., Schnare, M. N., Collett, J. R., D'Souza, L. M., Du, Y., Feng, B., Lin, N., Madabusi, L. V., Muller, K. M., Pande, N., Shang, Z., Yu, N., and Gutell, R. R. (2002) *BMC Bioinformatics* 3(1), 15
7. Milburn, M. V., Tong, L., deVos, A. M., Brunger, A., Yamaizumi, Z., Nishimura, S., and Kim, S. H. (1990) *Science* 247(4945), 939-945
8. Wimberly, B. T., Guymon, R., McCutcheon, J. P., White, S. W., and Ramakrishnan, V. (1999) *Cell* 97(4), 491-502
9. Poole, A. M., Jeffares, D. C., and Penny, D. (1998) *J Mol Evol* 46(1), 1-17
10. Vetter, I. R., and Wittinghofer, A. (2001) *Science* 294(5545), 1299-1304
11. Palade, G. E. (1955) *J Biophys Biochem Cytol* 1(1), 59-68
12. Karimi, R., Pavlov, M. Y., Buckingham, R. H., and Ehrenberg, M. (1999) *Mol Cell* 3(5), 601-609
13. Shine, J., and Dalgarno, L. (1975) *Nature* 254(5495), 34-38
14. Calogero, R. A., Pon, C. L., Canonaco, M. A., and Gualerzi, C. O. (1988) *Proc Natl Acad Sci U S A* 85(17), 6427-6431
15. Gualerzi, C. O., and Pon, C. L. (1990) *Biochemistry* 29(25), 5881-5889
16. Hartz, D., McPheeters, D. S., and Gold, L. (1989) *Genes Dev* 3(12A), 1899-1912
17. Antoun, A., Pavlov, M. Y., Andersson, K., Tenson, T., and Ehrenberg, M. (2003) *EMBO J* 22(20), 5593-5601
18. Rodnina, M. V., Savelsbergh, A., and Wintermeyer, W. (1999) *FEMS Microbiol Rev* 23(3), 317-333
19. Rodnina, M. V., Pape, T., Fricke, R., and Wintermeyer, W. (1995) *Biochem Cell Biol* 73(11-12), 1221-1227
20. Rodnina, M. V., Pape, T., Fricke, R., Kuhn, L., and Wintermeyer, W. (1996) *J Biol Chem* 271(2), 646-652
21. Brenner, S., Stretton, A. O., and Kaplan, S. (1965) *Nature* 206(988), 994-998
22. Weigert, M. G., and Garen, A. (1965) *Nature* 206(988), 992-994
23. Arkov, A. L., and Murgola, E. J. (1999) *Biochemistry (Mosc)* 64(12), 1354-1359
24. Brown, C. M., and Tate, W. P. (1994) *J Biol Chem* 269(52), 33164-33170
25. Zavialov, A. V., Buckingham, R. H., and Ehrenberg, M. (2001) *Cell* 107(1), 115-124

26. Hirashima, A., and Kaji, A. (1970) *Biochem Biophys Res Commun* 41(4), 877-883
27. Hirashima, A., and Kaji, A. (1972) *Biochemistry* 11(22), 4037-4044
28. Hirashima, A., and Kaji, A. (1972) *J Mol Biol* 65(1), 43-58
29. Ouzounis, C., and Kyrpides, N. (1996) *FEBS Lett* 390(2), 119-123
30. Olsen, G. J., and Woese, C. R. (1997) *Cell* 89(7), 991-994
31. Mathews, C. K., and van Holde, K.E. (1996) *Biochemistry*, 2 Ed., Benjamin/Cummings Publishing Company, Inc., Menlo Park, CA.
32. Bourne, H. R. (1995) *Philos Trans R Soc Lond B Biol Sci* 349(1329), 283-289
33. Caldon, C. E., Yoong, P., and March, P. E. (2001) *Mol Microbiol* 41(2), 289-297
34. Leipe, D. D., Wolf, Y. I., Koonin, E. V., and Aravind, L. (2002) *J Mol Biol* 317(1), 41-72
35. Caldon, C. E., and March, P. E. (2003) *Curr Opin Microbiol* 6(2), 135-139
36. Koonin, E. V., Wolf, Y. I., and Aravind, L. (2000) *Adv Protein Chem* 54, 245-275
37. Gideon, P., John, J., Frech, M., Lautwein, A., Clark, R., Scheffler, J. E., and Wittinghofer, A. (1992) *Mol Cell Biol* 12(5), 2050-2056
38. Trahey, M., and McCormick, F. (1987) *Science* 238(4826), 542-545
39. Scheffzek, K., Ahmadian, M. R., and Wittinghofer, A. (1998) *Trends Biochem Sci* 23(7), 257-262
40. Watson, N., Linder, M. E., Druey, K. M., Kehrl, J. H., and Blumer, K. J. (1996) *Nature* 383(6596), 172-175
41. Sprang, S. R. (1997) *Annu Rev Biochem* 66, 639-678
42. Boguski, M. S., and McCormick, F. (1993) *Nature* 366(6456), 643-654
43. Kawashima, T., Berthet-Colominas, C., Wulff, M., Cusack, S., and Leberman, R. (1996) *Nature* 379(6565), 511-518
44. Wittinghofer, A., Goody, R. S., Roesch, P., and Kalbitzer, H. R. (1982) *Eur J Biochem* 124(1), 109-115
45. Berchtold, H., Reshetnikova, L., Reiser, C. O., Schirmer, N. K., Sprinzl, M., and Hilgenfeld, R. (1993) *Nature* 365(6442), 126-132
46. Kjeldgaard, M., Nissen, P., Thirup, S., and Nyborg, J. (1993) *Structure* 1(1), 35-50
47. Pel, H. J., Moffat, J. G., Ito, K., Nakamura, Y., and Tate, W. P. (1998) *RNA* 4(1), 47-54
48. Pon, C. L., Paci, M., Pawlik, R. T., and Gualerzi, C. O. (1985) *J Biol Chem* 260(15), 8918-8924
49. Katunin, V. I., Savelsbergh, A., Rodnina, M. V., and Wintermeyer, W. (2002) *Biochemistry* 41(42), 12806-12812
50. Bourne, H. R., Sanders, D. A., and McCormick, F. (1990) *Nature* 348(6297), 125-132
51. Freistroffer, D. V., Pavlov, M. Y., MacDougall, J., Buckingham, R. H., and Ehrenberg, M. (1997) *EMBO J* 16(13), 4126-4133
52. Ravel, J. M. (1967) *Proc Natl Acad Sci U S A* 57(6), 1811-1816

53. Ravel, J. M., Shorey, R. L., and Shive, W. (1967) *Biochem Biophys Res Commun* 29(1), 68-73
54. Nathans, D., von, E., Monro, R., and Lipmann, F. (1962) *Fed Proc* 21, 127-133
55. Kolakofsky, D., Dewey, K. F., Hershey, J. W., and Thach, R. E. (1968) *Proc Natl Acad Sci U S A* 61(3), 1066-1070
56. Bodley, J. W., and Lin, L. (1970) *Nature* 227(253), 60-61
57. Bernabeu, C., Vazquez, D., and Ballesta, J. P. (1976) *Eur J Biochem* 69(1), 233-241
58. Arai, N., and Kaziro, Y. (1975) *J Biochem (Tokyo)* 77(2), 439-447
59. Parmeggiani, A., and Sander, G. (1981) *Mol Cell Biochem* 35(3), 129-158
60. Rodnina, M. V., Stark, H., Savelsbergh, A., Wieden, H. J., Mohr, D., Matassova, N. B., Peske, F., Daviter, T., Gualerzi, C. O., and Wintermeyer, W. (2000) *Biol Chem* 381(5-6), 377-387
61. Mohr, D., Wintermeyer, W., and Rodnina, M. V. (2002) *Biochemistry* 41(41), 12520-12528
62. Savelsbergh, A., Mohr, D., Wilden, B., Wintermeyer, W., and Rodnina, M. V. (2000) *J Biol Chem* 275(2), 890-894
63. Gudkov, A. T. (1997) *FEBS Lett* 407(3), 253-256
64. Moller, W., Schrier, P. I., Maassen, J. A., Zantema, A., Schop, E., Reinalda, H., Cremers, A. F., and Mellema, J. E. (1983) *J Mol Biol* 163(4), 553-573
65. Agthoven, A. J., Maassen, J. A., Schrier, P. I., and Moller, W. (1975) *Biochem Biophys Res Commun* 64(4), 1184-1191
66. Sander, G., Marsh, R. C., and Parmeggiani, A. (1972) *Biochem Biophys Res Commun* 47(4), 866-873
67. Hernandez, F., Vazquez, D., and Ballesta, J. P. (1977) *Eur J Biochem* 78(1), 267-272
68. Sander, G., Marsh, R. C., Voigt, J., and Parmeggiani, A. (1975) *Biochemistry* 14(9), 1805-1814
69. Schrier, P. I., and Moller, W. (1975) *FEBS Lett* 54(2), 130-134
70. Munishkin, A., and Wool, I. G. (1997) *Proc Natl Acad Sci U S A* 94(23), 12280-12284
71. Agrawal, R. K., Linde, J., Sengupta, J., Nierhaus, K. H., and Frank, J. (2001) *J Mol Biol* 311(4), 777-787
72. Moazed, D., Robertson, J. M., and Noller, H. F. (1988) *Nature* 334(6180), 362-364
73. Rosendahl, G., and Douthwaite, S. (1994) *Nucleic Acids Res* 22(3), 357-363
74. Thompson, J., Musters, W., Cundliffe, E., and Dahlberg, A. E. (1993) *EMBO J* 12(4), 1499-1504
75. Saarma, U., Remme, J., Ehrenberg, M., and Bilgin, N. (1997) *J Mol Biol* 272(3), 327-335
76. Wriggers, W., Agrawal, R. K., Drew, D. L., McCammon, A., and Frank, J. (2000) *Biophys J* 79(3), 1670-1678
77. Bilgin, N., and Ehrenberg, M. (1994) *J Mol Biol* 235(3), 813-824
78. Chan, Y. L., Sitikov, A. S., and Wool, I. G. (2000) *J Mol Biol* 298(5), 795-805

79. O'Connor, M., and Dahlberg, A. E. (1996) *Nucleic Acids Res* 24(14), 2701-2705
80. Wilson, K. S., and Nechifor, R. (2004) *J Mol Biol* 337(1), 15-30
81. Endo, Y., and Wool, I. G. (1982) *J Biol Chem* 257(15), 9054-9060
82. Zeidler, W., Egle, C., Ribeiro, S., Wagner, A., Katunin, V., Kreutzer, R., Rodnina, M., Wintermeyer, W., and Sprinzl, M. (1995) *Eur J Biochem* 229(3), 596-604
83. Mohr, D., Wintermeyer, W., and Rodnina, M. V. (2000) *EMBO J* 19(13), 3458-3464
84. Laursen, B. S., Siwanowicz, I., Larigauderie, G., Hedegaard, J., Ito, K., Nakamura, Y., Kenney, J. M., Mortensen, K. K., and Sperling-Petersen, H. U. (2003) *J Mol Biol* 326(2), 543-551
85. Larigauderie, G., Laalami, S., Nyengaard, N. R., Grunberg-Manago, M., Cenatiempo, Y., Mortensen, K. K., and Sperling-Petersen, H. U. (2000) *Biochimie* 82(12), 1091-1098
86. Crick, F. H. (1968) *J Mol Biol* 38(3), 367-379
87. Guerrier-Takada, C., Gardiner, K., Marsh, T., Pace, N., and Altman, S. (1983) *Cell* 35(3 Pt 2), 849-857
88. Lazcano, A., and Miller, S. L. (1996) *Cell* 85(6), 793-798
89. Orgel, L. E. (2004) *Crit Rev Biochem Mol Biol* 39(2), 99-123
90. Woese, C. R. (2001) *RNA* 7(8), 1055-1067
91. Jeffares, D. C., Poole, A. M., and Penny, D. (1998) *J Mol Evol* 46(1), 18-36
92. Ogle, J. M., Brodersen, D. E., Clemons, W. M., Jr., Tarry, M. J., Carter, A. P., and Ramakrishnan, V. (2001) *Science* 292(5518), 897-902
93. Ogle, J. M., Murphy, F. V., Tarry, M. J., and Ramakrishnan, V. (2002) *Cell* 111(5), 721-732
94. Potapov, A. P. (1982) *FEBS Lett* 146(1), 5-8
95. Davies, J., Gilbert, W., and Gorini, L. (1964) *Proc Natl Acad Sci U S A* 51, 883-890
96. Topal, M. D., and Fresco, J. R. (1976) *Nature* 263(5575), 289-293
97. Purohit, P., and Stern, S. (1994) *Nature* 370(6491), 659-662
98. Powers, T., and Noller, H. F. (1995) *RNA* 1(2), 194-209
99. Yusupov, M. M., Yusupova, G. Z., Baucom, A., Lieberman, K., Earnest, T. N., Cate, J. H., and Noller, H. F. (2001) *Science* 292(5518), 883-896
100. Green, R., and Noller, H. F. (1997) *Annu Rev Biochem* 66, 679-716
101. Monro, R. E. (1967) *J Mol Biol* 26(1), 147-151
102. Noller, H. F. (1993) *J Bacteriol* 175(17), 5297-5300
103. Noller, H. F., Hoffarth, V., and Zimniak, L. (1992) *Science* 256(5062), 1416-1419
104. Bispink, L., and Matthaei, H. (1973) *FEBS Lett* 37(2), 291-294
105. Barta, A., and Kuechler, E. (1983) *FEBS Lett* 163(2), 319-323
106. Barta, A., Steiner, G., Brosius, J., Noller, H. F., and Kuechler, E. (1984) *Proc Natl Acad Sci U S A* 81(12), 3607-3611
107. Breitmeyer, J. B., and Noller, H. F. (1976) *J Mol Biol* 101(3), 297-306

108. Moazed, D., and Noller, H. F. (1991) *Proc Natl Acad Sci U S A* 88(9), 3725-3728
109. Gale, E. F., Cundliffe, E., Reynolds, P.E., Garrett, R.A. (1981) Antibiotic inhibitors of ribosome function. In. *Molecular Basis of Antibiotic Action*, Wiley, London
110. Cocito, C., Di Giambattista, M., Nyssen, E., and Vannuffel, P. (1997) *J Antimicrob Chemother* 39 Suppl A, 7-13
111. Douthwalte, S., Voldborg, B., Hansen, L. H., Rosendahl, G., and Vester, B. (1995) *Biochem Cell Biol* 73(11-12), 1179-1185
112. Mankin, A. S. (2001) *Mol Biol (Mosk)* 35(4), 597-609
113. Noller, H. F. (1993) *Faseb J* 7(1), 87-89
114. Green, R., Switzer, C., and Noller, H. F. (1998) *Science* 280(5361), 286-289
115. Joseph, S., and Noller, H. F. (1996) *EMBO J* 15(4), 910-916
116. Moazed, D., and Noller, H. F. (1989) *Cell* 57(4), 585-597
117. Moazed, D., and Noller, H. F. (1990) *J Mol Biol* 211(1), 135-145
118. Samaha, R. R., Green, R., and Noller, H. F. (1995) *Nature* 377(6547), 309-314
119. Merryman, C., Moazed, D., Daubresse, G., and Noller, H. F. (1999) *J Mol Biol* 285(1), 107-113
120. Mitchell, P., Osswald, M., and Brimacombe, R. (1992) *Biochemistry* 31(11), 3004-3011
121. Schindler, D. G., and Davies, J. E. (1977) *Nucleic Acids Res* 4(4), 1097-1110
122. Olsnes, S., Refsnes, K., and Pihl, A. (1974) *Nature* 249(458), 627-631
123. Endo, Y., and Tsurugi, K. (1987) *J Biol Chem* 262(17), 8128-8130
124. Reisbig, R., Olsnes, S., and Eiklid, K. (1981) *J Biol Chem* 256(16), 8739-8744
125. Brigotti, M., Rambelli, F., Zamboni, M., Montanaro, L., and Sperti, S. (1989) *Biochem J* 257(3), 723-727
126. Fernandez-Puentes, C., and Vazquez, D. (1977) *FEBS Lett* 78(1), 143-146
127. Montanaro, L., Sperti, S., Mattioli, A., Testoni, G., and Stirpe, F. (1975) *Biochem J* 146(1), 127-131
128. Holmberg, L., and Nygard, O. (1994) *Biochemistry* 33(50), 15159-15167
129. Hausner, T. P., Atmadja, J., and Nierhaus, K. H. (1987) *Biochimie* 69(9), 911-923
130. Endo, Y., Gluck, A., and Wool, I. G. (1993) *Nucleic Acids Symp Ser* (29), 165-166
131. Macbeth, M. R., and Wool, I. G. (1999) *J Mol Biol* 285(3), 965-975
132. Macbeth, M. R., and Wool, I. G. (1999) *J Mol Biol* 285(2), 567-580
133. Nierhaus, K. H., Schilling-Bartetzko, S., and Twardowski, T. (1992) *Biochimie* 74(4), 403-410
134. Wool, I. G., Gluck, A., and Endo, Y. (1992) *Trends Biochem Sci* 17(7), 266-269
135. Agrawal, R. K., Penczek, P., Grassucci, R. A., and Frank, J. (1998) *Proc Natl Acad Sci U S A* 95(11), 6134-6138
136. Conn, G. L., Draper, D. E., Lattman, E. E., and Gittis, A. G. (1999) *Science* 284(5417), 1171-1174
137. Ryan, P. C., Lu, M., and Draper, D. E. (1991) *J Mol Biol* 221(4), 1257-1268

138. Conn, G. L., Gutell, R. R., and Draper, D. E. (1998) *Biochemistry* 37(34), 11980-11988
139. Lu, M., and Draper, D. E. (1995) *Nucleic Acids Res* 23(17), 3426-3433
140. Xing, Y., and Draper, D. E. (1995) *J Mol Biol* 249(2), 319-331
141. Rosendahl, G., and Douthwaite, S. (1993) *J Mol Biol* 234(4), 1013-1020
142. Xing, Y., and Draper, D. E. (1996) *Biochemistry* 35(5), 1581-1588
143. Egebjerg, J., Douthwaite, S., and Garrett, R. A. (1989) *EMBO J* 8(2), 607-611
144. Wimberly, B. T., Brodersen, D. E., Clemons, W. M., Jr., Morgan-Warren, R. J., Carter, A. P., Vonrhein, C., Hartsch, T., and Ramakrishnan, V. (2000) *Nature* 407(6802), 327-339
145. Gabashvili, I. S., Gregory, S. T., Valle, M., Grassucci, R., Worbs, M., Wahl, M. C., Dahlberg, A. E., and Frank, J. (2001) *Mol Cell* 8(1), 181-188
146. Alksne, L. E., Anthony, R. A., Liebman, S. W., and Warner, J. R. (1993) *Proc Natl Acad Sci U S A* 90(20), 9538-9541
147. Carter, A. P., Clemons, W. M., Brodersen, D. E., Morgan-Warren, R. J., Wimberly, B. T., and Ramakrishnan, V. (2000) *Nature* 407(6802), 340-348
148. Uchiumi, T., Hori, K., Nomura, T., and Hachimori, A. (1999) *J Biol Chem* 274(39), 27578-27582
149. Uchiumi, T., Honma, S., Endo, Y., and Hachimori, A. (2002) *J Biol Chem* 277(44), 41401-41409
150. Maassen, J. A., and Moller, W. (1978) *J Biol Chem* 253(8), 2777-2783
151. Maassen, J. A., and Moller, W. (1981) *Eur J Biochem* 115(2), 279-285
152. Van Dyke, N., and Murgola, E. J. (2003) *J Mol Biol* 330(1), 9-13
153. Van Dyke, N., Xu, W., and Murgola, E. J. (2002) *J Mol Biol* 319(2), 329-339
154. Tate, W. P., McCaughan, K. K., Ward, C. D., Sumpter, V. G., Trotman, C. N., Stoffler-Meilicke, M., Maly, P., and Brimacombe, R. (1986) *J Biol Chem* 261(5), 2289-2293
155. Stark, M. J., and Cundliffe, E. (1979) *Eur J Biochem* 102(1), 101-105
156. Stark, M. J., Cundliffe, E., Dijk, J., and Stoffler, G. (1980) *Mol Gen Genet* 180(1), 11-15
157. Yang, X., and Ishiguro, E. E. (2001) *J Bacteriol* 183(22), 6532-6537
158. Choli, T. (1989) *Biochem Int* 19(6), 1323-1338
159. Ryan, P. C., and Draper, D. E. (1989) *Biochemistry* 28(26), 9949-9956
160. Hausner, T. P., Geigenmuller, U., and Nierhaus, K. H. (1988) *J Biol Chem* 263(26), 13103-13111
161. Mazumder, R. (1973) *Proc Natl Acad Sci U S A* 70(7), 1939-1942
162. Lockwood, A. H., Sarkar, P., Maitra, U., Brot, N., and Weissbach, H. (1974) *J Biol Chem* 249(18), 5831-5834
163. Pestka, S. (1970) *Biochem Biophys Res Commun* 40(3), 667-674
164. Modolell, J., Cabrer, B., Parmeggiani, A., and Vazquez, D. (1971) *Proc Natl Acad Sci U S A* 68(8), 1796-1800
165. Grunberg-Manago, M., Dondon, J., and Graffe, M. (1972) *FEBS Lett* 22(2), 217-221
166. Cameron, D. M., Thompson, J., March, P. E., and Dahlberg, A. E. (2002) *J Mol Biol* 319(1), 27-35

167. Ballesta, J. P., and Vazquez, D. (1972) *Proc Natl Acad Sci U S A* 69(10), 3058-3062
168. Brandi, L., Marzi, S., Fabbretti, A., Fleischer, C., Hill, W. E., Gualerzi, C. O., and Stephen Lodmell, J. (2004) *J Mol Biol* 335(4), 881-894
169. Rodnina, M. V., Savelsbergh, A., Matassova, N. B., Katunin, V. I., Semenkov, Y. P., and Wintermeyer, W. (1999) *Proc Natl Acad Sci U S A* 96(17), 9586-9590
170. Weisblum, B., and Demohn, V. (1970) *J Bacteriol* 101(3), 1073-1075
171. Pestka, S., Weiss, D., Vince, R., Wienen, B., Stoffler, G., and Smith, I. (1976) *Mol Gen Genet* 144(3), 235-241
172. Highland, J. H., Howard, G. A., Ochsner, E., Hasenbank, R., Gordon, J., and Stoffler, G. (1975) *J Biol Chem* 250(3), 1141-1145
173. Thompson, J., Schmidt, F., and Cundliffe, E. (1982) *J Biol Chem* 257(14), 7915-7917
174. Cundliffe, E., and Thompson, J. (1979) *Nature* 278(5707), 859-861
175. Thompson, J., and Cundliffe, E. (1991) *Biochimie* 73(7-8), 1131-1135
176. Thompson, J., Cundliffe, E., and Stark, M. (1979) *Eur J Biochem* 98(1), 261-265
177. Moore, P. B. (2001) *Biochemistry* 40(11), 3243-3250
178. Cate, J. H., Yusupov, M. M., Yusupova, G. Z., Earnest, T. N., and Noller, H. F. (1999) *Science* 285(5436), 2095-2104
179. Ban, N., Nissen, P., Hansen, J., Moore, P. B., and Steitz, T. A. (2000) *Science* 289(5481), 905-920
180. Harms, J., Schluenzen, F., Zarivach, R., Bashan, A., Gat, S., Agmon, I., Bartels, H., Franceschi, F., and Yonath, A. (2001) *Cell* 107(5), 679-688
181. Schluenzen, F., Tocilj, A., Zarivach, R., Harms, J., Gluehmann, M., Janell, D., Bashan, A., Bartels, H., Agmon, I., Franceschi, F., and Yonath, A. (2000) *Cell* 102(5), 615-623
182. Grimes, J. M., Fuller, S. D., and Stuart, D. I. (1999) *Acta Crystallogr D Biol Crystallogr* 55 (Pt 10), 1742-1749
183. Brimacombe, R. (1991) *Biochimie* 73(7-8), 927-936
184. Graifer, D. M., Juzumiene, D. I., Wollenzien, P., and Karpova, G. G. (1994) *Biochemistry* 33(13), 3878-3884
185. Dontsova, O. A., Rosen, K. V., Bogdanova, S. L., Skripkin, E. A., Kopylov, A. M., and Bogdanov, A. A. (1992) *Biochimie* 74(4), 363-371
186. Dontsova, O., Dokudovskaya, S., Kopylov, A., Bogdanov, A., Rinke-Appel, J., Junke, N., and Brimacombe, R. (1992) *EMBO J* 11(8), 3105-3116
187. Stade, K., Rinke-Appel, J., and Brimacombe, R. (1989) *Nucleic Acids Res* 17(23), 9889-9908
188. Stiege, W., Stade, K., Schuler, D., and Brimacombe, R. (1988) *Nucleic Acids Res* 16(6), 2369-2388
189. Juzumiene, D. I., Shapkina, T. G., and Wollenzien, P. (1995) *J Biol Chem* 270(21), 12794-12800
190. Tranque, P., Hu, M. C., Edelman, G. M., and Mauro, V. P. (1998) *Proc Natl Acad Sci U S A* 95(21), 12238-12243

191. Noah, J. W., Shapkina, T. G., Nanda, K., Huggins, W., and Wollenzien, P. (2003) *Biochemistry* 42(49), 14386-14396
192. Osswald, M., Doring, T., and Brimacombe, R. (1995) *Nucleic Acids Res* 23(22), 4635-4641
193. Doring, T., Mitchell, P., Osswald, M., Bochkariov, D., and Brimacombe, R. (1994) *EMBO J* 13(11), 2677-2685
194. Abdurashidova, G. G., Tsvetkova, E. A., and Budowsky, E. I. (1991) *Nucleic Acids Res* 19(8), 1909-1915
195. Ciesiolka, J., Nurse, K., Klein, J., and Ofengand, J. (1985) *Biochemistry* 24(13), 3233-3239
196. Ehresmann, C., Ehresmann, B., Millon, R., Ebel, J. P., Nurse, K., and Ofengand, J. (1984) *Biochemistry* 23(3), 429-437
197. Chan, Y. L., Correll, C. C., and Wool, I. G. (2004) *J Mol Biol* 337(2), 263-272
198. Nag, B., Johnson, A. E., and Traut, R. R. (1995) *Indian J Biochem Biophys* 32(6), 343-350
199. Kastner, B., Trotman, C. N., and Tate, W. P. (1990) *J Mol Biol* 212(2), 241-245
200. Girshovich, A. S., Bochkareva, E. S., and Vasiliev, V. D. (1986) *FEBS Lett* 197(1-2), 192-198
201. Skold, S. E. (1983) *Nucleic Acids Res* 11(14), 4923-4932
202. Pon, C. L., Brimacombe, R., and Gualerzi, C. (1977) *Biochemistry* 16(26), 5681-5686
203. Seo, H. S., and Cooperman, B. S. (2002) *Bioorg Chem* 30(3), 163-187
204. Muralikrishna, P., Alexander, R. W., and Cooperman, B. S. (1997) *Nucleic Acids Res* 25(22), 4562-4569
205. Alexander, R. W., Muralikrishna, P., and Cooperman, B. S. (1994) *Biochemistry* 33(40), 12109-12118
206. Muralikrishna, P., and Cooperman, B. S. (1994) *Biochemistry* 33(6), 1392-1398
207. Muralikrishna, P., and Cooperman, B. S. (1991) *Biochemistry* 30(22), 5421-5428
208. Ehresmann, C., Baudin, F., Mougel, M., Romby, P., Ebel, J. P., and Ehresmann, B. (1987) *Nucleic Acids Res* 15(22), 9109-9128
209. Desai, N. A., and Shankar, V. (2003) *FEMS Microbiol Rev* 26(5), 457-491
210. Zimmermann, R. A., Muto, A., Fellner, P., Ehresmann, C., and Branlant, C. (1972) *Proc Natl Acad Sci U S A* 69(5), 1282-1286
211. Bear, D. G., Schleich, T., Noller, H. F., and Garrett, R. A. (1977) *Nucleic Acids Res* 4(7), 2511-2526
212. Egebjerg, J., Leffers, H., Christensen, A., Andersen, H., and Garrett, R. A. (1987) *J Mol Biol* 196(1), 125-136
213. Vester, B., and Garrett, R. A. (1984) *J Mol Biol* 179(3), 431-452
214. Peattie, D. A., and Gilbert, W. (1980) *Proc Natl Acad Sci U S A* 77(8), 4679-4682
215. Peattie, D. A., and Herr, W. (1981) *Proc Natl Acad Sci U S A* 78(4), 2273-2277
216. Batey, R. T., and Williamson, J. R. (1996) *J Mol Biol* 261(4), 550-567

217. Mougel, M., Philippe, C., Ebel, J. P., Ehresmann, B., and Ehresmann, C. (1988) *Nucleic Acids Res* 16(7), 2825-2839
218. Stern, S., Changchien, L. M., Craven, G. R., and Noller, H. F. (1988) *J Mol Biol* 200(2), 291-299
219. Stern, S., Powers, T., Changchien, L. M., and Noller, H. F. (1988) *J Mol Biol* 201(4), 683-695
220. Meier, N., and Wagner, R. (1984) *Nucleic Acids Res* 12(3), 1473-1487
221. Moazed, D., and Noller, H. F. (1989) *Nature* 342(6246), 142-148
222. Moazed, D., and Noller, H. F. (1986) *Cell* 47(6), 985-994
223. Huttenhofer, A., and Noller, H. F. (1994) *EMBO J* 13(16), 3892-3901
224. Matassova, A. B., Rodnina, M. V., and Wintermeyer, W. (2001) *RNA* 7(12), 1879-1885
225. La Teana, A., Gualerzi, C. O., and Dahlberg, A. E. (2001) *RNA* 7(8), 1173-1179
226. Dahlquist, K. D., and Puglisi, J. D. (2000) *J Mol Biol* 299(1), 1-15
227. Powers, T., and Noller, H. F. (1993) *Proc Natl Acad Sci U S A* 90(4), 1364-1368
228. Muralikrishna, P., and Wickstrom, E. (1989) *Biochemistry* 28(19), 7505-7510
229. Pogozelski, W. K., and Tullius, T. D. (1998) *Chem Rev* 98(3), 1089-1108
230. Noller, H. F., Green, R., Heilek, G., Hoffarth, V., Huttenhofer, A., Joseph, S., Lee, I., Lieberman, K., Mankin, A., Merryman, C., and et al. (1995) *Biochem Cell Biol* 73(11-12), 997-1009
231. Samaha, R. R., Joseph, S., O'Brien, B., O'Brien, T. W., and Noller, H. F. (1999) *Proc Natl Acad Sci U S A* 96(2), 366-370
232. Beauclerk, A. A., Cundliffe, E., and Dijk, J. (1984) *J Biol Chem* 259(10), 6559-6563
233. Strycharz, W. A., Nomura, M., and Lake, J. A. (1978) *J Mol Biol* 126(2), 123-140
234. Miller, S. P., and Bodley, J. W. (1991) *Nucleic Acids Res* 19(7), 1657-1660
235. Larsson, S. L., Sloma, M. S., and Nygard, O. (2002) *Biochim Biophys Acta* 1577(1), 53-62
236. Perentesis, J. P., Miller, S. P., and Bodley, J. W. (1992) *Biofactors* 3(3), 173-184
237. Sigman, D. S., Graham, D. R., D'Aurora, V., and Stern, A. M. (1979) *J Biol Chem* 254(24), 12269-12272
238. Sigman, D. S. (1990) *Biochemistry* 29(39), 9097-9105
239. Mazumder, A., Chen, C. B., Gaynor, R., and Sigman, D. S. (1992) *Biochem Biophys Res Commun* 187(3), 1503-1509
240. Muth, G. W., Thompson, C. M., and Hill, W. E. (1999) *Nucleic Acids Res* 27(8), 1906-1911
241. Chen, C. H., Mazumder, A., Constant, J. F., and Sigman, D. S. (1993) *Bioconjug Chem* 4(1), 69-77
242. Hermann, T., and Heumann, H. (1995) *RNA* 1(10), 1009-1017
243. Bullard, J. M., van Waes, M. A., Bucklin, D. J., and Hill, W. E. (1995) *J Mol Biol* 252(5), 572-582

244. Bullard, J. M., van Waes, M. A., Bucklin, D. J., Rice, M. J., and Hill, W. E. (1998) *Biochemistry* 37(5), 1350-1356
245. Bucklin, D. J., van Waes, M. A., Bullard, J. M., and Hill, W. E. (1997) *Biochemistry* 36(26), 7951-7957
246. Muth, G. W., Hennelly, S. P., and Hill, W. E. (1999) *RNA* 5(7), 856-864
247. Muth, G. W., and Hill, W. E. (2001) *Methods* 23(3), 218-232
248. Caruthers, M. H., Barone, A. D., Beaucage, S. L., Dodds, D. R., Fisher, E. F., McBride, L. J., Matteucci, M., Stabinsky, Z., and Tang, J. Y. (1987) *Methods Enzymol* 154, 287-313
249. Helene, C., and Thuong, N. T. (1989) *Genome* 31(1), 413-421
250. Meyer, H. A., Triana-Alonso, F., Spahn, C. M., Twardowski, T., Sobkiewicz, A., and Nierhaus, K. H. (1996) *Nucleic Acids Res* 24(20), 3996-4002
251. White, G. A., Wood, T., and Hill, W. E. (1988) *Nucleic Acids Res* 16(22), 10817-10831
252. Cheung, J., and Lin, A. (1999) *J Biomed Sci* 6(4), 277-284
253. Donis-Keller, H. (1979) *Nucleic Acids Res* 7(1), 179-192
254. Murakawa, G. J., Chen, C. H., Kuwabara, M. D., Nierlich, D. P., and Sigman, D. S. (1989) *Nucleic Acids Res* 17(13), 5361-5375
255. Bonincontro, A., Cinelli, S., Mengoni, M., Onori, G., Risuleo, G., and Santucci, A. (1998) *Biophys Chem* 75(2), 97-103
256. Thomas, G. J., Jr., Prescott, B., and Hamilton, M. G. (1980) *Biochemistry* 19(15), 3604-3613
257. Klein, D. J., Moore, P. B., and Steitz, T. A. (2004) *J Mol Biol* 340(1), 141-177
258. Holmberg, L., and Nygard, O. (1996) *J Mol Biol* 259(1), 81-94
259. Thederahn, T. B., Kuwabara, M.D., Larsen, T.A., Sigman, D.S. (1989) *Journal of the American Chemical Society* 111, 4941-4946
260. Que, B. G., Downey, K. M., and So, A. G. (1980) *Biochemistry* 19(26), 5987-5991
261. Johnson, G. R. A., Nazhat, N.B. (1989) *Journal of the American Chemical Society* 85, 677-689
262. Pecci, L., Montefoschi, G., and Cavallini, D. (1997) *Biochem Biophys Res Commun* 235(1), 264-267
263. Moro-Oka, Y., Fujisawa, K., Kitajima, N. (1995) *Pure and Applies Chemistry* 67, 241-248
264. Gorbunova, N. V., Purmal, A.P., Skurlatov, Y., Travin, S.O. (1977) *International Journal of Chemical Kinetics* 9, 983-1005
265. Bowen, W. S., Hill, W. E., and Lodmell, J. S. (2001) *Methods* 25(3), 344-350
266. Muth, G. W. (1999) I. Synthesis, Bio-Conjugation, Electronic and Spectral Properties of Phenanthroline Analogs II. Phenanthroline Cleavage of RNA. In. *Department of Chemistry*, The University of Montana, Missoula
267. Tam, M. F., and Hill, W. E. (1981) *Biochemistry* 20(22), 6480-6484
268. Lodmell, J. S., Tapprich, W. E., and Hill, W. E. (1993) *Biochemistry* 32(15), 4067-4072
269. Arkov, A. L., Freistroffer, D. V., Pavlov, M. Y., Ehrenberg, M., and Murgola, E. J. (2000) *Biochimie* 82(8), 671-682

270. Stoffler, G., Cundliffe, E., Stoffler-Meilicke, M., and Dabbs, E. R. (1980) *J Biol Chem* 255(21), 10517-10522
271. Cundliffe, E., Dixon, P., Stark, M., Stoffler, G., Ehrlich, R., Stoffler-Meilicke, M., and Cannon, M. (1979) *J Mol Biol* 132(2), 235-252
272. Brot, N., Tate, W. P., Caskey, C. T., and Weissbach, H. (1974) *Proc Natl Acad Sci U S A* 71(1), 89-92
273. Haseltine, W. A., Block, R., Gilbert, W., and Weber, K. (1972) *Nature* 238(5364), 381-384
274. Draper, D. E., Xing, Y., and Laing, L. G. (1995) *J Mol Biol* 249(2), 231-238
275. Cundliffe, E. (1986) Involvement of specific portions of rRNA in defined ribosomal functions: a study utilizing antibiotics. In: Hardesty, B., Kramer, G. (ed). *Structure, function, and genetics of ribosomes*, Springer-Verlag, New York
276. Porse, B. T., Leviev, I., Mankin, A. S., and Garrett, R. A. (1998) *J Mol Biol* 276(2), 391-404
277. Lentzen, G., Klinck, R., Matassova, N., Aboul-ela, F., and Murchie, A. I. (2003) *Chem Biol* 10(8), 769-778
278. Tam, M. F., Dodd, J. A., and Hill, W. E. (1981) *J Biol Chem* 256(12), 6430-6434
279. Christiansen, J., Egebjerg, N.L., Larsen, N., Garrett, R.A. (1990) Analysis of rRNA structure: experimental and theoretical considerations. In: Spedding, G. (ed). *Ribosomes and Protein Synthesis: a practical approach*, Oxford University Press, Oxford; New York
280. Stern, S., Moazed, D., and Noller, H. F. (1988) *Methods Enzymol* 164, 481-489
281. Wilson, K. S., and Noller, H. F. (1998) *Cell* 92(3), 337-349
282. Dijk, J., Garrett, R. A., and Muller, R. (1979) *Nucleic Acids Res* 6(8), 2717-2729
283. Laing, L. G., and Draper, D. E. (1994) *J Mol Biol* 237(5), 560-576
284. Bodley, J. W., Zieve, F. J., Lin, L., and Zieve, S. T. (1970) *J Biol Chem* 245(21), 5656-5661
285. Eckstein, F., Kettler, M., and Parmeggiani, A. (1971) *Biochem Biophys Res Commun* 45(5), 1151-1158
286. Jucker, F. M., and Pardi, A. (1995) *RNA* 1(2), 219-222
287. Stark, H., Rodnina, M. V., Wieden, H. J., van Heel, M., and Wintermeyer, W. (2000) *Cell* 100(3), 301-309
288. Stark, M., and Cundliffe, E. (1979) *J Mol Biol* 134(4), 767-769
289. George, S. (2003) Functional Characterization of Ribosomal Protein L11 Mutants in Esherichia Coli. In. *Division of Biological Sciences*, University of Montana, Missoula
290. Wagner, E. G., Jelenc, P. C., Ehrenberg, M., and Kurland, C. G. (1982) *Eur J Biochem* 122(1), 193-197
291. Jelenc, P. C., and Kurland, C. G. (1979) *Proc Natl Acad Sci U S A* 76(7), 3174-3178
292. Nomura, M., Gourse, R., and Baughman, G. (1984) *Annu Rev Biochem* 53, 75-117

293. Baughman, G., and Nomura, M. (1984) *Proc Natl Acad Sci U S A* 81(17), 5389-5393
294. Ehrenberg, M., Bilgin, N. & Kurland C.G. (1990) Design and use of a fast and accurate in vitro translation system. In: Spedding, G. (ed). *Ribosomes and Protein Synthesis: A Practical Approach*, Oxford University Press, New York
295. Naaktgeboren, N., Roobol, K., Gubbens, J., and Voorma, H. O. (1976) *Eur J Biochem* 70(1), 39-47